POLITECNICO DI TORINO

Corso di Laurea Magistrale

in Ingegneria Energetica e Nucleare

Tesi di Laurea Magistrale

"Life cycle environmental analysis of a hydrogen-based P2P storage system for remote applications"

Relatori

Prof. Massimo Santarelli

Dr. Kyrre Sundseth

Candidato

David Bionaz

Anno Accademico 2018/2019

Abstract

Climate change and global warming, mainly caused by the GHG emissions increase, are threatening our planet and a huge energy transition is needed, including the decarbonisation of energy sources, a larger and larger penetration of renewables (with the dramatic growth of wind and solar intermittent energies) and the necessary development of energy storage technologies. The integration of RES in hydrogen-based P2P storage systems is the most credible option with medium/long-term capacity and H_2 can be also used as a clean energy vector, flexibly transportable across different sectors and regions. In particular, islands and remote areas can become isolated mini-grids based on RES and P2P systems, avoiding more expensive and impacting solutions, such as submarine electric connections or on-site diesel generators, and having a huge global development potential. In this framework, the European Remote project takes place, aiming at demonstrating the technical and economic feasibility and the energy and environmental advantages of hydrogen-based P2P energy storage systems, designed and implemented in four remote demo cases, creating smart micro-grids almost totally relying on local RES. The aim of this thesis is to provide an environmental analysis of the complete hydrogen-based P2P energy storage system of the demo case 4, located in the harsh environment of the Norwegian Froan Islands and composed by PV panels, wind turbines, a diesel generator (covering 5% of the load), the H_2 storage system (water electrolyser, H_2 tank and PEM fuel cell) and Li-ion batteries. The impacts of this system are assessed in comparison with the ones of different scenarios, such as a reference fossil fuel case, with on-site diesel generators, or the actual situation, in which the Norwegian mainland electricity is transmitted through submarine cables. The climate impacts of each component or subsystem, mainly evaluated from literature data, are studied in a holistic view, according to a Life Cycle Assessment philosophy and methodology, in terms of Global Warming Impact (CO_2 equivalent emissions with time horizon of 100 years) per MWh of electricity generated or carried by sea cables. The Diesel case has very high GHG emissions (1,031.9 $kgCO_2eq/MWh$), more or less 7 times the ones of the Remote scenario (145.7 $kgCO_2eq/MWh$) and producing around 12,657.2 tons of CO_2eq more than the RES P2P plant, during the 25 years lifetime. The Cable case, instead, presents a lower impact (120.8 $kgCO_2eq/MWh$), because of a lower contribution of the diesel generators (2%), the relatively small distance from the mainland and the very low carbon intensity of the Norwegian electricity, almost totally produced from RES (98%). Further scenarios are also studied through sensitivity analyses, in which some relevant parameters are modified, in order to evaluate their relative contribution to the total GWI. Among the additional scenarios, the Remote-2% case, in which a lower contribution of generators is assumed for the demo case 4 (2% as in the Cable scenario), presents the lowest GWI (119.5 $kgCO_2eq/MWh$), while the Cable additional scenarios, in which a double connections length and a higher electricity carbon intensity are considered, reveal larger GWI

(from 211.4 to 595.2 $kgCO_2eq/MWh$), showing the high sensitivity of the final results to these parameters. In conclusion, apart from the very low GWI of the Cable scenario in the particular Froan Islands situation, the application of H_2-based P2P storage systems in remote isolated micro-grids offers high climate change benefits in comparison with other scenarios, especially with fossil fuel ones.

Keywords: P2P storage systems, Hydrogen, Remote areas, LCA, Global Warming Impact.

Abstract (italiano)

I cambiamenti climatici e il riscaldamento globale, causato principalmente dall'aumento delle emissioni di gas a effetto serra, stanno minacciando il nostro pianeta ed è necessaria una forte transizione energetica, comprendente la decarbonizzazione delle fonti energetiche, una penetrazione sempre più ampia di energie rinnovabili intermittenti (con le energie eolica e solare in grande crescita) e il necessario sviluppo delle tecnologie di accumulo dell'energia. L'integrazione delle energie rinnovabili nei sistemi di stoccaggio *P2P* a base di idrogeno è l'opzione più credibile con capacità a medio-lungo termine e l'idrogeno può essere anche utilizzato come vettore di energia pulita, trasportabile in modo flessibile in diversi settori energetici e regioni. In particolare, isole e aree remote possono diventare *mini-grid* isolate basate su sistemi con fonti di energia rinnovabile (*RES*) e stoccaggio *P2P*, evitando soluzioni più costose e impattanti, come connessioni elettriche sottomarine o generatori diesel installati in loco, rivelando quindi un enorme potenziale di sviluppo globale. In questo quadro, si svolge il progetto europeo *Remote* avente l'obiettivo di dimostrare la fattibilità tecnica ed economica e i vantaggi energetici e ambientali dei sistemi di accumulo di energia *P2P* a base di idrogeno, progettati e realizzati in quattro casi dimostrativi in località remote, creando *micro-grid* intelligenti quasi completamente basate su fonti di energia rinnovabile locale. Lo scopo di questa tesi è di fornire un'analisi ambientale dell'intero sistema di accumulo di energia *P2P* a base di idrogeno del caso dimostrativo 4, situato nell'ambiente rigido e ostile delle isole norvegesi Froan e composto da pannelli fotovoltaici, turbine eoliche, un generatore diesel (che copre il 5% del carico), il sistema di stoccaggio di idrogeno (elettrolizzatore, serbatoio e cella a combustibile *PEM*) e batterie agli ioni di litio. Gli impatti di questo sistema sono valutati rispetto a quelli di diversi scenari, un caso studio di riferimento basato sull'uso di combustibile fossile in generatori diesel sull'isola e la situazione attuale, in cui l'elettricità prodotta nel continente norvegese viene trasmessa attraverso cavi sottomarini. Gli impatti climatici di ciascun componente o sottosistema, principalmente valutati da dati presenti in letteratura, sono studiati in una visione olistica, secondo una filosofia e una metodologia di *Life Cycle Assessment* (*LCA*), in termini di impatto sul riscaldamento globale (emissioni di CO_2 equivalente con orizzonte temporale di 100 anni) per MWh di elettricità generata o trasportata da cavi sottomarini. Lo scenario *Diesel* ha emissioni di gas a effetto serra (*GHG*) molto elevate (1.031,9 $kgCO_2eq/MWh$), circa 7 volte quelle dello scenario *Remote* (145,7 $kgCO_2eq/MWh$), producendo, nei 25 anni di vita, circa 12.657,2 tonnellate di CO_2eq in più rispetto al sistema *P2P* basato su energie rinnovabili. Lo scenario *Cable* presenta invece un impatto inferiore (120,8 $kgCO_2eq/MWh$), a causa di un minore contributo dei generatori diesel (2%), della distanza relativamente piccola dalla terraferma e della bassissima intensità di carbonio dell'elettricità norvegese, quasi totalmente prodotta da *RES* (98%). Si sono poi studiati ulteriori scenari attraverso un'analisi di sensibilità, in cui alcuni parametri rilevanti sono stati

modificati al fine di valutare il loro contributo relativo al *GWI* totale. Tra gli scenari aggiuntivi, il caso *Remote-2%*, in cui si ipotizza un contributo inferiore dei generatori (2% come nello scenario *Cable*) per il caso dimostrativo 4, presenta il *GWI* più basso (119,5 kgCO_2eq/MWh), mentre gli scenari *Cable* aggiuntivi, in cui si considerano una doppia lunghezza dei collegamenti e una maggiore intensità di carbonio dell'elettricità, rivelano un *GWI* maggiore (da 211,4 a 595,2 kgCO_2eq/MWh), mostrando l'elevata sensibilità dei risultati finali a questi parametri. In conclusione, a parte il bassissimo *GWI* dello scenario *Cable* nella particolare situazione delle isole Froan, l'applicazione di sistemi di stoccaggio *P2P* a base di idrogeno in *micro-grids* intelligenti in zone remote ed isolate offre alti vantaggi in termini di cambiamenti climatici rispetto ad altri scenari, in particolare con il caso che prevede l'utilizzo di combustibile fossile.

Parole chiave: Sistemi di stoccaggio *P2P*, Idrogeno, Aree remote, LCA, Impatto sul riscaldamento globale (GWI).

Acknowledgements

First of all, I would like to thank my academic supervisor of the Polytechnic University of Turin, Prof. Massimo Santarelli, for providing me the great opportunity to undertake this project, my co-supervisor in SINTEF AS, Dr. Kyrre Sundseth, for receiving me so warmly in Trondheim (Norway), and both of them for their important support and guidance during this project.

Vorrei poi ringraziare tutte le persone che mi sono sempre state accanto, sia nei momenti felici che in quelli più bui, e con le quali ho condiviso e affrontato esperienze e periodi più o meno lunghi del percorso che mi ha portato sin qui. Non farò nomi per non dimenticare nessuno, ma sono sicuro che ognuno di voi si sentirà rappresentato e menzionato in una o più parti.

Un grazie enorme alla mia famiglia, sempre presente, che mi ha supportato in ogni istante. Ai miei nonni con la loro preziosa esperienza e i loro innumerevoli racconti di vita, ai miei genitori che mi crescono e proteggono ogni giorno, a mia sorella, riferimento costante, che con mio cognato mi ha regalato la gioia di essere zio di una bimba stupenda, ai miei zii, cugini e parenti facenti parte di questa magnifica grande famiglia per cui rimarrò sempre Dadi.

Un altrettanto grande grazie a tutte le persone che sono accanto a me in qualità di amici, da coloro che conosco sin da tenera età, fino a chi ho incontrato recentemente. Grazie a chi ha iniziato a chiamarmi Bio tra le mura di un roseo liceo ed è tutt'ora qui nonostante viaggi intercontinentali e lavori navali. Grazie a chi ha vissuto letteralmente con me in questi anni, sopportandomi, supportandomi e regalandomi perle giornaliere in via San Secondo. Grazie a chi ha iniziato a chiamarmi Dave tra le mura di un oratorio e tra le montagne della magica Valle. Grazie a chi mi ha accompagnato tra mille lezioni, progetti e risate nelle aule di questo Politecnico. Grazie a chi ha reso i miei Erasmus delle esperienze indimenticabili, tra serate tacos nella Lyon dei giovani talenti e aperinorway rigorosamente a base di salmone nella nordica Trondheim. Un grazie in particolare a chi ha vissuto da vicino e in prima persona questi mesi di preparazione e scrittura tesi. A chi ha iniziato a chiamarmi Dad tra i fiordi, a chi anche da lontano mi forniva consulenze ingegneristiche, a chi ha supervisionato minuziosamente il design e la resa grafica, a chi mi ha fornito vitto e alloggio nelle giornate trascorse a Torino.

Grazie a tutti coloro che hanno condiviso con me feste danzanti, serate tra amici, pranzi in famiglia, supermercati notturni, confessionali profondi, fusa feline, navigazioni a vela, sessioni di studio, tour automobilistici in ogni luogo e orario, sushi ingolfanti, grigliate notturne, tornei di carte, esami impossibili, progetti infiniti, concerti, palcoscenici Al Buio, karaoke ignoranti, compleanni, tuffi al mare, aperitivi e tisanine, viaggi indimenticabili e molto altro ancora.

Questo traguardo non sarebbe stato possibile senza di voi e senza il vostro immenso appoggio che mi dimostrate giornalmente.

Grazie.

Contents

List of figures

List of tables

Acronyms

AC	Alternating Current
BOP	Balance of Plant
CCS	Carbon Capture and Storage
CDR	Carbon Dioxide Removal
CED	Cumulative Energy Demand
CH_4	Methane
CIGRE	International Council for Large Electric Systems
Cl	Chlorine
CO_2	Carbon Dioxide
CO_2eq	Equivalent Carbon Dioxide
COP	Conference of the Parties
Cu	Copper
DC	Direct Current
ELY	Electrolyser
EOL	End of Life
EPBT	Energy Payback Time
EU	European Union
FC	Fuel Cell
G2P	Gas to Power
GHG	Greenhouse Gases
GWI	Global Warming Impact
GWP	Global Warming Potential
H_2	Hydrogen
HVDC	High Voltage Direct Current
I	Iodine
ICE	Internal Combustion Engine
IPCC	Intergovernmental Panel on Climate Change

ISO	International Standards Organization
LCA	Life Cycle Assessment
LCI	Life Cycle Inventory
LCIA	Life Cycle Impact Assessment
LHV	Low Heating Value
Li	Lithium
LMP	Lithium Metal Polymer
LT-PEM	Low Temperature – PEM
MV	Medium Voltage
MVAC	Medium Voltage Alternating Current
NOCT	Normal Operating Cell Temperature
NVE	Norwegian Water Resources and Energy Directorate
P2G	Power to Gas
P2H	Power to Hydrogen
P2P	Power to Power
PEM	Proton Exchange (or Polymer Electrolyte) Membrane
PEMFC	PEM Fuel Cell
PEMWE	PEM Water Electrolysis
PR	Performance Ratio
PV	Photovoltaic
RES	Renewable Energy Sources
RUL	Remaining Useful Life
S	Sulfur
SAGES	Smart Autonomous Green Energy Station
SDG	Sustainable Development Goal
SF	Safety Factor
Si	Silicon
SOC	State of Charge
SOEC	Solid Oxide Electrolysis Cell
SS	Stainless Steel

UN	United Nations
UNFCCC	United Nations Framework Convention on Climate Change
UPS	Uninterruptible Power Supply
VRE	Variable Renewable Energy
WOW	Waiting on Weather
WT	Wind Turbine
WTT	Well-To-Tank
XLPE	Cross-Linked Polyethylene

1 Introduction

1.1 General background

Climate change is threatening almost irreversibly human society and the entire planet, amplifying, in the recent future, the existing risks and creating new ones for natural and human systems. Anthropogenic forcings on climate, such as the dramatic increase in GHG emissions and concentrations, are the dominant causes of the observed increase in global average surface temperature. It has increased by 0.85 °C between 1880 and 2012, as reported in the IPCC Fifth Assessment Report, and, if the current warming rate continues, the world will reach a global warming of 1.5 °C by around 2040 [1] [2] (Figure 1-1, Figure 1-2).

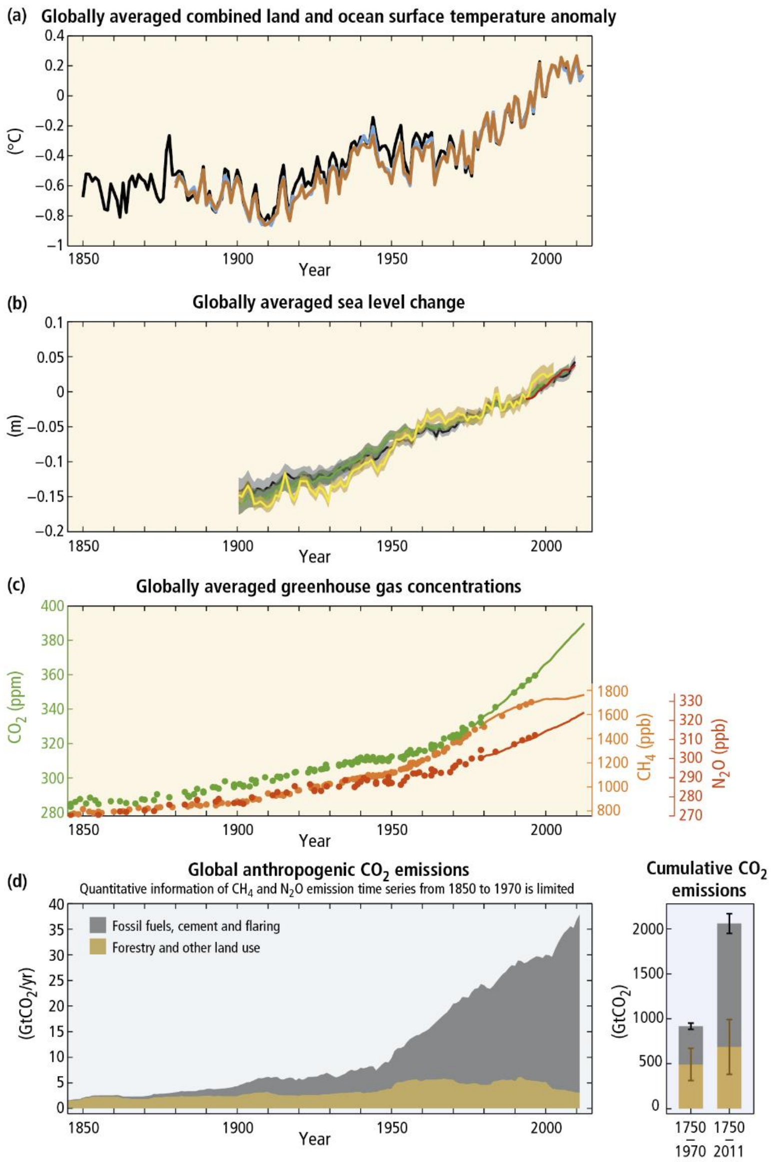

Figure 1-1: Relationship between the observations of a changing global climate system (a, b, c) and CO_2 emissions (d) [2].

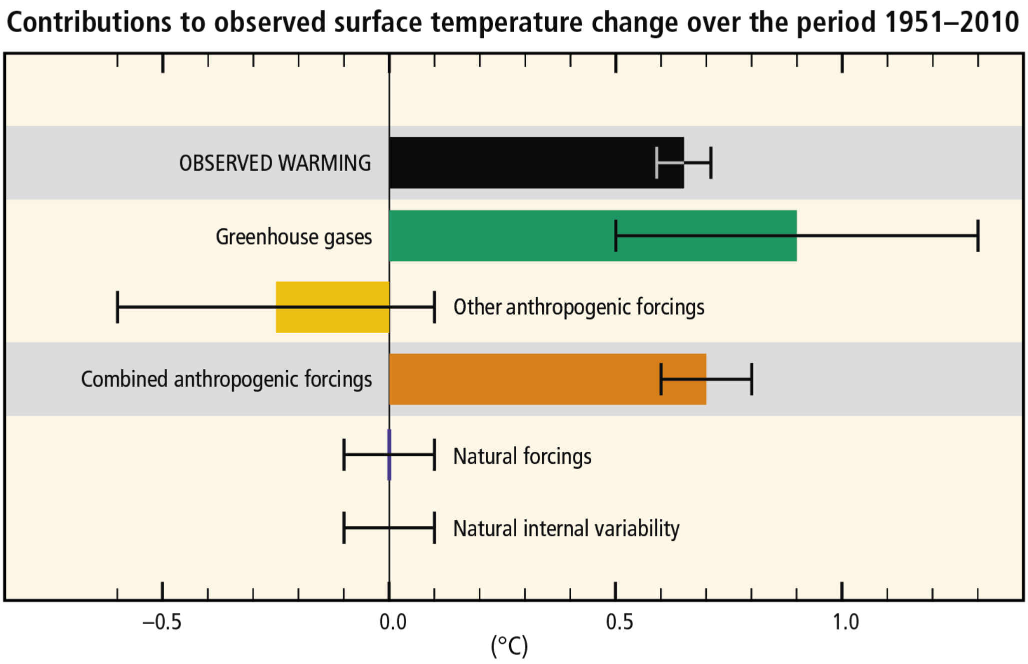

Figure 1-2: Mid-points (bars) and assessed likely ranges (whiskers) for trends regarding observed warming and various contributions over the 1951–2010 period [2].

Reducing risks of climate change is then only affordable with a substantial reduction of GHG emissions to zero in next decades, even if some risks from climate damages will be unavoidable [2]. This can be achieved only by a huge transformation in the energy, industry, transport, buildings, agriculture, forestry and other land-use sectors. In particular, the energy system will face a great transformation, such as the use of new technologies, the decarbonisation of energy sources, a larger and larger penetration of renewables, an increase in electrification with low carbon intensity, a more and more efficient energy systems and a reduction of the energy demand with a change in individual and collective behaviour [1] [2] [3].

Climate change is a problem at global scale and international and cooperative responses are critical in order to reduce emissions in the short term and to achieve an effective mitigation of the problem. In September 2015, at the UN Sustainable Development Summit, the 2030 Agenda for Sustainable Development was adopted by all United Nations Member States. According to [4], the document of the adopted resolution, "this Agenda is a plan of action for people, planet and prosperity" now and into the future, seeking "to strengthen universal peace in larger freedom" and recognizing also "that eradicating poverty in all its forms and dimensions, including extreme poverty, is the greatest global challenge and an indispensable requirement for sustainable development". Furthermore, in a global "collaborative partnership" spirit, it shows the determination "to take the bold and transformative steps which are urgently needed to shift the world on to a sustainable and resilient path", and to "heal and secure our planet" [4]. This shared blueprint has at its core the 17 Sustainable Development Goals (SDGs), which are "an urgent call for action by all countries (developed and developing)" and the "world's best plan to build a better world for people and our planet by 2030” [I]. They aim at ending poverty and deprivations (for example of food and clean water), at reducing inequalities, at improving human rights, gender equality, peace, justice, prosperity, economic growth, job opportunities, health, education, innovation, industry and infrastructures, cities and communities, all while protecting the environment, ensuring responsible consumption and production, tackling climate change, preserving nature (seas, oceans, forests, land…) and producing clean and affordable energy. The integrated and indivisible SDGs, balancing the three dimensions of sustainable development (economic, social and environmental), are summarized in Figure 1-3 [I] [4].

Figure 1-3: Sustainable Development Goals [II].

In the same year, in December 2015, at the Paris climate conference (COP 21), 195 countries adopted the Paris agreement, the first-ever, universal, legally binding, global climate deal. The main purpose was to define an action plan in order to hold “the increase in the global average temperature to well below 2 °C above pre-industrial levels pursuing efforts to limit the temperature increase to 1.5 °C above pre-industrial levels” [5] [6]. Following the principles of equity, poverty eradication and sustainable development, some global and regional climate-resilient pathways can be and must be pursued. In the great number of possible scenarios, the 1.5 °C emission pathways, providing chance of remaining below 1.5 °C or returning to 1.5 °C by 2100, require quickly and substantial societal and technological transformations. They should mix adaptation and mitigation efforts with sustainable development strategies across multiple scales (international, national, regional and local) to support technologically, economically and politically this transition. Adaptation aims at reducing vulnerability to the threatening effects of climate change, while mitigation refers to the reduction of GHG emissions or the absorption of gases already emitted with for example Carbone Dioxide Removal (CDR) systems or Carbon dioxide Capture and Storage (CCS) technologies [2] [3].

In 2015, in order to create a united and compact front against climate changes, EU built the Energy Union. It is a "European priority project, identified by the Juncker Commission as one of the ten political priorities, in which five dimensions are closely interlinked: energy security, solidarity and trust; a fully integrated European energy market; energy efficiency contributing to moderation of demand; decarbonising the economy; and research, innovation and competitiveness" [7]. In particular, renewable energy is one of the most important Energy Union's priorities contributing to the five dimensions mentioned above and it is a key pillar for the energy transition towards a low-carbon economy and society, necessary to mitigate climate change [8] [9]. Following the adoption of the Paris agreement and according to its directives, the EU also fixed precise targets to achieve in the future. The "2020 package" and the "2030 climate and energy framework" set three key targets for the year 2020 and 2030: 20% cut in GHG emissions from 1990 levels in 2020 and 40% in 2030, 20% share for renewable energy in 2020 and 32% in 2030, 20% improvement in energy efficiency in 2020 and 32.5% in 2030. The final aim is a climate-neutral Europe by 2050 through a strategic long-term vision presented by the Commission on 28/11/2018 [III]. The decarbonisation of the European zone is well under way and the share of renewable energy in the EU energy mix is continually rising and is on the track to reach the 2020 energy targets [7] [10]. In 2017, renewable energy sources accounted for 29.9% of the EU-28's total production of primary energy, with an increase of 65.6% compared to 2007 [11], as we can see in Figure 1-4 (modified from [11]).

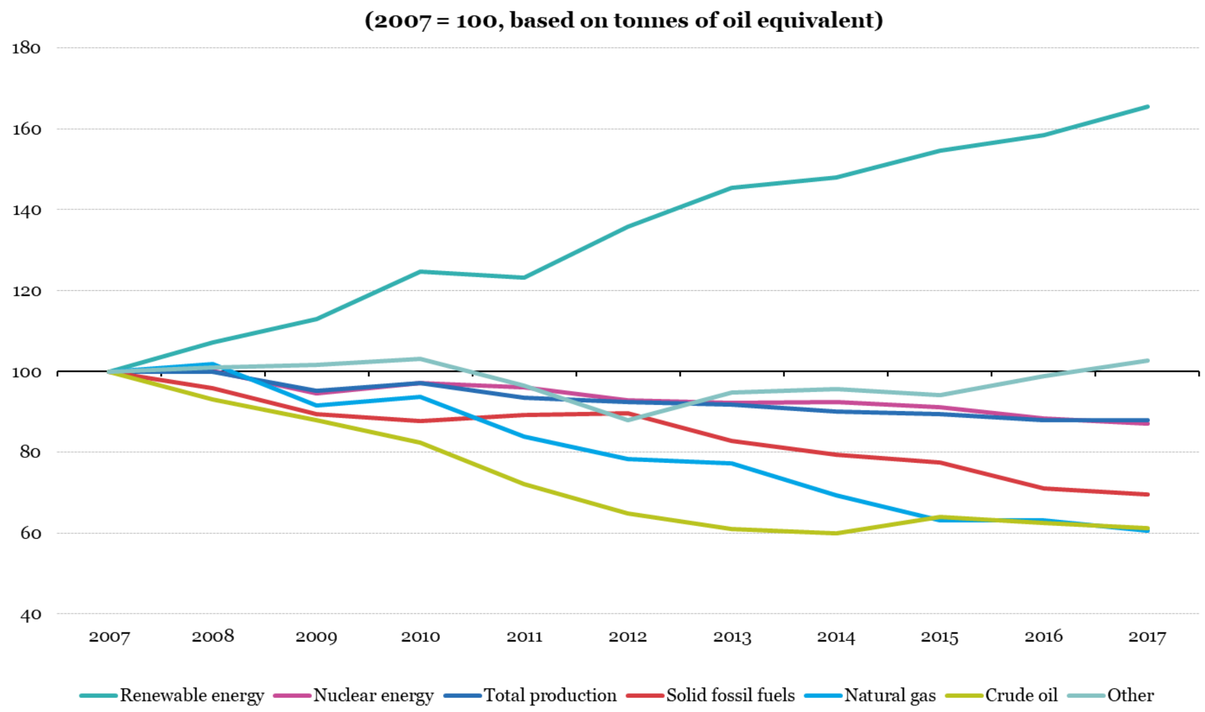

Figure 1-4: Development of the EU-28 production of primary energy (by fuel type) in the period 2007-2017 [11].

Moreover, the share of energy from renewable sources in gross final energy consumption in the EU-28 is continuously growing year after year, from 8.5% in 2004 to 12.6% in 2009, 16.7% in 2015, 17.0% in 2016 and finally to 17.5% in 2017 [12] (Figure 1-5).

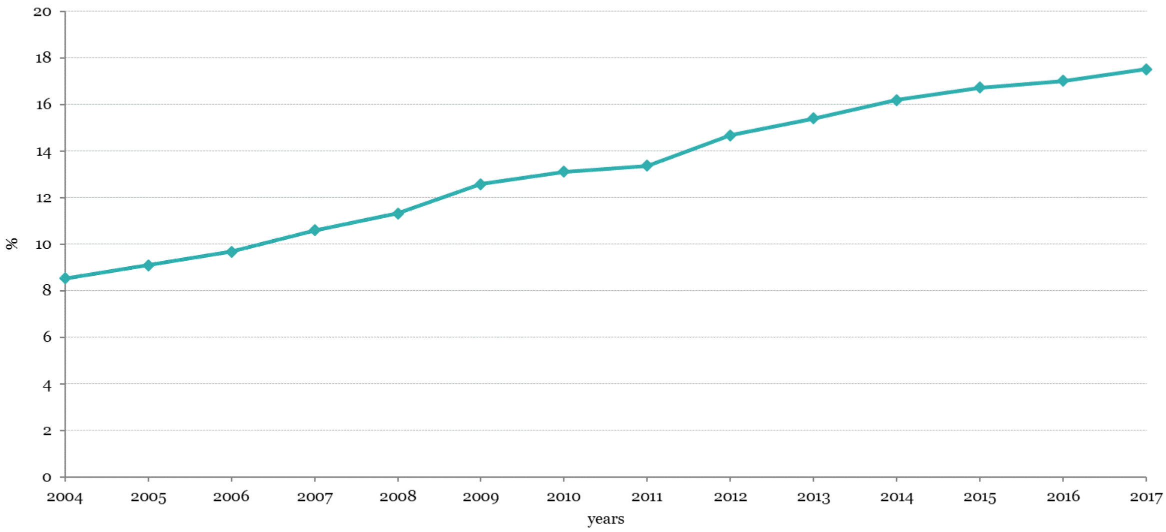

Figure 1-5: Share of energy from renewable sources in EU-28 gross final consumption of energy, 2004-2017.

This increasing consumption of renewables allows the EU to decrease significantly its demand for fossil fuels and it is one of the major drivers of the reduction of GHG emissions. Compared with 1990 levels, in 2017, EU total GHG emissions, including international aviation and indirect CO_2 emissions, were down by 21.7%, exceeding the Europe 2020 targets [13], as shown in Figure 1-6 (modified from [13]).

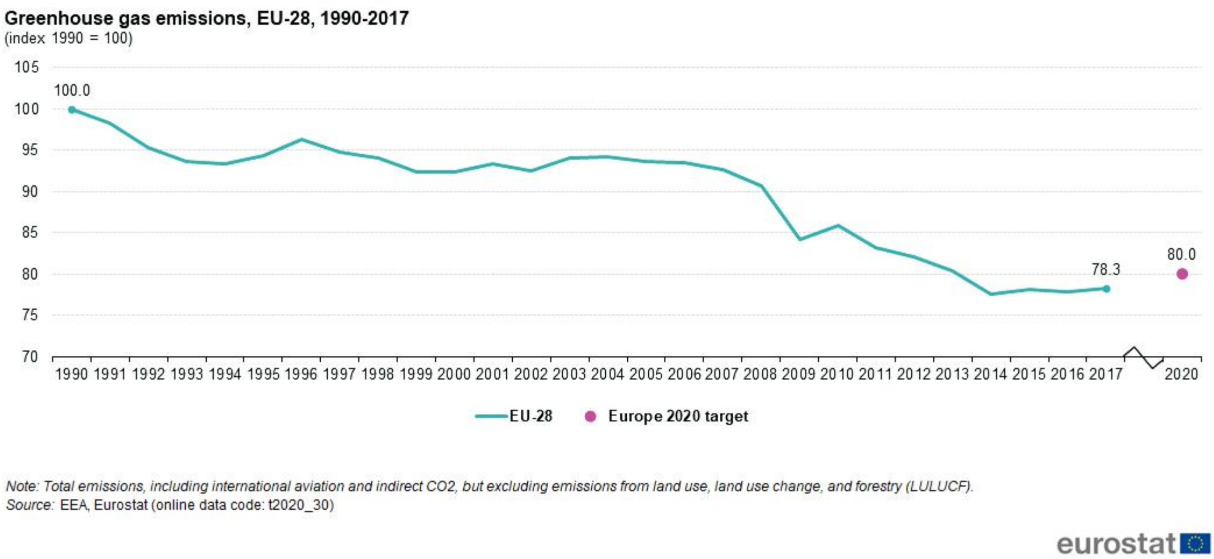

Figure 1-6: EU-28 greenhouse gas emissions trend over the period 1990-2017 [13].

In absolute terms, the dominant RES market sectors are yet heating and cooling, followed by renewable electricity, which is instead the first one concerning the share of renewable energy in gross final energy consumption by sector (30.7% in 2017), followed by heating/cooling and transport (Figure 1-7). The electricity sector has seen the fastest growth in renewable share doubling 2004 value, a growth driven especially by the increasing onshore and offshore wind power and solar PV electricity generation [9][8][13].

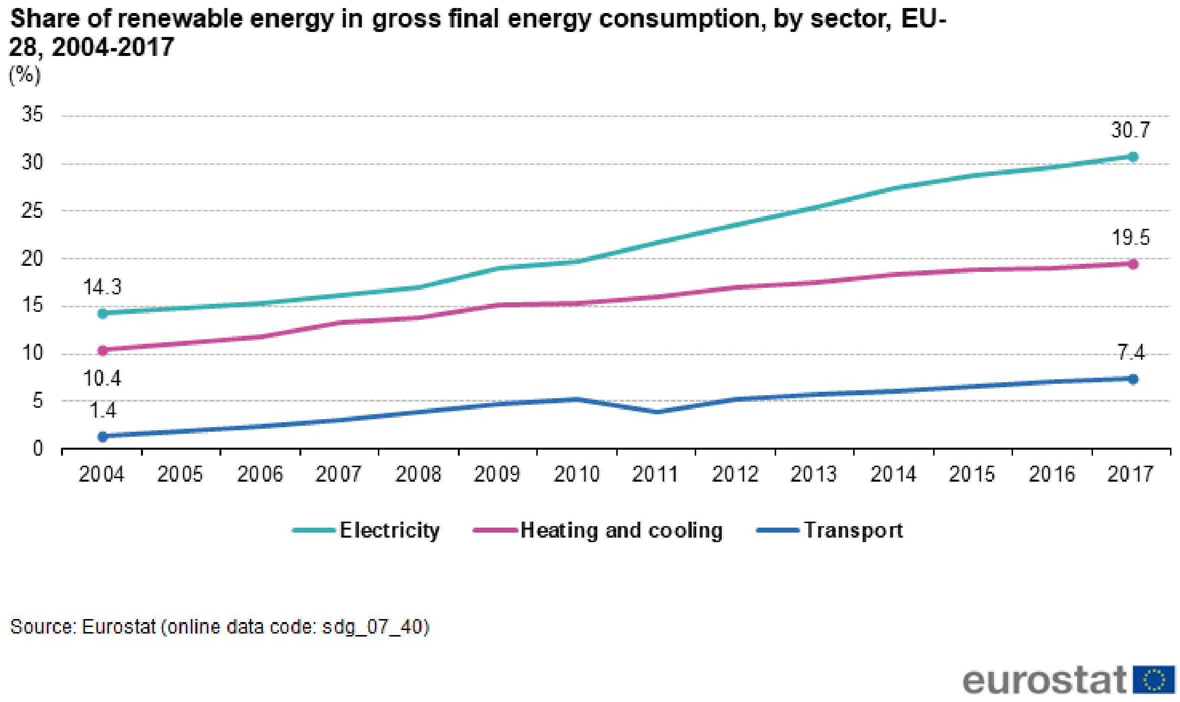

Figure 1-7: Share of renewable energy in EU-28 gross final energy consumption (by sector), over the period 2004-2017 [13].

Among renewables energies, in 2017, the most important RES remained still bioenergy (wood, solid biofuels, renewable waste, biogas and bioliquids), accounting for about 60.5% of the total primary renewable energy production. Nevertheless, wind and solar energy have continued to grow the fastest in terms of relative shares, thanks to a rapid expansion in the two technologies. In particular, in 2017, the wind power became for the first time the most importance source regarding the gross electricity generation from renewable sources in the EU-28, with a share of 37.2% and with a production increase of about 3.5 times compared with 2007. The solar power has also seen a dramatic growth in its electricity production, rising to about 31.6 times the generation assessed in 2007, with a share in 2017 of 12.3% [12]. This trend, confirmed by the fact that in 2017 the 85% of all newly installed power capacity in the EU was of renewable origin (mostly due to wind and solar power), is necessary to meet the EU targets and more generally the 1.5 °C limit [8]. In fact, in the high-renewables EU scenario presented by [14], variable RES penetration will be more than 60% by 2050 and, in all the 1.5 °C pathways, the share of energy from renewable sources (including biomass, hydro, solar, wind and geothermal) must increase, reaching 38-88% in 2050 [3].

The “new” and disruptive renewables like solar and wind (onshore and offshore) have therefore demonstrated substantial technological improvements in performance, cost reductions, dramatic growth trajectories and they seem to well contribute to 1.5 °C-consistent pathways, but there are still challenges to be solved in order to achieve a high penetration and enable a deployment at significant scale [15] [5]. Possible barriers are, for example, the intermittency, the both seasonal, daily and hourly weather variability, the difficult predictability of the natural source (solar irradiance, wind…), the reduction of the inertia of the energy system and the difference between load and production curves. Periods with a production far in excess of demand, needing then curtailment, will alternate with times when the low power generation from sun and wind will require a non-renewable generation capacity. In addition, the large intermittency in power flows will stress very much the transmission and distribution systems [14]. In order to ensure power network stability and reliability and to maintain the continuous balance between energy generation and load, we need flexibility from every corner of the energy system and there are four main options that can be taken into account: dispatchable generation, transmission and distribution expansion, demand side management, and energy storage [14]. In particular, the development of bulk electricity energy storage is one of the most significant and necessary solution and the European commission recognized it as an important component for the transition towards a decarbonized power sector [16] [14].

Energy storage is in fact a game changer, since it is a key to enable a higher penetration of RES in the grid and it can provide many services to the energy sector. It allows the electricity time shift, converting the RES power surplus in a storable form (avoiding curtailments) and providing an available amount of energy when demand overcomes the production (avoiding other forms of power generation). It can convert the electricity into other energy carriers, such as heat or hydrogen, which can be useful for other purposes. It gives stability, flexibility and a frequency reserve for the grid ensuring a continuous balance between supply and demand and avoiding large investments on transmission and distribution infrastructures [14]. Then, the role of energy storage is expected to gain importance, as intermittent renewables, like PV and wind, increasing their share in the electricity mix. There are many different types of energy storage, which can be categorized into mechanical (pumped hydroelectric storage, compressed air energy storage, flywheels), electrochemical (conventional and flow batteries), electrical (capacitors, supercapacitors and superconducting magnetic energy storage), thermal (sensible/latent heat storage), thermochemical (solar fuels) and chemical ones (hydrogen storage with fuel cell) [16]. Batteries are easy to implement and they have seen the main increase in energy storage in the last years. They have also become a strategic part of the innovation priorities for reaching the Energy Union objectives because of their increasing performance and falling costs [10]. Despite these positive aspects, the feasibility of battery storage has some drawbacks concerning the still high costs for storage of more than one day, the availability of manufacturing resources and the environmental impacts of its production such as the high CO_2 footprint and the difficult recyclability [15]. Instead, renewably chemical storage is still under the research and demonstration phase, but it is increasingly seen as a feasible storage option for renewables energy. Among the various range of possibilities, the integration of diffuse and intermittent RES (PV, wind, wave) in hydrogen-based power-to-power (P2P) storage systems is seen as the most credible option and it can become a disruptive technology solution, with medium to long-term storage capabilities (days, weeks or even months) [15]. Furthermore, even if batteries are generally cheaper and they have better roundtrip efficiencies, this solution has a longer lifetime and a higher temperature tolerance, useful in extreme climates [17].

Hydrogen is a versatile, clean and flexible energy vector, crucial to achieve the decarbonisation objective and the energy transition. Even if current hydrogen is still almost completely (95%) produced by fossil sources through steam-methane reforming or oil and coal gasification, in a lower-carbon energy future with a high share and penetration of renewables, the hydrogen will be mainly produced via renewables ways, such as the water electrolysis from RES. There are also other possible renewables ways to produce hydrogen, such as steam reforming of biomethane/biogas, biomass gasification and pyrolysis, combined dark fermentation and anaerobic digestion, photocatalysis, thermochemical water splitting, supercritical water gasification of biomass, but or they need CCS or they are not yet mature technologies [17]. The main disadvantage of water electrolysis is the high initial investment and final hydrogen costs, but they are decreasing year after year, thanks to the development in the technology and the increasing demand of hydrogen. In total, according to the scenario presented by [18], the annual demand for hydrogen would increase from about 325 TWh in 2015 to 2,250 TWh in 2050, representing roughly a quarter of the EU's total energy demand, due to the new uses in power, transportation, industry and buildings [18]. In fact, if produced from RES, hydrogen would enable large-scale renewables integration and power generation and it can be used both as fixed seasonal storage of renewable electricity and as renewable fuel to provide sectors that would be otherwise difficult to decarbonise through electrification, such as industry, buildings and transport. Moreover, regions with high RES production can use hydrogen as energy carrier in order to feed countries with limited or more expensive renewable potential. In fact, it can be transported flexibly across sectors and regions through pipelines, ships or trucks in gaseous, liquid or in other forms of storage. Then, it could be transformed again in electricity with fuel cells or it can be simply used as a fuel or as a source material for the synthetisation of other chemicals [19] [18] [17]. Figure 1-8 resumes in a schematic view the possible paths for the hydrogen produced from RES.

Hydrogen and electricity are then complementary energy carriers needed for the energy transition and, in the future, H_2 could transport and distribute the renewable energy over long distances, also in those cases where the electricity grid has insufficient capacity or it is too

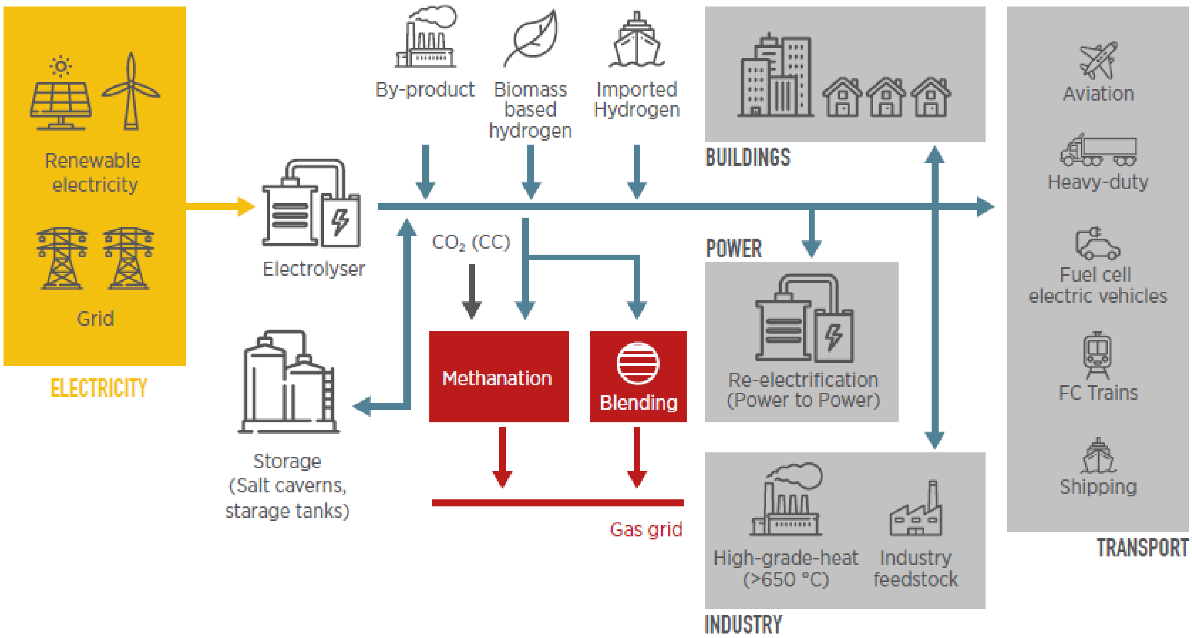

Figure 1-8: Integration of RES into end uses by means of hydrogen [17].

impractical or expensive. It is the case, for example, of offshore renewable production, where, instead of building expensive submarine cables, hydrogen can be produced on site and then transported with cheaper pipelines. Island or remote areas, hardly connectable by electric grid or still fed by expensive diesel generators and imported fuels, can instead only rely on on-site renewables with a well-sized storage solution. This solution would provide a reliable, cheaper and more accessible electricity to the inhabitants, helping a socioeconomic development of the rural communities and an improved self-sufficiency. Furthermore, it would decrease the environmental impact providing clean energy 24/7 and replacing the diesel generators that also require more maintenance. A reduced noise, odour and an improved air quality could also make touristic island more attractive [20] [17] [21]. The off-grid renewable energy solutions (stand-alone systems and isolated mini-grids) have a huge global development potential and they represent a large market (on a scale of hundreds of GW). They consist generally in replacing or hybridising the existing off-grid diesel generators or transmission cables with RES plants and hydrogen storage systems in combination with batteries for the short term [22] [17]. These off-grid systems are cost-competitive, rapidly deployable, easily customisable to different conditions, in accordance with emerging technologies and they represent a unique opportunity to change the socioeconomic and energetic landscape of rural areas and islands [20]. In accordance with these concepts, in May 2017, in Malta, UE Commission signed a political declaration to accelerate the energy transition of islands towards RES solutions, in order to reduce the heavy reliance on imported fossil fuels [10].

In this framework, under Horizon 2020, the biggest EU Research and Innovation program ever, the Remote project takes place. It aims at demonstrating the technical and economic feasibility and the high energy and environmental advantages of two hydrogen-based P2P energy storage systems (integrated or not) designed and implemented in four demo cases located in three different countries (Norway, Italy and Greece) and in different types of remote areas, which are all ideal candidates for this energy storage solution. Thanks to this project, experience of fuel cells and H_2-based storage solutions will be gained, promoting their future and larger deployment and providing a starting point to show the feasibility of hydrogen as multi-purpose energy vector [23] [21]. These systems would create smart micro-grids based only on local RES, avoiding the import and the local use of fossil fuels or the dependence on transmission lines usually transmitting energy from fossil fuels. Renewable energy sources, different according to the location, will be exploited to fully meet the local energy loads and the storage system will manage the relevant fluctuations in the power production introduced by the RES. Surplus electricity can be used to charge a battery or to supply a water electrolyser that produces hydrogen, which is then stored in a pressurized container. In case of lack of RES energy, the demand can be covered by the electricity generation of the fuel cell through hydrogen consumption or by discharging the battery device. In particular, the battery is used both to provide electricity for the daily operation of the control unit and auxiliary equipment and as a daily electricity energy buffer. The hydrogen storage would provide instead a longer-term energy back up. An appropriate control system and a power management strategy are also essential in order to ensure the optimal energy and storage utilization, the performance, the efficiency, the lifetime of the different subsystems and the correct operation in specific ranges (regarding, for example, the battery state of charge, the pressure of the hydrogen tank or the number of start-ups and shut-downs) [24]. The four demo cases would then be able to provide a clean, renewable, secure and reliable power supply, they would eliminate the costs related to the transmission/distribution lines or to the transport of fossil fuels and they would determine a drastic reduction (or elimination) of the CO_2 emissions. Moreover, the sustainable development goals touched in the Remote project and in this thesis are summarized in Figure 1-9 (modified from [II]).

Figure 1-9: Sustainable Development Goals touched in the Remote project and in this thesis [II].

1.2 Aim of the thesis

The aim of this thesis work is to provide an environmental analysis of the complete hydrogen-based P2P energy storage system of the demo case 4, located in the Froan Islands in Norway. After a literary review of similar previous studies, a description of the Remote case study and the explanation of the methodology applied in the analysis, the environmental impacts of the designed system will be assessed in comparison with the ones of different scenarios, such as a reference fossil fuel scenario (diesel fuelled internal combustion engines) or the actual situation using the Norwegian electricity generated in the mainland and transmitted by submarine cables. In particular, the climate change benefits, in terms of CO_2 equivalent emissions (with time horizon of 100 years) per MWh of electricity generated or carried by sea cables, will be evaluated from literature data through a life cycle assessment philosophy, with the aim of providing the potential environmental impacts in a holistic view, including lifetime direct impacts as well as lifecycle indirect impacts. Additional scenarios are also studied through a sensitivity analysis, in which some relevant parameters are modified, in order to evaluate their relative impacts to the total GWI.

2 Literary review

In literature we can find a lot of studies approaching hydrogen technologies, confirming the big interest on this topic. Several papers discuss the H_2 production from different sources and through different methodologies, such as studies [25], [26], [27], [28], [29], [30], [31] and [32]. They compare the performances (environmental impacts via LCA, production costs, energy and exergy efficiencies,…) of alternative ways of producing hydrogen (conventional and not), such as coal or biomass gasification, dark fermentation of lignocellulosic biomass, steam reforming of natural gas, water electrolysis (with PEM or SOEC technologies) from grid electricity or from renewables energies (wind and solar), thermochemical water-splitting using solar or nuclear energy (with for example Cu-Cl or S-I cycles), water photo-splitting and auto-maintained methane decomposition. A more specific interest in the LCA of different electrolysis technologies, mainly based on renewable sources, in present and future energy systems, is present in papers [33], [34], and [42].

Regarding the produced hydrogen, various pathways are studied through environmental (via LCA), technical, energetical and economic analyses. Papers [35], [36] and [37] deepen the fuel cell systems in mobility and transportation, in comparison with conventional ICEs, while study [38] analyses the impacts of renewable hydrogen used as cooking fuel compared to conventional ones. The LCA of uninterruptible power supply (UPS) systems, battery and hydrogen-based, is also present in paper [43], comparing the ICE conventional case, and in paper [76], with a focus in EOL scenarios. Other studies (such as [39], [40], [87], [41], [44] and [45]) investigate instead the production and utilisation of hydrogen in power-to-gas (P2G) systems, enabling the storage of surplus electricity from fluctuating RES and directly using the produced hydrogen for different final scopes. It can be directly transported by pipelines or pressurized tanks towards the final application (heat or electricity generation, fuel for mobility, chemical industries…) or it can be used to synthetize methane, in order to be fed into the existing gas infrastructure and then used for similar scopes.

Different RES storage systems, usually studied for the energy supply of off-grid and stand-alone situations, in particular for remote sites, such as mountainous areas or islands (like in the Remote case), are also analysed in the literature. Papers about stationary application of batteries and/or hydrogen-based power-to-power (P2P) systems, in which H_2 is stored and consumed onsite, in order to produce, through fuel cells, the electricity needed by the load when the RES can't supply enough energy, are the most relevant in the framework of this thesis. They involve different type of RES (wind turbines, PV panels, hydroelectric converters,…) sometimes integrated with diesel generators or electricity connections to the grid, various sizes (from the load of one small house to the energy supply of entire remote villages and islands), disparate locations around the world, assorted technologies and several analysis approaches (environmental impacts via LCA, costs, technical feasibility, reliability, sizing, optimization models, management strategies, energy and exergy efficiencies,…).

A list of papers, presenting case studies in which the RES storage is provided by the only stationary application of batteries, is here reported: [46], [47], [48], [49], [50], [78], [89], [95], [117], [123], [124], [51]. The following list of studies involves instead H_2-based P2P RES storage systems (with also the contribution of batteries in some cases): [52], [53], [54], [55], [56], [57], [58], [59], [60], [61], [62], [63], [64], [65], [66], [67], [68], [69], [70], [71], [72], [77], [79], [81], [83]. In particular, some papers (such as [84], [85], [91], [93], [97], [98] and [99]) examine and compare the two RES storage technologies (battery and hydrogen systems), evaluating different scenarios, including battery only, hydrogen P2P storage only and the hybrid storage case (H_2 and battery together). Even if, from a commercial point of view, hydrogen-based power systems seem to be more expensive than Li-ion batteries, they present lower environmental impacts according to [91] and [93]. Moreover, some of the cited papers assess that the hybrid storage technology, with the simultaneous presence of batteries (efficient for short-term time intervals) and hydrogen systems (more cost-effective for long-term storage) [97], is a very adequate, reliable [98] and efficient solution from the economic [84] [85] and environmental point of views, enabling the increase of sustainability and energy independency of small islands and the decarbonization of energy sectors, such as transports [99].

Among the papers investigating hydrogen-based power-to-power (P2P) storage systems, a few of them perform an LCA analysis ([66], [69], [61], [63], [91], [93], [99], [55]), but none of them presents the LCA results of such RES storage systems located in a remote island, comparing the final environmental impacts with the ones caused by alternative scenarios, such the ones previously assessed in this thesis. Then, according to our knowledge, the present thesis is one of the first studies assessing the environmental impacts (through an LCA analysis) of an hybrid battery and hydrogen-based P2P storage system for the energy supply of remote areas almost totally relying on RES (wind and PV), in comparison with an electricity transmission case (using submarine cables), with a fossil fuel scenario, in which the electricity is provided by on-site diesel generators, and with further additional scenarios.

3 Description of the case study

3.1 Froan Islands

The site of Froan Islands is located in a harsh environment off the west coast of Norway at about the 64th North parallel, almost the same latitude of Trondheim, and it takes about 20 minutes by boat from the mainland (Figure 3-1). It consists of several islands on which there are 20 houses, a fish farm and 40-50 weekend cottages. The remaining fish farm and the summer tourists are the main source of income and the onsite electricity consumption is also mainly related to the high occupancy of tourists during the summer and to the heating and lighting in winter time. The islands are a nature reserve and conservation area since 1979 (Ramsar area since 2003), to protect the flora and fauna and conserve living and nesting areas for birds, seals etc. in the distinctive coastal land-scape [23] [21] [24].

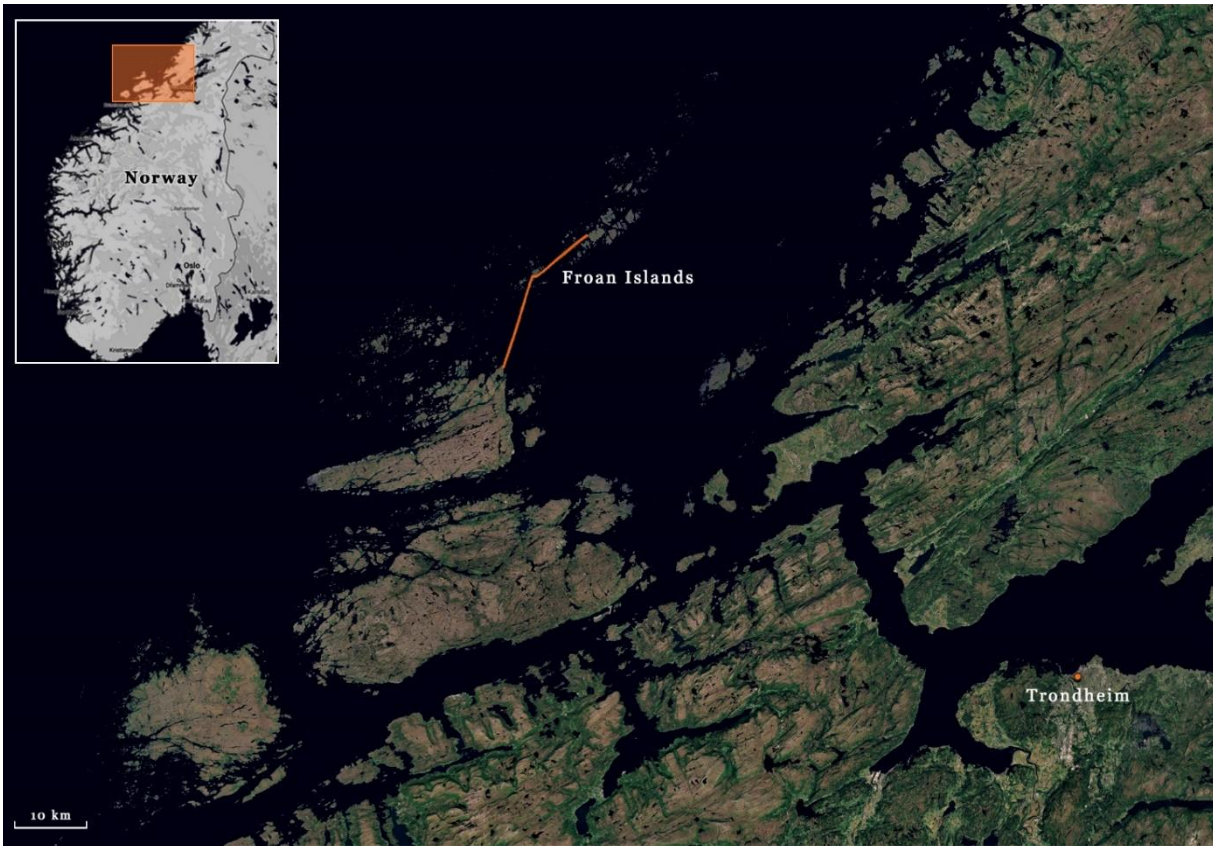

Figure 3-1: Localization of the Froan Islands in the map of Norway.

3.2 Current and future scenarios

Today, the site is interconnected by electric grid with a connection of about 23.4 km to the mainland composed of two outdated sea cables, owned by TrønderEnergi Nett AS, which are estimated to last for about 3 years, creating a sense of urgency to find and evaluate alternative solutions. The immediate solution would be to replace the sea cables, but the too high cost and the invasive replacement require finding alternative solutions. The easiest alternative option could be the installation onsite of diesel generators. However, the related polluting issues, the cost related to the transportation of the fuel and the status of the islands being natural reserve seem to make this choice impracticable [23] [21] [24].

The solution proposed by the Remote project, instead, aims at a local and renewable production of energy through the installation, on the Froan Islands, of a RES plant without any connection with the mainland and with a microgrid RES production higher than 95%. Due to the dark Norwegian winter months, the occasional consecutive days without wind, the natural intermittence of renewable sources and the variable demand over days, weeks and seasons, a storage system is also needed to make this option totally self-sustainable. Therefore, the examined plant consists of PV panels and wind turbines to generate the energy and a hybrid storage system where a bank of batteries is coupled with a non-integrated P2G+G2P system including an electrolyser (by Hydrogenics), a storage tank (by Powidian) and a fuel cell (by Ballard Power Systems Europe A/S). A diesel generator is also required occasionally (less than 5%). The production and consumption of energy are regulated by the Energy Management system (by Powidian). It communicates, in real time, with each subsystem, analysing, managing and monitoring (also with satellite links) every component and physical quantity, in order to create a fully integrated system, known as SAGES (Smart Autonomous Green Energy Station). In particular, the secured data connection is provided with a cybersecurity software developed with the help of Airbus Defence & Space, in order to avoid the risk of hacking. Moreover, in case of plant functioning alarms, the possible remote control of the system can help the diagnostic assistance, facilitating or avoiding onsite maintenance and visits. Diagnosis and prognosis algorithms assess the state of health and the Remaining Useful Life (RUL) of each component in order to optimize their maintenance and lifetime, while predictive algorithms, based on weather-based renewable power forecasts and self-learning load profiling, are also used to optimize the management strategy of power, energy and storage, in order to offer a reliable, safe and best performance solution. When the energy produced by the PV panels and the wind turbines is enough, the plant supplies directly the load through the AC bus of the internal grid. If it is in excess, it is stored or curtailed when the maximum capacity of storage is reached. The surplus energy first charges the battery bank and, once totally charged, it produces hydrogen thanks to the electrolyser. In case of lack of RES to supply user's needs, the short-term and quick-response storage of the battery bank maintains stability and power conditions in the microgrid (frequency and voltage) and meanwhile the fuel cell starts to supply the load. Thanks to the battery bank, the fuel cell and the electrolyser can always operate at the nominal point of efficiency avoiding also abrupt starts and stops of the hydrogen chain. The hydrogen system, instead, acts as longer-term storage of energy. The explained non-integrated P2P solution enables the optimized utilization of local RES, ensuring the supply all year round and the almost total independency from shipped-in fossil fuels and diesel generators. This would mean a significant reduction of polluting emissions (in particular CO_2 emissions), a decreased impact to the fragile wildlife and plants on the islands and the no more necessity of submarine cables, avoiding large investments for TrønderEnergi Nett AS. The onsite renewable production of electricity would determine also a reduction of its local cost. Moreover, this solution might open to future possibilities of using the oxygen produced by the electrolyser for fish farming and of exploiting the excess RES energy for other purposes besides the storage system, such as hydrogen for mobility. More generally, the Remote project offers the huge opportunity to develop and demonstrate a medium power SAGES and a cost-effective hydrogen-based energy storage system in a North European site, facing the specific challenges of a remote location with harsh environment and very high requirements in renewable energy utilisation. This would enable the possible replicability of this hydrogen concept on some of the other populated Norwegian and North European islands having similar challenges [23] [21] [24].

The proposed isolated microgrid plant of the Remote project is here considered as the base case and it is compared with two further scenarios. One in which the sea cables are substituted (Cable scenario) and one in which diesel generators are installed to cover the load (Diesel scenario). Additional scenarios are also considered, modifying some relevant parameters, such as the contribution of diesel generators in the Remote plant, the submarine cables length and the carbon intensity of the mainland electricity, in order to evaluate their relative impacts to the total GWI.

4 Environmental analysis

4.1 Methodology

In this thesis, an environmental analysis of the different scenarios is carried on in terms of global warming impact (GWI), in particular in terms of CO_2 equivalent with time horizon of 100 years. The CO_2 equivalent emission represents “the amount of carbon dioxide emission that would cause the same integrated radiative forcing, over a given time horizon, as an emitted amount of a greenhouse gas (GHG) or a mixture of GHGs” and they are obtained multiplying the GHG emission by its Global Warming Potential (GWP) for the given time horizon [100]. The GWP is “an index measuring the radiative forcing following an emission of a unit mass of a given substance, accumulated over a chosen time horizon, relative to that of the reference substance, carbon dioxide (CO_2)”, representing then the combined effect of their effectiveness in causing radiative forcing and their remaining time in the atmosphere [100]. Among the several possibilities, we choose the cited emissions metric and time horizon, since the 100-year GWP (GWP100) was also adopted by the United Nations Framework Convention on Climate Change (UNFCCC) and its Kyoto Protocol and it is now widely used as a common scale for comparing GHG emissions [2] [100]. All the papers mentioned in this environmental analysis use this default metric and the specification about the time horizon will be omitted from now on. Moreover, the environmental analysis carried on, including all the studies and paper mentioned and all the data used, follows a Life Cycle Assessment (LCA) philosophy, organization and methodology in order to implement a life cycle thinking approach. The LCA is an objective and systematic technique for a quantitative evaluation of energy and environmental loads related to a process or activity, carried out by identifying energy and materials used and waste released into the environment. LCA studies the environmental aspects and potential impacts throughout the entire life cycle of the process or activity (cradle-to-grave), including extraction and processing of raw materials, manufacture, transport, distribution, use, reuse, recycling and final disposal. The International Standards Organization (ISO) has also defined and adopted standards that provide references for the correct application of LCA analysis, the UNI EN ISO 14040: 2006 [104] and UNI EN ISO 14044: 2006 [105].

According to [104] and [105], a rigorous LCA study is divided into four main phases, here briefly described:

- Goal and scope definition: in this phase, the context, the reasons, the investigated product, the system boundaries, the data sources, the assumptions and the functional unit are described and defined. The functional unit is the reference unit for all the LCA process.

- Life Cycle Inventory (LCI): it is an inventory analysis of the input/output data with regard to the studied system, involving data collection (about for example energy and raw materials requirements, releases to air, water and land during the life cycle…) and calculation procedures necessary to meet the goal of the defined study.
- Life Cycle Impact Assessment (LCIA): this phase aims at evaluating the extent of potential environmental impacts using LCI results. In general, the inventory data are associated with specific environmental impact categories and class indicators.
- Life Cycle Interpretation: it is the final phase of the LCA procedure, in which the LCI/LCIA results are summarized, interpreted, evaluated and discussed as a basis for conclusions, recommendations and decision-making, in a unifying presentation of results in accordance to the goal and scope definition.

The present environmental analysis is mainly based on data found in literature and it is divided in similar parts. In the first part, the objective, the general boundaries and the functional unit are described. Then, for each scenario and for each component or subsystem, the data sources, the assumptions, the specific boundaries and the inventory of all the data needed will be defined, in order to evaluate the potential environmental impacts. Lastly, a comparation of the results and the analysis of additional scenarios will be presented as a basis for the final conclusions.

4.1.1 Goal and scope definition

The goal of this environmental analysis is to evaluate and compare the global warming impact, in terms of CO_2-equivalents with time horizon of 100 years (CO_2eq), related to the Remote plant designed for the Froan Islands and based on Renewable Energy Sources (RES), in comparison with the GWI of alternative scenarios, such as the Cable and Diesel scenarios. The study is performed aiming at considering the entire life cycle of the plant, cradle-to-grave, including extraction and processing of raw materials, manufacture, installation, use, recycling and final disposal. Transports are not considered because of the lack of data about the actual location of the industries that have in charge the manufacture of the different components. However, transports would have a small contribution to the final result and they are negligible. Moreover, the final results without transport would be more general and applicable to similar cases in different locations. Regarding the other steps of the life cycle, the specific boundaries are defined for each component in the next sections. Concerning the physical boundary, it is fixed before the distribution of the electricity through the islands, so at the exit of the electricity produced by the RES plant or by the diesel generators and at the arrival on the Froan Islands of the electricity of the sea cable. The distribution is not considered since it is in common with the different scenarios. Since the function of the plant is to generate electricity and considering also the chosen physical boundary, we report the results based on the electricity produced in Froan or supplied by the submarine cable. The functional unit considered is the kg of CO_2eq emitted referred to 1 MWh generated or supplied by the sea cable. In order to compare the different scenarios, results are expressed in the same functional unit. Figure 4-1 (modified from [21]) sums up the general physical system boundaries for the three scenarios.

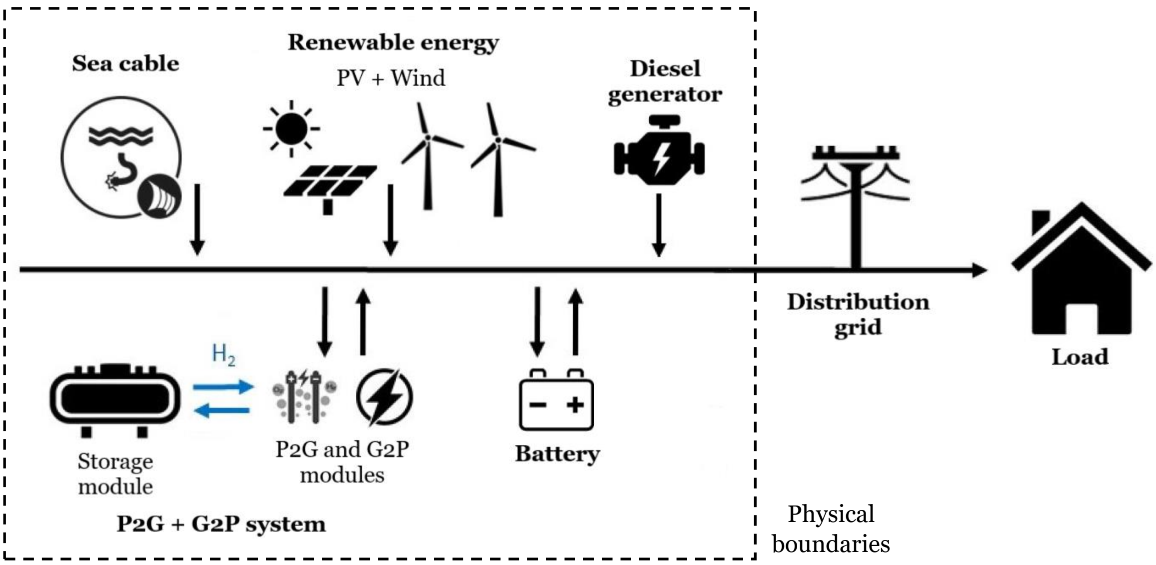

Figure 4-1: General LCA physical system boundaries for the different scenarios [21].

4.2 Remote scenario

A scheme of the renewable base case with qualitative energy and mass exchanges is shown in Figure 4-2, taken and modified from [24].

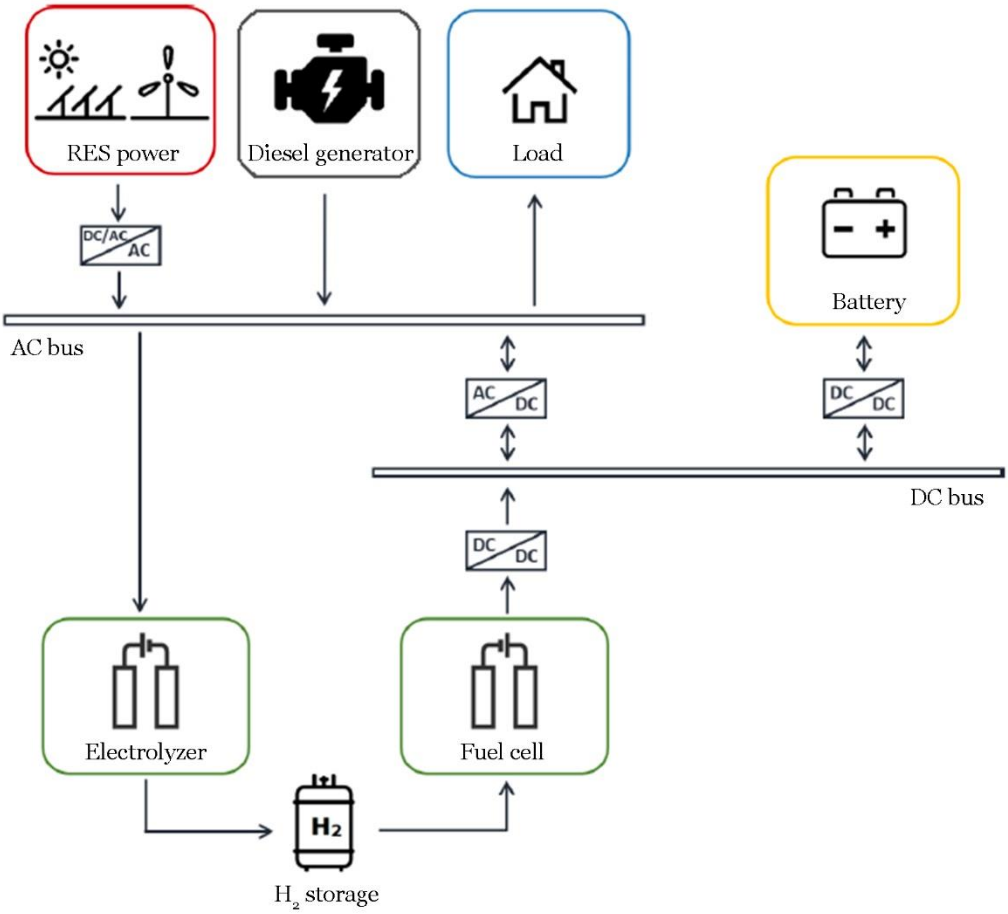

Figure 4-2: Scheme of the components and qualitative energy and mass exchanges in the Remote scenario [24].

A 2 years simulation of the RES plant has been made during the Remote project in order to evaluate the exact energy and mass exchanges between the components and the load. Assuming that the energy derived from RES is the 95% of the total energy needed by the load, a 5% of energy supplied by the diesel generator is added. The values of these exchanges are shown in the following tables (Table 4-1, Table 4-2, Table 4-3, Table 4-4).

Table 4-1: Annual energy exchanges of the PV pannels.

PV pannels				
Total energy delivered	Energy to load	Energy to storage	Energy curtailed	Energy delivered and curtailed
MWh/y	*MWh/y*	*MWh/y*	*MWh/y*	*MWh/y*
104.999	58.701	46.298	90.472	195.471

Table 4-2: Annual energy exchanges of the wind turbines.

Wind turbines				
Total energy delivered	Energy to load	Energy to storage	Energy curtailed	Energy delivered and curtailed
MWh/y	*MWh/y*	*MWh/y*	*MWh/y*	*MWh/y*
523.926	263.695	260.231	790.580	1,314.506

Table 4-3: Annual energy and mass exchanges of the water ELY, the FC, the battery and the diesel generators.

Water Electrolyzer			**Fuel cell**			**Battery**		**Diesel generators**
Energy from RES	H_2 to storage	Heat lost	H_2 from storage	Energy to load	Heat lost	Energy from RES	Energy to load	Energy to load
MWh/y	*kg/y*	*MWh/y*	*kg/y*	*MWh/y*	*MWh/y*	*MWh/y*	*MWh/y*	*MWh/y*
105.602	1,920.029	21.120	1,920.029	35.165	19.200	200.923	185.171	28.565

Table 4-4: Annual energy exchanges of the load of Froan Islands.

Load Froan				
Energy directly from RES	Energy from storage	Energy from RES plant	Energy from Diesel generator	Total energy to load
MWh/y	*MWh/y*	*MWh/y*	*MWh/y*	*MWh/y*
322.396	220.336	542.733	28.565	571.297

The assumed lifetime of the plant is 25 years. Then, we can calculate the total energy provided and the total hydrogen produced (Table 4-5, Table 4-6, Table 4-7, Table 4-8).

Table 4-5: Total energy exchanges of the PV pannels.

PV pannels				
Total energy delivered	Energy to load	Energy to storage	Energy curtailed	Energy delivered and curtailed
MWh	*MWh*	*MWh*	*MWh*	*MWh*
2,624.978	1,467.518	1,157.460	2,261.797	4,886.775

Table 4-6: Total energy exchanges of the wind turbines.

Wind turbines				
Total energy delivered	Energy to load	Energy to storage	Energy curtailed	Energy delivered and curtailed
MWh	*MWh*	*MWh*	*MWh*	*MWh*
13,098.150	6,592.387	6,505.763	19,764.500	32,862.650

Table 4-7: Total energy and mass exchanges of the water ELY, the FC, the battery and the diesel generators.

Water Electrolyzer			Fuel cell			Battery		Diesel generators
Energy from RES	H_2 to storage	Heat lost	H_2 from storage	Energy to load	Heat lost	Energy from RES	Energy to load	Energy to load
MWh	*kg*	*MWh*	*kg*	*MWh*	*MWh*	*MWh*	*MWh*	*MWh*
2,640.040	48,000.726	528.008	48,000.726	879.133	480.007	5,023.087	4,629.277	714.122

Table 4-8: Total energy exchanges of the load of Froan Islands.

Load Froan				
Energy directly from RES	Energy from storage	Energy from RES plant	Energy from Diesel generator	Total energy to load
MWh	*MWh*	*MWh*	*MWh*	*MWh*
8,059.904	5,508.410	13,568.315	714.122	14,282.437

A detailed analysis for each component is now presented.

4.2.1 PV panels

4.2.1.1 Remote plant characteristics

One of the renewable energy sources of our plant is the photovoltaic conversion from the solar energy. A PV plant ground-mounted of 250 kW is considered. It has to produce a total energy of about 195.5 MWh/y of which 90.5 MWh/y are curtailed and 105 MWh/y are delivered directly to the load (58.7 MWh/y) and to the storage system (46.3 MWh/y). Due to the lack of knowledge about the precise technology used, we assume to use the PV panels already chosen for a different demo case present in the Remote project, the LG NeON® R solar module LG365Q1C-A5, provided by LG Electronics USA [108]. In Table 4-9 the main characteristics are summarized.

Table 4-9: Main characteristics of the LG NeON® R solar module LG365Q1C-A5, LG Electronics USA [108].

Number of cells	Cell type	Panel dimensions	Weight	Product warranty	Module efficiency	Maximum power NOCT
-	-	*mm*	*kg*	*years*	*%*	*W*
6 x 10	Monocrystalline Si/ N-type	1700 x 1016 x 40	18.5	25	21.1	275

The degradation of the performances with time are not considered and we are only interested in the dimension of the plant installed in order to reach the designed peak power of 250 kW in NOCT conditions. Knowing the total power needed and the power and dimensions of each module, the total number of them and the total area can be calculated (Table 4-10).

Table 4-10: Capacity and dimensions of the PV plant in the Remote scenario.

PV plant power capacity	Maximum power NOCT	Number of modules	Area of modules	PV total area
kW	*W/module*	-	$m^2/module$	m^2
250	275	910	1.7272	1,571.75

The estimated production is then calculated multiplying the total area by the module efficiency, the Performance Ratio (PR), set at the default value of 0.75, and the local average solar irradiation given in the Froan data specifications. A check between the simulated yearly productivity and the estimated one shows that the area is enough (Table 4-11).

Table 4-11: Check between the simulated yearly productivity and the estimated one.

PV total area	Module efficiency	PR	Yearly average horizontal solar irradiation	Simulated PV production	Estimated PV production
m^2	*%*	-	*$kWh/m^2/year$*	*MWh/y*	*MWh/y*
1,571.752	21.1	0.75	869.6125	195.471	216.299

4.2.1.2 LCI from literature

A lot of studies have already assessed the environmental impact of different technologies and installations of PV panels. Some of them focus on PV panels building integrated ([27], [35]) or mounted on a rooftop [123], others consider technologies such as polycrystalline Si ([28], [109], [110]) or thin-film amorphous Si [35]. In the studies [47], [82], [111] and [110] ground-mounted monocrystalline Si PV panels are presented.

In particular, the study [82], not only it has the right type of technology and installation, but it is also the most recent (2018), the most similar in term of size and it has the most suitable data needed. The aim of the study is to compare the potential environmental impact of a small-scale PV plant with a small-scale hybrid solar-gas turbine system. We are interested in the part regarding the 100 kW_p PV plant composed by single-crystalline silicon panel mounted on ground and situated in Almeria, Spain. The general characteristics are summarized in Table 4-12. The total panel active surface is quantified in 653 m^2 with an efficiency of 14% and a Performance Ratio set at the default value of 0.75. The potential emissions of the plant are calculated throughout its lifetime of 30 years where the degradation of performance of the PV modules is not considered. The plant produces about 4784 MWh during its lifetime.

Table 4-12: General characteristics of the PV plant presented in paper [82].

Source	Year	Lifetime	PV technology	Efficiency	Size (power)	Size (area)	Total lifetime production
-	-	*years*	-	*%*	*kW*	*m^2*	*MWh*
82	2018	30	single-crystalline Si mounted on the ground	14	100	653	4,784.003

For this study, the boundaries are specified for a complete cradle-to-grave LCA. This includes the acquisition of raw materials, manufacturing processes and transport, in addition to construction, operation, maintenance and end of life phases. In particular, the amount of material for the mounting system and the electricity consumption required for its installation have been taken into account. The construction, transports (only those from the place of production of the components to the plant site), installation, maintenance (cleaning of panels) and disposal of the plant components, and in particular of photovoltaic panels and inverters, are also part of the analysis. In particular, the inverter is necessary for transforming the direct current produced by solar cells to alternating current and, since its lifetime is assumed to be 15 years, it must be changed once during the lifetime of the plant. This study does not consider all the components (cabling, power electronics, transformer etc.) required for the connection of the plants to the local electricity grids, since they are the same or significantly similar in terms of size and power required for both plants and can be omitted from the comparison. Moreover, the electrical and electronic components of the tracking system are omitted because of the lack of data. With reference to end of life phase, if materials are sent to a landfill, the impacts associated with disposal are accounted for; if they are sent to recycling, impacts are not included since the recycling phase is considered as counted in the product system to which the secondary raw material is intended. According to the boundaries assumed for our environmental analysis, the share of the impacts caused by transports is removed. Regarding the end of phase, because of the lack of specific and diversified data about the dismantling, the end-of-life operations and the landfill or recycling path, the materials are assumed to be sent to a landfill, as the study [82] does. In the following Table 4-13, the steps taken into account and the result of the study are presented.

Table 4-13: Resulting GHG emissions of study [82] and relative impact percentages of each LCA phase.

Steps taken into account in the LCA of [82]						Total GHG emissions rate	Total GHG emissions rate without transport
Extraction of raw materials	Manufacture of PV and components	Installation on site	Maintenance and electricity use and production	Transport	End of life treatments	*$kgCO_2eq/MWh$ delivered*	*$kgCO_2eq/MWh$ delivered*
90%	3.50%	1.50%	0.50%	3.50%	1%	43	41.495

Figure 4-3, modified from [82], summarizes the boundaries of the PV system LCA. The use phase contains also the installation on site and the maintenance.

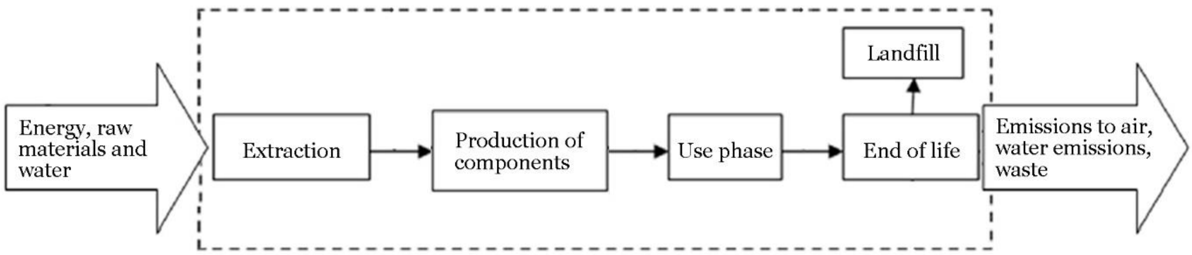

Figure 4-3: LCA boundaries of the PV system [82].

Knowing the kg of CO_2eq for each MWh produced and the total energy produced in paper [82], we can calculate the total amount of carbon dioxide emitted and the $kgCO_2$eq for each m^2 of PV panels (Table 4-14).

Table 4-14: GHG emissions per installed area of PV panels from the results of paper [82].

Total GHG emissions rate considered	Total lifetime production	Total GHG emissions	GHG emissions per area installed
$kgCO_2eq/MWh$ delivered	*MWh*	*$kgCO_2eq$*	*$kgCO_2eq/m^2$*
41.495	4,784.003	198,512.190	304.000

Multiplying this last value by the total area of the PV panels of our analysis, the total mass of CO_2eq emitted can be obtained and, dividing the total mass by the total energy produced by the Remote plant, the result expressed in functional unit is found (Table 4-15).

Table 4-15: Total GHG emissions rate (in functional unit) of the PV panels in the Remote scenario.

GHG emissions per area installed [82]	PV total area	Total GHG emissions	Total energy production	Total GHG emissions rate
$kgCO_2eq/m^2$	*m^2*	*$kgCO_2eq$*	*MWh*	*$kgCO_2eq/MWh$*
304.000	1,571.752	477,813.066	14,282.437	**33.455**

4.2.1.3 Comparison of the results with the literature

In order to verify and compare the result obtained with the literature, it can be also calculated the mass of CO_2eq normalized for each MWh produced by the PV panels only, both in the case of real production both in the case of ideal production with no curtailments (Table 4-16).

Table 4-16: Real and ideal GHG emissions rate per MWh delivered by the PV panels in the Remote scenario.

PV total energy delivered	PV real GHG emissions rate	PV total energy delivered and curtailed	PV ideal GHG emissions rate
MWh	*$kgCO_2eq/MWh$ delivered by PV*	*MWh*	*$kgCO_2eq/MWh$ deliverable by PV*
2,624.978	182.026	4,886.775	97.777

In literature various reviews on LCA results of photovoltaic systems can be found, such as studies [112], [113], [114] and [101], of which paper [101] is the most recent (2018). It reviews and analyses LCA studies on solar PV technologies, such as silicon and thin film, and it summarizes three impact assessment methods, namely, cumulative energy demand (CED), energy payback time (EPBT), and GHG emissions rate, based on data and information published in the literature. The findings of [101] are summarized in Table 4-17. The large range is due to several factors, such as local energy mix in manufacturing phase, different solar irradiations of the installation location and lifetime of PV plant.

Table 4-17: Ranges of CED, EPBT and GHG emissions of different PV technologies from [101].

Source	Type of solar PV technology	Range of CED	Range of EPBT	Range of GHG emissions
-	-	MJ/m^2	*years*	$gCO_2 eq/kWh$
101	Mono-Si	1123 - 8050	1.4 - 7.3	29.0 - 671.0
	Multi-Si	1034 - 5150	0.8 - 4.17	12.1 - 569.0
	a-Si	862 - 1731	1.1 - 3.2	8.1 - 57.0
	CdTe	811 - 1803	0.79 - 2.7	8.9 - 66.0
	CIS	1105 - 1684	1.3 - 2.8	33.0 - 95.0
	DsC	277 - 365	0.6 - 1.8	9.8 - 25.0
	Perovskite	379 - 821	0.2 - 5.4	56.65 - 497.2
	Quantum dot	370 - 1030	0.9 - 1.51	2.89 - 5.0

The values found in our analysis, both in case of real (182.026 gCO_2eq/kWh) and ideal (97.777 gCO_2eq/kWh) production, are in the range of GHG emissions reported by [101] for the monocrystalline-Si technology.

4.2.2 Wind turbines

4.2.2.1 Remote plant characteristics

The other RES of the Froan plant is the wind energy. Three wind turbines of 225 kW are installed in the plant for a total power capacity of 675 kW. According to the simulation they will produce a total amount of about 1314.5 MWh/y, of which 790.5 MWh/y will be curtailed and 524 MWh/y will be delivered to the load (263.7 MWh/y) and to the storage system (260.3 MWh/y). The onshore Vestas V27 is the selected wind turbine having a gearbox and an assumed lifetime of 25 years as the plant. The specific characteristics, taken from the datasheet [115], are summarized in Table 4-18.

Table 4-18: Main characteristics of the onshore WT Vestas V27 [115].

Rated power	Number of blades	Rotor diameter	Swept Area	Hub height	Average total weight	Cut-in wind speed	Rated wind speed	Cut-off wind speed
kW	-	*m*	m^2	*m*	*kg*	*m/s*	*m/s*	*m/s*
225	3	27	572.6	33.5	21,300	3.5	14	25

4.2.2.2 LCI from literature

In literature, a lot of studies have already performed an LCA on wind turbines of different sizes and hub heights (the height of the nacelle). Among the various studies found ([33], [27], [28], [35], [80], [116]), the paper [80] is the most recent (2013) and it offers a sensitivity analysis based on different sizes and hub heights. The objective of this study is to investigate, evaluate and compare the environmental effects of three medium scale (330 kW, 500 kW, 810 kW) and two large scale (2050 kW, 3020 kW) wind turbines with the hub heights of 50 m, 80 m and 100 m installed in Pınarbaşı-Kayseri (Turkey) using life cycle assessment methodology. We are interested in the medium scale turbines since they have the same order of magnitude of the characteristics of Vestas V27. The LCA of the selected wind turbines contains their whole lifespan: raw materials extraction, manufacturing, transport of all components, site erection and crane operations, wind turbine operation, maintenance, decommissioning and recycling stages (according to past studies cited in [80] and some other assumptions). The manufacturing and assembly stage includes the foundation (concrete, steel and iron) and the fuel consumption related to its construction, the tower (steel, aluminum, plastic, copper, paint), the nacelle (steel, copper, aluminum) that is a combination of the bedplate, frame, nacelle cover, generator, main shaft and gearbox, the rotor (steel, fiberglass, epoxy/resin) that includes blades, hub, nose cone and bolts, the cables for internal connections and connection to the grid and finally any other component (assumed to be composed of aluminum, copper, plastic and steel). Since the lifespan of the wind turbines is assumed to be 20 years, gearboxes are supposed to be replaced once during the operation. For the maintenance, distances and used materials are considered and the turbines are assumed to be inspected twice a year. Regarding the end of life scenario, the assumptions made in the paper [80] are here reported: 90% of all metals are recycled, 10% goes to the landfill, recycling process is performed 250 km away from the wind turbine site while concrete, plastics and other materials are land filled only 150 km away, recycled materials are used as raw materials to produce new wind turbines. Contributions due to the transports can't be removed because of the lack of specific data, however they have little impact on the total emissions. The scheme presented in Figure 4-4, taken from [80], summarizes the system boundaries considered in this analysis.

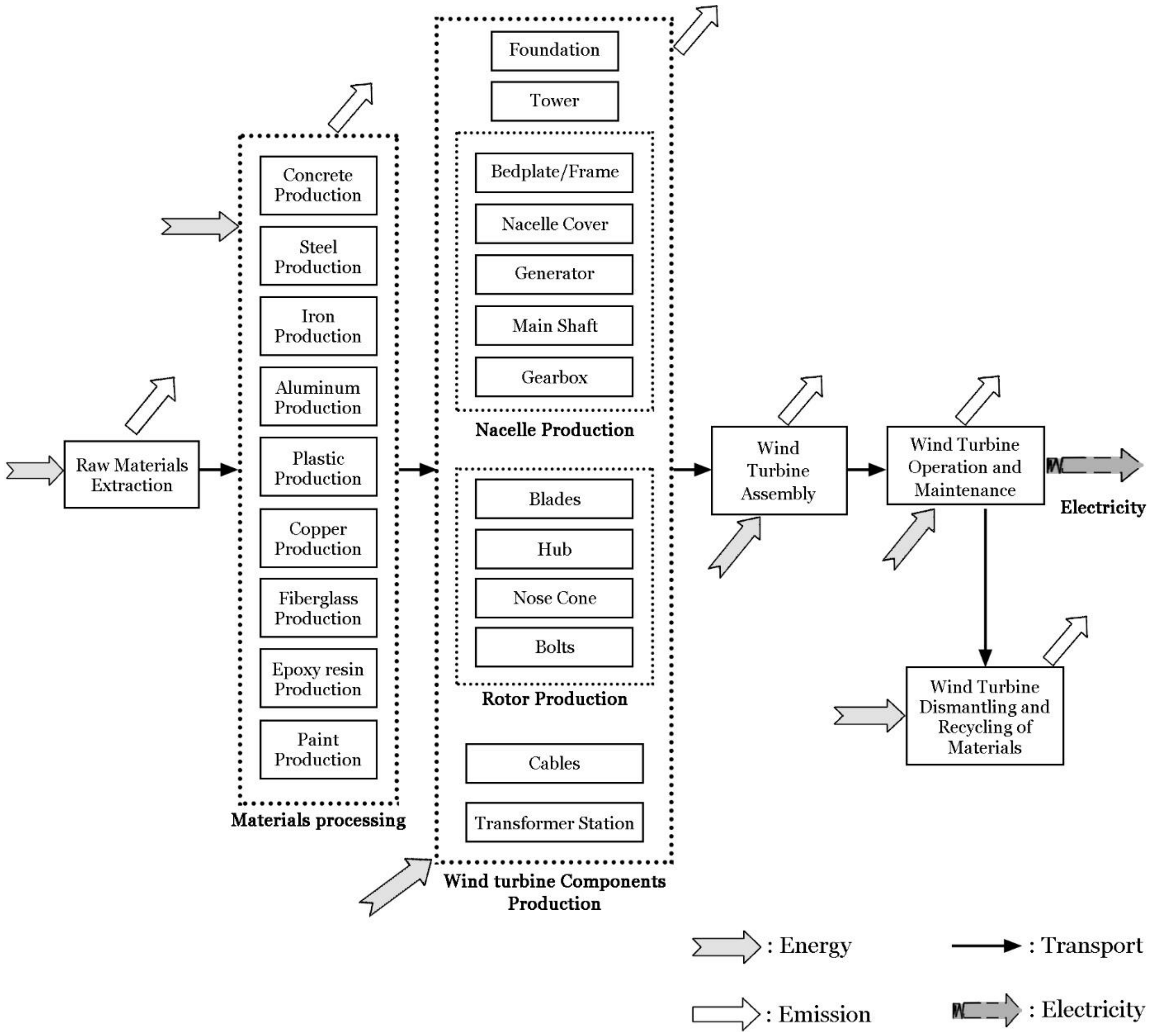

Figure 4-4: LCA boundaries of the WT system [80].

In the following Table 4-19, for each size and hub height studied, the more important results are presented, such as the GHG emissions for each MWh produced, the total energy and the total CO_2eq produced during the lifetime (20 years) and the CO_2eq emitted for each kW of wind power capacity.

Table 4-19: GHG emissions resulting from study [80] for different WTs.

Source	Size	WT Hub height	Rotor diameter	Swept area	Total energy produced	GHG emissions per energy produced	Total GHG emissions	GHG emissions per WT capacity
-	*kW*	*m*	*m*	m^2	*MWh*	$kgCO_2eq/MWh$	$kgCO_2eq$	$kgCO_2eq/kW$
80	330	50	33	876	9,420	40.36	380,191.2	1,152.095
	500	50	48	1,560	13,860	38.96	539,985.6	1,079.971
	810	50	53	2,198	23,600	26.57	627,052.0	774.138
	330	80	33	876	12,160	36.46	443,353.6	1,343.496
	500	80	48	1,560	18,060	32.01	578,100.6	1,156.201
	810	80	53	2,198	30,200	21.66	654,132.0	807.570
	330	100	33	876	14,920	33.96	506,683.2	1,535.404
	500	100	48	1,560	20,200	29.97	605,394.0	1,210.788
	810	100	53	2,198	33,400	20.41	681,694.0	841.598

Regarding the total mass of CO_2eq, the value for the wind turbine V27 (225 kW of capacity and 33.5 m of hub height) can be derived from the data of the other turbines. Plotting the curves showing the emissions of CO_2eq in function of the hub height and of the WT capacity, according to the results of [80], and using polynomial (second order) trend curves and equations, we can find the approximated values of the emitted mass of CO_2eq for our case. Curves, equations and the results are shown in the following tables (Table 4-20, Table 4-21) and figures (Figure 4-5, Figure 4-6).

Table 4-20: GHG emissions in function of hub heights and WT capacities, calculated from [80].

Total GHG emissions [kgCO$_2$eq]				
	Hub height [m]			
WT capacity [kW]	33.5	50	80	100
225	226752.481	241853.313	327198.313	425592.938
330	361733.707	380191.200	443353.600	506683.200
500	520468.596	539985.600	578100.600	605394.000
810	619453.229	627052.000	654132.000	681694.000

Table 4-21: GHG emissions in function of WT capacities and hub heights, calculated from [80].

Total GHG emissions [kgCO$_2$eq]				
	WT capacity [kW]			
Hub height [m]	225	330	500	810
33.5	226730.938	361733.707	520468.596	619453.229
50	241853.313	380191.200	539985.600	627052.000
80	327198.313	443353.600	578100.600	654132.000
100	425592.938	506683.200	605394.000	681694.000

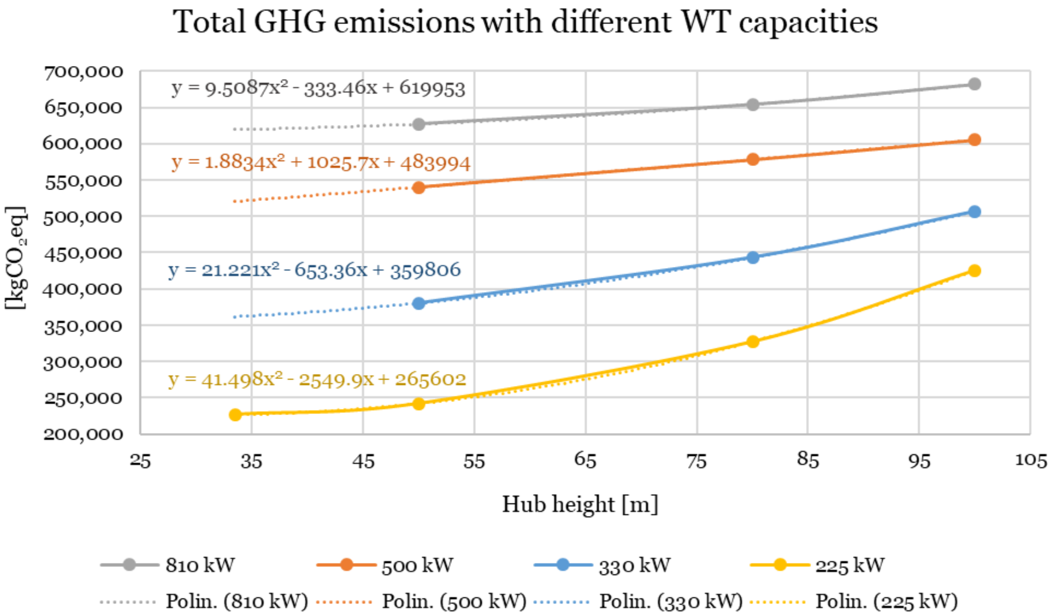

Figure 4-5: GHG emissions in function of hub heights and WT capacities, calculated from [80].

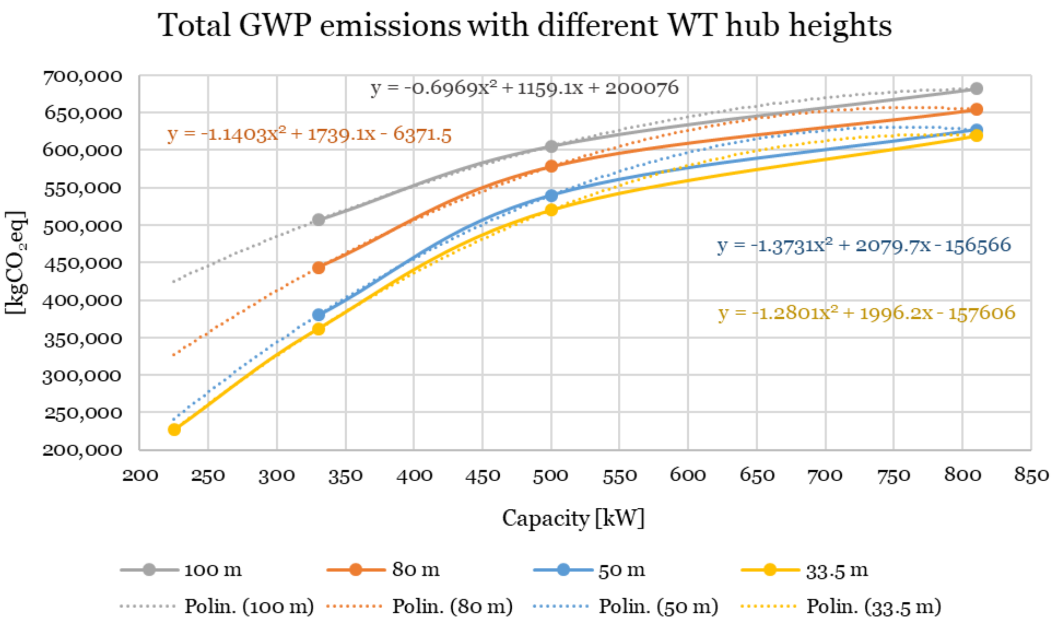

Figure 4-6: GHG emissions in function of WT capacities and hub heights, calculated from [80].

We calculate the arithmetic mean value of the two values orange-highlighted (present in Table 4-20 and Table 4-21) and we found the value of the total mass of CO_2eq assumed to be emitted from the lifecycle of the V27 wind turbine. Dividing the result by the capacity of 225 kW, the CO_2eq emitted for each kW of capacity can be also calculated to verify that it is similar to the other values of the study [80]. Since we have three turbines, the total mass of CO_2eq is tripled and then normalized by the kWh produced by the Remote plant (Table 4-22).

Table 4-22: Total GHG emissions rate (in functional unit) of the WTs in the Remote scenario.

Total GHG emissions of 1 WT	GHG emissions per WT capacity	Total GHG emissions of 3 WT	Total energy production	Total GHG emissions rate
$kgCO_2eq$	*$kgCO_2eq/kW$*	*$kgCO_2eq$*	*MWh*	*$kgCO_2eq/MWh$*
226,741.709	1,007.741	680,225.127	14,282.437	**47.627**

4.2.2.3 Comparison of the results with the literature

In order to compare the results with the literature, the total CO_2eq can be normalized by the energy produced only by the wind turbines (both in case of real production and in case no curtailment occurs), as we can see in Table 4-23.

Table 4-23: Real and ideal GHG emissions rate per MWh delivered by the WTs in the Remote scenario.

WT total energy delivered	WT real GHG emissions rate	WT total energy delivered and curtailed	WT ideal GHG emissions rate
MWh	*$kgCO_2eq/MWh$ delivered by WT*	*MWh*	*$kgCO_2eq/MWh$ deliverable by WT*
13,098.150	51.933	32,862.650	20.699

Various ranges of CO_2eq emitted for each kWh produced can be found in literature. Paper [80] presents both the range of its results and the one taken from previous studies [102] and [103], concerning the general wind energy production systems. Moreover, papers [149] and [150] present a review of LCA GHG emissions of wind power generation systems, based on previously published studies. The different ranges are shown in Table 4-24.

Table 4-24: Ranges of LCA GHG emissions of WTs systems from different papers.

Sources	Range of GHG emissions
-	*$kgCO_2eq/MWh$*
80	15.1 - 38.3
80 - 102 - 103	9.7 - 123.7
149	1.7 - 81
150	4.6 - 55.4

According to these ranges, it can be seen that the resulting emissions of our case are acceptable, both in case of real (51.933 $kgCO_2eq/MWh$) and ideal (20.699 $kgCO_2eq/MWh$) production.

4.2.3 Battery

4.2.3.1 Remote plant characteristics

The battery is a very important component of our plant, crucial for the short-term and quick-response storage. A bank of 5 Lithium-ion (Li-ion) batteries with a capacity of 110 kWh, an efficiency of 96.00% and a State of Charge (SOC) between 20% and 90% is considered. Table 4-25 resumes the main characteristics. They should store about 200 MWh/y and they will provide to the load about 185 MWh/y.

Table 4-25: Characteristics of the Remote battery system.

Technology	Number of batteries	Capacity of each battery	Efficiency	SOC
-	-	*kWh*	*%*	*%*
Li-ion	5	110	96	20 - 90

4.2.3.2 LCI from literature

A lot of studies have been already carried on about the LCA of batteries. Among the various paper found in literature ([118], [73], [74], [75], [120], [78], [121]), the study [74] is the most recent (2017) and it analyses the same battery technology of Remote batteries with the same efficiency and a similar capacity. This paper quantifies and compares the environmental performances of Lithium Metal Polymer (LMP) and Li-ion stationary batteries of different capacities (6 MWh for a centralized and 75 kWh for a distributed grid configuration in Quebec), through the LCA methodology covering their entire life cycle. We are interested in the analysis of the GHG emissions related to the Li-ion technology for a distributed grid configuration and with a capacity of 75 kWh. Table 4-26 resumes the main characteristics of the chosen battery.

Table 4-26: Main characteristics of the battery system present in [74].

Source	Year	Technology	Capacity	Lifetime		Efficiency
-	-	-	*kWh*	*cycles*	*years*	*%*
74	2017	Li-ion	75	5000	15	96

As already mentioned, a cradle-to-grave approach is adopted, including the extraction of raw materials, the manufacture of the battery and its components (assumed to take place in China), the installation on site, the maintenance and use phase, the production and delivery of the stored electricity, the transport and the end of life treatments. A metal packaging and a battery container are also included in the analysis. Regarding the use phase, batteries require little maintenance (two annual visits) and the monitoring is performed by remote technologies (one computer providing information). Concerning the end of life phase, it is estimated that the batteries are not recycled and that they are transported by truck and treated in a facility at approximately 4500 km away from the operation site. Instead, steel containers are considered to be completely recyclable. Finally, the production of the electricity stored in the batteries is assumed to come from wind power sources, but we assume to not consider this contribution in order to not account the production of energy twice in the final results. We assume also to not consider the delivery of electricity according to the physical system boundaries assumed. Concerning the transports, no sufficient data are available in order to remove their contribution for our analysis. A summary of the system boundaries is shown in Figure 4-7, taken from [74]. The use phase contains also the maintenance, while the transports are included in each phase.

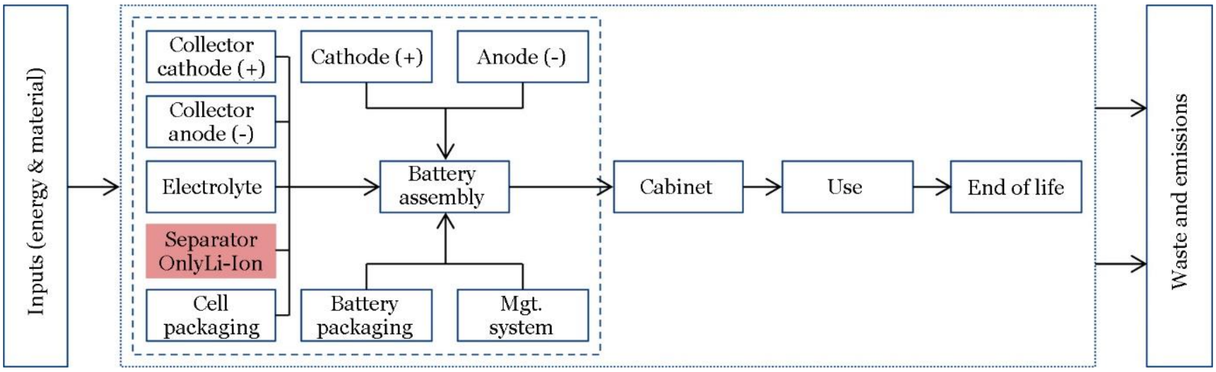

Figure 4-7: LCA boundaries of the battery system [74].

The final results of [74], regarding the GHG emissions of the Li-ion battery of 75 kWh, are presented in the Table 4-27, including the percentage of impact of each lifecycle phase.

Table 4-27: Resulting GHG emissions of study [74] and relative impact percentages of each LCA phase.

Steps taken into account in the LCA of [74]							Total GHG emissions per battery capacity	Total GHG emissions rate
Extraction of raw materials	Manufacture of battery and components	Installation on site	Container	Maintenance and use	Transport	End of life treatments	*$kgCO_2eq/kWh$*	*$kgCO_2eq/MWh$ delivered*
78%			7%	11%	In each phase	4%	130.73	34.0

We assume as input datum for the Li-ion batteries of the Remote plant the emissions of CO_2eq per kWh of battery capacity. The assumed lifetime of the batteries is the same assumed in [74]

(15 years), so the batteries are required to be replaced once during the plant lifetime of 25 years. This involves a total number of batteries of 110 kWh equal to 10. With these data, we can calculate the total CO_2eq emissions related to the batteries and, dividing the total GHG emissions by the plant energy production, the result in the functional unit assumed. Table 4-28 resumes the values obtained.

Table 4-28: Total GHG emissions rate (in functional unit) of the battery system in the Remote scenario.

GHG emissions per battery capacity [74]	Capacity of each battery	Total GHG emissions of 1 battery	Total GHG emissions of 10 batteries	Total energy production	Total GHG emissions rate
$kgCO_2eq/kWh$	*kWh*	*$kgCO_2eq$*	*$kgCO_2eq$*	*MWh*	*$kgCO_2eq/MWh$*
130.73	110	14,380.30	143,803.0	14,282.437	**10.069**

4.2.3.3 Comparison of the results with the literature

The amount of kg of CO_2eq emitted per kWh provided by the battery can be also calculated in order to verify the results (Table 4-29).

Table 4-29: Total GHG emissions rate of the battery system in the Remote scenario (per electricity delivered by the battery).

Total energy delivered by the battery	GHG emissions rate
MWh	*$kgCO_2eq/MWh$ delivered by the battery*
4,629.277	31.064

Since the value of 31.064 $kgCO_2eq/MWh$ is very close to the value of the study [74] (34.0 $kgCO_2eq/MWh$) and very similar to the values that we can find in other papers present in literature, as we can see in Table 4-30, we can conclude that the results are reliable.

Table 4-30: LCA GHG emissions rates of battery systems from different papers present in literature.

Source	Year	Technology	Battery capacity	GHG emissions rate
-	-	-	*kWh*	*kgCO₂ eq/MWh delivered by the battery*
Remote	-	Li-ion	550	31.064
73	2017	Li manganese	-	27.80
		Li iron phosphate	-	16.10
74	2017	Li metal polymer	75	25.6
		Li metal polymer	6000	20.5
		Li-ion	75	34.0
		Li-ion	6000	28.9
75	2016	Li iron phosphate	0.006	28.4
78	2015	Li-ion	329	25
		Li-ion	1,054,093	49

4.2.4 Electrolyser

4.2.4.1 Remote plant characteristics

The electrolyser is the first part of the non-integrated hydrogen storage system, the power-to-gas (P2G) side, which transforms the surplus energy in hydrogen. According to the simulations, it should receive about 105.6 MWh/y from the RES and produce more or less 1920 kg of hydrogen per year with a heat loss of 21.12 MWh/y.

Hydrogenics, the company in charge to build this component, proposed a PEM (Polymer Electrolyte or Proton Exchange Membrane) electrolyser (HyLYZER-10/30) developed to offer a reliable and high efficiency solution and designed to operate fully continuous with a minimal need for human attendance and maintenance, ensuring a constant flow of hydrogen. This outdoor version, equipped with an ISO steel container of 20 feet, is an all-in hydrogen generator producing 10 Nm^3/h of hydrogen at a purity of up to 99,998 % and a pressure of 30 barg, consuming at full load 55 kW. The characteristics of the electrolyser are summarized in Table 4-31. As a default, the equipment is manufactured in conformity with CE (ATEX directive 94/9/EC) and it includes the water purification system (reverse osmosis), power rectifiers, compressed air generator, H_2 purification system and cooling (dry cooler and chiller) [23].

Table 4-31: Main characteristics of the electrolyser system in the Remote plant [23].

Type	Size	Output pressure	H_2 purity	Production rate	Modulation range	Efficiency LHV	Electricity consumption	Ambient temperature (min / max)	Container
-	*kW*	*barg*	*%*	*Nm^3/h*	*%*	*%*	*kWh/kgH_2 produced*	*°C*	*feet*
PEM HyLYZER-10/30	55	30	99.998	10	10-100	63.00	52	-20 / +35	20

4.2.4.2 LCI from literature

In literature there are several studies considering the Life Cycle Assessment of different hydrogen production systems. Some of them assess the potential environmental impact of integrating hydrogen in an energy system in an isolated territory, such as paper [55] that includes electricity production from a wind turbine, PEM electrolysis and fuel cell stacks, hydrogen storage and transportation and final applications. Paper [33], instead, studies only the renewable hydrogen production from wind power with compression and storage. In the study [43], the environmental impacts of an uninterruptible power supply (UPS) based on hydrogen technologies (alkaline electrolyser) using renewable energy sources is compared to a UPS system based on internal combustion engine. A focus on hydrogen mobility is instead present in paper [35], where an LCA of hydrogen and gasoline vehicles is conducted, and in paper [41], which studies a hydrogen refuelling station with an on-site alkaline electrolyser operating with electricity provided by wind turbines, a compressor and a storage system. Finally, a list of various studies that compare the life cycle assessment of different hydrogen production methods is presented:

- [27] including steam reforming of natural gas, coal gasification, water electrolysis via wind and solar electrolysis, thermochemical water splitting with a Cu-Cl cycle;

- [32] presenting LCA and water footprint of H_2 production through steam reforming of natural gas, coal gasification, water electrolysis via proton exchange membrane (PEM) or solid oxide electrolyser cell (SOEC), biomass gasification and reforming, and dark fermentation of lignocellulosic biomass;

- [40] evaluating LCA (cradle-to-gate) of power-to-gas technology to store surplus electricity from fluctuating renewable sources such as wind power or photovoltaics, by generating hydrogen (H_2) via water electrolysis, with optional methane (CH_4) synthesis from carbon dioxide (CO_2) and H_2. The results are compared to those of reference processes, such as steam reforming of natural gas and crude oil as well as natural gas extraction;

- [34] reviewing twenty-one studies that address the LCA of hydrogen production technologies, a majority of them employing electrolytic technologies;

- [28] assessing new processes under development for producing hydrogen (water photo-splitting, solar two-step thermochemical cycles and auto-maintained methane decomposition with different lay-outs) using a life cycle methodology and comparing them to conventional ones (methane steam reforming with CCS and electrolysis with different electricity sources);

- [30] evaluating and comparing the environmental impacts of various hydrogen production processes considering several energy sources and using life cycle analysis (steam methane reforming, renewable based electrolysis, nuclear based high temperature electrolysis, Cu–Cl and S–I thermochemical cycles);

- [25] investigating the environmental aspects of hydrogen production by natural gas steam reforming and production upon renewable energy sources (solar PV, solar thermal, wind power, hydro power, biomass).

Paper [42] is the most recent document discussing the life cycle assessment of hydrogen production from PEM water electrolysis (PEMWE) in present and future scenarios and comparing it to the reference process of steam methane reforming. However, the big size of the studied PEMWE (1 MW) makes it difficult to scale the results towards our PEM electrolyser of 55 kW. This is why we use as reference the study [87].

In this paper, the environmental performance of P2G using Life Cycle Assessment (LCA) is investigated according to ISO 14040-14044 (from raw material acquisition, production, use, to end-of-life treatment, recycling and final disposal). In particular, different approaches applied for CO_2 Capture and Utilization are discussed, a wide range of technology and system processes variations are investigated (supply of electricity, electrolysis technologies and CO_2 source, hydrogen or methane as product gases), the comparison of these P2G systems with conventional technologies is assessed, sensitivity analyses are performed and further environmental impacts in addition to the GWI are quantified. We are only interested in the production of hydrogen through electrolysis, the Power-to-Hydrogen (P2H) part of the study. It contains the electrolyser stack, the balance of plant (BOP), the transformer (voltage conversion), the rectifier (AC/DC conversion) and a compression stage before the supply, where hydrogen pression reaches 350-700 bar. For the P2H part, the reference unit is 1 MJ of hydrogen generated, considering the LHV of hydrogen equal to 10.8 MJ/Nm^3. The boundary of the system is set at the point of compressed hydrogen production, not considering any specific final application on any transport. In the electrolysis system, the analysis includes the consumption of electricity and water (1.1 kg per Nm^3 of hydrogen production), the raw materials required for electrodes, the nitrogen bottle, the buffer tank, the hydrogen dryer and heat exchanger, the materials required in operation and maintenance and the waste treatment and disposal. Regarding the compression of hydrogen, the study includes the electricity consumption needed for the compression and the raw materials required for the compressor. In our analysis, the electricity consumption of the electrolyser system and of the compressor is then removed in order not to take into account the emissions related to the electricity twice, since they have been already considered in our PV and wind systems. The manufacture of a container of 20 feet of steel high grade is also added in the boundaries of the original system. The compressor is not present in the Remote plant, but its contribution to the environmental impact is assumed negligible compared to the total plant so it has been left inside the boundaries. Figure 4-8 resumes the assumed boundaries.

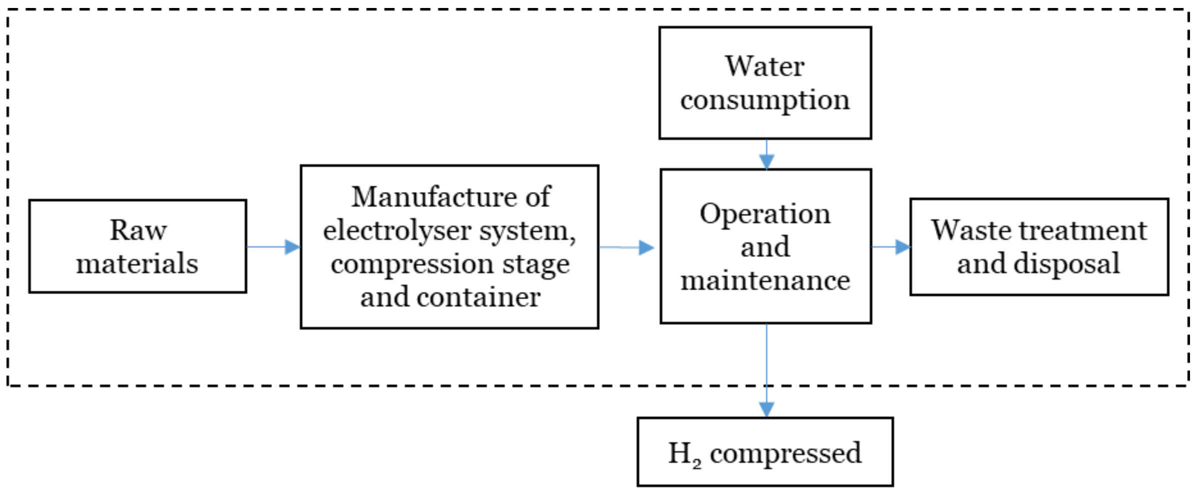

Figure 4-8: LCA boundaries assumed for the electrolyser system.

Among the different scenarios, we select the Polymer Electrolyte Membrane as electrolysis technology and the renewable energy sources (wind turbines and solar photovoltaics) of the Swiss context as electricity supply. The environmental impacts of electricity generation from RES located in Switzerland differ depending on the annual electricity generation, affected by location-specific resources and factors (such as wind condition, solar irradiance) and technology parameters, as well as the performance and lifetime of the turbines and PV panels. Assuming that the same technologies are applied in different locations, the ranges of parameters, performances and environmental impacts are shown in the Table 4-32, derived and modified from [87].

Table 4-32: Ranges of parameters and GHG emissions rate for PV and WT systems in different locations [87].

	Renewable electricity type					
	Electricity from PV			Electricity fron WT		
Parameters	Annual yield	Lifetime	GHG emissions rate	Full-load hours	Lifetime	GHG emissions rate
	$kWh/KW_p/y$	*years*	$kgCO_2 eq/MWh$ *produced*	*h/y*	*years*	$kgCO_2 eq/MWh$ *produced*
	850 - 1500	20 - 30	50 - 132	1000 - 2600	10 - 30	8 - 62

The electrolysis is performed at low temperature (less than 100°C) under the pressure of less than 30 bars. The considered PEM electrolyser has a capacity of 100 kW, an operation load density of 3.75 W/cm^2 and a lifetime of 67000 hours (Table 4-33).

Table 4-33: Main characteristics of the electrolyser system in paper [87].

Source	Year	Type	Size	Output pressure	Operation load density	Lifetime
-	-	-	*kW*	*bar*	W/cm^2	*hours*
87	2016	PEM	100	< 30	10	67000

The total system consumption is assumed equal to 4.9 kWh/Nm^3 H_2, according to the average system power consumption for PEM electrolyser described by [106] in 2015. 95% of the system energy consumption is assumed to be dedicated to the stack (4.655 kWh/Nm^3 H_2), while the remaining 5% is consumed in the BOP (0.245 kWh/Nm^3 H_2). Concerning the compression stage, the average energy consumption is assumed to be 3.1 kWh/kg H_2, based on [107]. Table 4-34 summarizes the different energy consumptions calculated with different units knowing the LHV of hydrogen (10.8 MJ/Nm^3) and its density in normal conditions (0.08994 kg/Nm^3), calculated with the ideal gas law.

Table 4-34: Electricity consumption of the electrolyser system and the compression phase [87] [106] [107].

Electricity consumption [87] [106] [107]						
PEM stack (95%)	BOP (5%)	Total electrolysis system		Compression		Total system
$kWh/Nm^3\ H_2$	*$kWh/Nm^3\ H_2$*	*$kWh/Nm^3\ H_2$*	*$kWh/MJ\ H_2$*	*$kWh/kg\ H_2$*	*$kWh/MJ\ H_2$*	*$kWh/MJ\ H_2$*
4.655	0.245	4.9	0.4537	3.1	0.0258	0.4795

The results of the analysis, expressed in kg of CO_2 emitted per MJ of hydrogen produced, are presented in Table 4-35. We consider the results of the four scenarios of RES considering the upper and lower values of the PV and wind systems. Knowing the carbon intensity of the RES (Table 4-32) and the energy consumption of the total system (stack+BOP+compressor) (Table 4-34), we can also find the GHG emissions related to the electricity consumption. This contribution is then removed from the total environmental impact in order to find the emissions of the only electrolyser system. An average value is then calculated.

Table 4-35: GHG emissions rates of the electrolyser system with and without electricity contribution [87].

Renewable electricity type	Total GHG emissions rate	Electricity GHG emissions rate	Electricity consumption GHG emissions rate	System GHG emissions rate without electricity
-	*$gCO_2eq/MJ\ H_2$ produced*	*$kgCO_2eq/MWh$ produced*	*$gCO_2eq/MJ\ H_2$ produced*	*$gCO_2eq/MJ\ H_2$ produced*
WT lower	5.04	8	3.836	1.204
WT upper	30.7	62	29.730	0.970
PV lower	25.2	50	23.976	1.224
PV upper	64.8	132	63.297	1.503
Average value	-	-	-	1.225

Knowing the total hydrogen produced, obtained multiplying the electrolyser power (100 kW) with the hours of lifetime (67000 h) and dividing by the energy consumption of the PEM electrolyser (4.655 $kWh/Nm^3\ H_2$), we can also find the total emissions. The GHG emissions are then divided by the capacity of the electrolyser to find the kg of CO_2eq per kW (Table 4-36).

Table 4-36: Total GHG emissions per ELY capacity calculated from paper [87].

System GHG emissions rate without electricity		Total hydrogen produced		Total GHG emissions	GHG emissions per ELY capacity
$gCO_2eq/MJ\ H_2$ produced	*$gCO_2eq/kg\ H_2$ produced*	*$Nm^3\ H_2$*	*$kg\ H_2$*	*$kgCO_2eq$*	*$kgCO_2eq/kW$*
1.225	147.115	1,439,312.567	129,456.893	19,045.017	190.450

The average value of 190.45 kg CO_2eq/kW is assumed for our analysis. Multiplying this value by the size of the Froan electrolyser (55 kW), we obtain the total GHG emissions related to the PEM electrolysis system. Based on the simulation of the plant, the working hours of the electrolyser are about 61813 h during the 25 years of lifetime assumed for the plant. This value is lower than the 67000 hours of lifetime assumed in [87], so we can consider only one electrolyser for the entire lifetime of our plant. Concerning the environmental impact of the stainless steel 20 feet container, we assume the total mass of 3900 kg stated in [42] and the emission factor of stainless steel (2.9 kg CO_2/kg SS) presented in [86] and discussed more in the detail in Section 4.2.5, dedicated to the hydrogen storage. The impact due to the container is easily found (Table 4-37).

Table 4-37: GHG emissions related to the ELY system and the container present in the Remote plant.

GHG emissions per ELY capacity	ELY capacity	Total ELY GHG emissions	Container mass [42]	SS GHG emissions factor [86]	Container GHG emissions
kgCO₂eq/kW	*kW*	*kgCO₂eq*	*kg SS*	*kgCO₂eq/kg SS*	*kgCO₂eq*
190.450	55	10,474.759	3900	2.9	11,310

Summing the emissions related to the electrolyser system and the container, the total result is obtained. Dividing this value by the total energy produced by our plant, we found the result in functional unit (Table 4-38).

Table 4-38: Total GHG emissions rate (in functional unit) of the battery system in the Remote scenario.

Total GHG emissions	Total energy production	Total GHG emissions rate
kgCO₂eq	*MWh*	*kgCO₂eq/MWh*
21,784.759	14,282.437	**1.525**

4.2.4.3 Comparison of the results with the literature

The emissions per hydrogen mass and energy unit are also obtained in order to compare the results with the literature (Table 4-39).

The results are difficult to compare because the majority of the studies doesn't separate the electrolysis part from the electricity production system. However, the emission rates are of the same order of magnitude of the ones obtained from [87] (1.225 gCO_2eq/MJ H_2) and of the ones

Table 4-39: Total GHG emissions rate of the electrolyser system in the Remote scenario (per hydrogen produced by the ELY).

Total hydrogen produced by the electrolyser		GHG emissions rate	
kg H_2	*MJ H_2*	*$gCO_2eq/kg\ H_2$ produced by the ELY*	*$gCO_2eq/MJ\ H_2$ produced by the ELY*
48,000.726	5,763,701.732	453.842	3.780

obtainable from [42] (1.769 – 3.349 $gCO_2eq/MJ\ H_2$), using a technique similar to the one used in this chapter to remove the electricity contribution from the total GHG emissions. The resulting values of our study are bigger than the ones of [87] because in that paper the container is not considered and, in general, they are bigger than the values found because the electrolysis systems studied in the literature have the only scope of producing hydrogen, while in our study the hydrogen is only produced in case of surplus energy from RES and when the electricity is not charging the battery. A lower amount of hydrogen produced induces higher values of the normalized CO_2 emissions.

4.2.5 Hydrogen storage

4.2.5.1 Remote plant characteristics

The second part of the non-integrated hydrogen storage system is the physical tank storing the gas. The proposed hydrogen storage solution provided by Powidian for the Remote plant of Froan contains about 100 kg of hydrogen, for about 3.33 MWh of gross energy content (with a LHV of hydrogen equal to 120 MJ/kg H_2) and it is composed by two main parts: the vessel and all the accessories (valves, pressure reducer…). Due to the availability of space without particular constraints and the difficult accessibility, the technical solution proposed is a 30 bar storage, which avoid the use of the compression stage. This low-pressure installation involves a bigger volume of the hydrogen tank, but it brings significant advantages, such as the higher round-trip efficiency, lower maintenance, longer durability and improved reliability. The lifetime is assumed 25 years. In the following Table 4-40 the detailed data of the tank [23].

Table 4-40: Main characteristics of the hydrogen storage system in the Remote plant [23].

Tank	Material	H_2 capacity	Useful gross energy (LHV)	Volume capacity	Total length	External radius	Working pressure	Test pressure	Design temperature	Lifetime
-	-	*kg H_2*	*MWh H_2*	*m^3*	*m*	*m*	*bar*	*bar*	*°C*	*years*
Cylindrical	Stainless Steel	100	3.333	41	9.5	1.25	30	45	-40 / +30	25

4.2.5.2 LCI and comparison with the literature

Concerning the material of the storage tank, we assume the austenitic stainless-steel type 316 (EN 1.4401) considered, with its lower carbon version 316L (EN 1.4404), "the benchmark for resistance to hydrogen embrittlement in gaseous hydrogen environments" [122]. We choose type 316 instead of 316L because of the higher values of tensile and yield strength of the former. In Table 4-41 some properties relevant for our study are presented.

Table 4-41: Relevant properties of the stainless-steel assumed as storage tank material.

Stainless Steel type	Yield strength 0.2%	Tensile strength	Density @ 20°C
-	*MPa*	*MPa*	*g/cm^3*
316 (EN 1.4401)	205	515	8.027

In order to find the total mass of stainless steel for the tank, we calculate the thickness required to withstand the internal pressure. We set as maximum pressure (p_{max}) the test pressure of 45 bar and we assume a safety factor (SF) of 1.5. Dividing the yield strength (σ_{yield}) by the safety factor (equation (1) we obtain the allowable stress (σ_{all}), the value of which is used as hoop (σ_θ) and longitudinal (σ_{long}) stresses. Knowing these values and using the relations for thin-walled cylindric pressure vessels (equations (2-(3), where r is the internal radius and t is the thickness of the tank, we can calculate the thicknesses related to the hoop and longitudinal stresses (equations (4-(5). We calculate also the thickness related to Tresca criterion with equation (6. As a first approximation, we assume the internal radius equal to the external radius (r_{ext}).

$$\sigma_{all} = \frac{\sigma_{yield}}{SF} = \frac{205\ MPa}{1.5} = 136.67\ MPa \tag{1}$$

$$\sigma_\theta = \frac{p_{max} \cdot r}{t} \tag{2}$$

$$\sigma_{long} = \frac{p_{max} \cdot r}{2 \cdot t} \tag{3}$$

$$t_\theta = \frac{p_{max} \cdot r}{\sigma_\theta} = \frac{4.5\ MPa\ \cdot 1.25\ m}{136.67\ MPa} = 4.116\ cm \tag{4}$$

$$t_{long} = \frac{p_{max} \cdot r}{2 \cdot \sigma_{long}} = \frac{4.5\ MPa\ \cdot 1.25\ m}{2\ \cdot\ 136.67\ MPa} = 2.058\ cm \tag{5}$$

$$t_{Tresca} = \sqrt{\frac{(p_{max} \cdot r)^2 + (\frac{p_{max} \cdot r}{2})^2 - (p_{max} \cdot r) \cdot (\frac{p_{max} \cdot r}{2})}{\sigma_{all}^2}} = 3.564\ cm \tag{6}$$

We choose the biggest value among the obtained thicknesses t=4.116 cm. The internal radius, according to equation (7, will be:

$$r = r_{ext} - t = 125\ cm - 4.116\ cm = 120.884\ cm \tag{7}$$

Assuming the tank composed by a central cylinder and two final semi-spheres having the same radius and knowing the total length (L), the external radius and the internal one, we can calculate (equation (8) the total volume (V) of material of the tank as summation of the volume of the cylindric part (V_{cyl}) and the one of the two semi-spheres part (V_{sph}).

$$V_{SS} = V_{cyl} + V_{sph} = \pi \cdot (r_{ext}^2 - r^2) \cdot (L - 2 \cdot r_{ext}) + \frac{4}{3}\pi \cdot (r_{ext}^3 - r^3) = 3.00738\ m^3 \tag{8}$$

The total mass of stainless steel (m_{SS}) is (equation (9):

$$m_{SS} = \rho_{SS316} \cdot V_{SS} = 8027 \frac{kg}{m^3} \cdot 3.00738\ m^3 = 24140.3\ kg \tag{9}$$

Since all the calculations are made under the assumption of internal radius equal to the external one and since we have found a new internal radius, we can iterate the operations described in the equations from (1 to (9, substituting in every iteration the old internal radius with the new one found, until we reach a relative error of the final m_{SS} minor than 10^{-5}. The relative error (E_{rel}) is calculated with the following equation (10, where "i" is the present iteration and "i-1" is the previous one.

$$E_{rel} = \left| \frac{m_{SS}(i) - m_{SS}(i-1)}{m_{SS}(i-1)} \right| \tag{10}$$

At the fifth iteration we obtain a relative error of $1.19 \cdot 10^{-6}$. In Table 4-42 we resume the final results obtained.

Table 4-42: Volume and mass of SS required for the H_2 tank, calculated through iterations.

	Thickness	Internal radius	Volume of SS	Mass of SS	Relative error
Iterations	*cm*	*cm*	*m^3*	*kg*	-
1^{st}	4.1160	1.208841	3.007384	24140.268	-
2^{nd}	3.9803	1.210197	2.910375	23361.582	0.03226
3^{rd}	3.9848	1.210152	2.913572	23387.239	0.00110
4^{th}	3.9846	1.210154	2.913466	23386.394	3.612E-05
5^{th}	3.9847	1.210153	2.913470	23386.422	1.19E-06

The total mass of stainless steel needed is of the same order of magnitude of the value stated by [43] (16964 kg) for a hydrogen storage tank of steel high grade for a capacity of 20 m^3 at a maximum operational pressure of 25 bar. The value found by our analysis is reasonable higher due to the bigger volume capacity and the higher operational pressure.

Regarding the environmental impact of the storage tank, document [86] quantifies the CO_2 emitted from the production of stainless steel specifying three sources: the extraction and preparation of ores and the production of ferro-alloys including the electricity needed, the electricity consumed within the stainless steel industry and finally the production process at stainless steel sites. The first part includes the emissions from the raw material extraction, the processes to produce primary elements (chromium, nickel, molybdenum and others), carbon steel scrap and stainless-steel scrap and the electricity required for mining and ferro-alloy production. If the production derives only from raw materials, the CO_2 emissions are 4.2 $kgCO_2$/kg SS, while the emissions decrease to 1.92 $kgCO_2$/kg SS if around 50% of recycled stainless-steel scrap is used. The second part takes into account only the electricity required from the plant for the SS production. The emissions are 0.54 $kgCO_2$/kg SS. The third part concerns the direct CO_2 emissions during the production phase, including the use of fuel, giving an average value of 0.44 $kgCO_2$/kg SS. The total emissions (Table 4-43) are 2.90 $kgCO_2$/kg SS, assuming the 50% recycling case, and 5.18 $kgCO_2$/kg SS, in case of production derived only from raw materials.

Table 4-43: CO_2 emissions factors for the production of stainless steel through different phases [86].

CO_2 emission factors [86] (2015)					
Raw material (50% recycling)	Raw material (no recycling)	Electricity	Direct production	Total emissions (50% recycling)	Total emissions (no recycling)
$kgCO_2$/kg SS	*$kgCO_2$/kg SS*	*$kgCO_2$/kg SS*	*$kgCO_2$/kg SS*	*$kgCO_2$/kg SS*	*$kgCO_2$/kg SS*
1.92	4.20	0.54	0.44	2.90	5.18

In study [43], instead, the total mass of steel high grade (16964 kg) produces an amount of CO_2 emissions equal to about 76000 $kgCO_2$, including the manufacture from raw materials, the installation on site and the transports. Maintenance and end-of-life phases are not considered. The resulting environmental impact is 4.48 $kgCO_2$ per kg of steel high grade, almost exclusively due to the manufacturing phase. However, [43] states that the predominant part of the materials used in the studied system can be recycled and used as material inputs in manufacturing phase. This is why we assume the 50% recycling case stated by [86] with the lower value of total emissions. Multiplying the total mass of our storage tank by the emission factor of 2.90 $kgCO_2$/kg SS, the total CO_2 emissions can be found. Dividing this result with the total electricity production of the Froan plant, the emissions per functional unit are obtained. Table 4-44 resumes the results.

Table 4-44: Total GHG emissions rate (in functional unit) of the H_2 storage tank in the Remote scenario.

Mass of SS for the tank	CO_2 emission factor (50% recycling) [86]	Total GHG emissions	Total energy production	Total GHG emissions rate
kg	*$kgCO_2$/kg SS*	*$kgCO_2$ eq*	*MWh*	*$kgCO_2$ eq/MWh*
23386.422	2.90	67820.623	14282.437	**4.749**

Concerning the system boundaries related to the storage system, only the production of materials required for the tank is included. Its manufacture, the transports, the installation, the use and maintenance phase and the end of life processes are outside the boundaries because of lack of data. However, it can be assumed that the most relevant part involving the environmental impact is the production of stainless steel, while the contribution of the other phases is less important.

4.2.6 Fuel cell

4.2.6.1 Remote plant characteristics

The gas-to-power (G2P) side is the third part of the non-integrated hydrogen storage system, constituted by the fuel cell, which transforms the hydrogen stored in electricity again. According to the simulations, it should receive about 1920 kg of hydrogen from the storage tank and provide to the load more or less 35.16 MWh/y of electricity with a heat loss of 19.2 MWh/y.

The solution proposed by Ballard Power Systems Europe A/S (BPSE) for the Remote project is a low-temperature proton exchange membrane (LT-PEM) fuel cell system, in a containerized solution (2x10 feet ISO container), specially designed for the cold, coastal and harsh Nordic climate environment. Since the system is located in a remote area, the design has been focused on some essential properties, such as the reliability, durability, easy installation, easy and low-cost serviceability and remote monitoring and control. The solution proposed is in conformity with CE (EN 62282-3-100), it is equipped with the newest generation fuel cell technology and it combines the relevant and best features of the existing stationary (remote area installations) and motive (long lifetime) products of BPSE. The fuel cell has a power rating of 100 kW (peak) with an efficiency of 50% (LHV) and a consumption rate of 0.804 Nm^3 of hydrogen per kWh of electricity produced. The required hydrogen purity must be grade 3.5 or higher (99.95%) and the operational gage pressure is 0.5 bar. The characteristics already mentioned and some extra information are summarized in Table 4-45 [23] [24].

Table 4-45: Main characteristics of the fuel cell system in the Remote plant [23] [24].

Type	Container	Power rating	Efficiency LHV	H_2 consumption rate		Required H_2 purity	Modulation range	Pressure	Temperature range	Relative humidity
-	*ft*	*kW (peak)*	*%*	*Nm^3/kWh produced*	*NLPM /kW*	*%*	*%*	*barg*	*°C*	*%*
LT-PEM	2 x 10	100	50	0.804	13.4	99.95	6 - 100	0.5	-20 / +46	5 - 95

4.2.6.2 LCI from literature

In literature, a lot of papers discuss the LCA of PEM fuel cells for mobility application. For example, [127] and [128] examine PEMFC systems for road passenger vehicles with a particular attention in document [128] to production and EOL processes in current and future scenarios. Paper [130] studies a fuel cell mounted in a cargo bike. Document [37] discusses the role of hydrogen and fuel cell systems from the sustainability point of view and presents two case studies on the LCA of fuel cell vehicles with different hydrogen production systems and study [131] presents and compares four case studies of mobile fuel cells stacks and two more case studies on stationary stacks. Fewer studies present the LCA of fuel cells for stationary applications, like hydrogen storage systems in energy plants, such as paper [132] that assesses the environmental performance of different electricity storage technologies for grid applications such as pumped hydro, compressed air, batteries and hydrogen. Among these studies only few ones report the specific data regarding only the fuel cells such as [55] and [43].

For our study we analyse paper [76], which evaluates environmental impacts cradle-to-grave of a 3 kW uninterruptible power supply system with polymer membrane fuel cell (called FCH-UPS) with an LCA method according to FC-HyGuide document [134] and ISO standards 14040 [104] and 14044 [105]. The cradle-to-grave type of the LCA analysis includes manufacturing from production of raw materials with materials and energy inputs, transportation, operation and EOL. Maintenance of the system is excluded. In particular, the main components considered in the study (especially in the manufacturing phase) are: PEM fuel cell stack, air and hydrogen recirculation blowers, external heat exchanger, air humidifier, cabinet, lead batteries, controls and regulation systems and others balance of plant components needed. The manufacture of the hydrogen production facility is not included. For our study the contributions of the cabinet and the lead batteries are removed in order to consider only the fuel cell. A 20-feet container is then added to the total contribution. Transportations via railway, cargo ship and truck of the components from manufacturing to final assembly site and then to utilisation site are included, but they have almost negligible influence to the total environmental impact, so they are neglected for our study. Considering the operating phase, two geographical locations (Oslo, Norway and Marrakesh, Morocco) with different electrical energy mixes are evaluated and compared regarding the environmental impacts for the hydrogen production with electrolysis onsite. The operating phase is not considered for our study because the emissions related to the hydrogen production have been already assessed. Three different end of life (EOL) scenarios reducing environmental impacts during manufacturing stage are presented: base, feasible and realistic scenario. The base case scenario considers the total landfilling of materials, while feasible and realistic scenarios consider also the recycle and reuse of them. In the feasible case, the highest theoretical recycling (32%) and reuses (68%) possibilities for all materials are considered, reducing drastically the input of new materials in the manufacturing phase. However, this scenario is technically complex to implement. The third scenario, the realistic one, is between the previous ones and represents the highest expected amount of reused and recycled materials according to available technologies. In this hypothesis, 50% of the mass is reused, 41% is recycled and only 9% is landfilled. For our study, the base case scenario in assumed for the EOL because of the more accurate data regarding the different contributions of each component of the fuel cell system. A summary of the system boundaries considered in our analysis is shown in Figure 4-9.

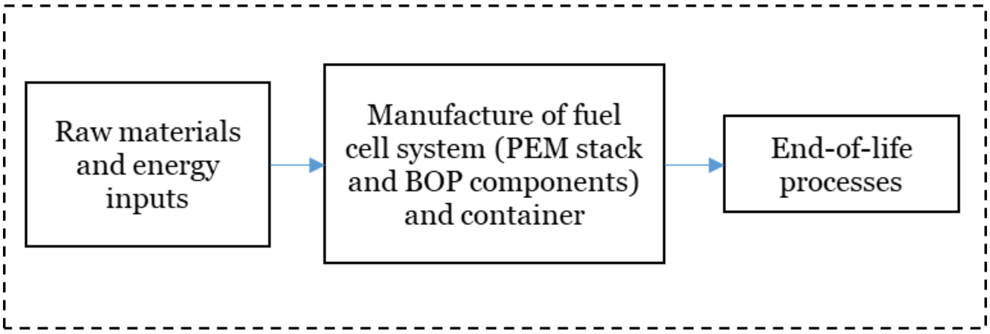

Figure 4-9: LCA boundaries assumed for the fuel cell system.

The functional unit proposed is 1 kWh of produced uninterrupted electric energy and the lifetime of the system is considered to be 10,000 h. In the following Table 4-46 the basic technical data of the 3 kW FCH-UPS system, produced by Electro Power Systems from Torino, are presented.

Table 4-46: Main characteristics of the fuel cell system in paper [76].

Source	Year	Type and electrolyte	Rated power	Rated voltage output	Rated current output	Efficiency	Rated H_2 consumption	H_2 purity	Lifetime	
-	-	-	*kW*	*V*	*A*	-	*kg/MWh*	*%*	*years*	*hours*
76	2018	PEM Nafion™	3	24	125	0.5	88.3334	99.99	10	10,000

The total environmental impacts due to the manufacturing phase are shown in Table 4-47 with the relative contributions of each component.

Table 4-47: Resulting GHG emissions and percentages of each components contribution for the manufacturing phase of the fuel cell system of paper [76].

Environmental impact for manufacturing phase [76]								
Air blower	H_2 blower	Battery	Humidifier	External climate	FC stack	Cabinet	Auxiliary components	Total absolute value
%	*%*	*%*	*%*	*%*	*%*	*%*	*%*	*$kgCO_2eq$*
3.5	1.2	23.0	0.4	4.4	35.9	21.4	10.2	2180

From the total value of 2180 $kgCO_2eq$ we remove the 23.0% of the battery and the 21.4% of the cabinet and we obtain 1212.08 $kgCO_2eq$. According to [76], the relative contribution of EOL processes is 0.2% compared with manufacturing phase being 99.8%. Then, dividing the total manufacture emissions (2180 $kgCO_2eq$) by 0.998 and multiplying it by 0.002, we obtain the impact of the landfill process, 4.37 $kgCO_2eq$. Summing the manufacture and EOL contributions, a total value of 1216.45 kgCO_2eq is found. Dividing it by the capacity of the fuel cell, we obtain the GHG emissions per kW installed, 405.48 kgCO_2eq/kW (Table 4-48).

Table 4-48: GHG emissions (manufacture and EOL) per FC rated power (without battery and cabinet) [76].

Manufacture GHG emissions (no battery and cabinet)	End-of-life GHG emissions (no battery and cabinet)	Total GHG emissions (no battery and cabinet)	GHG emissions per FC rated power
$kgCO_2eq$	$kgCO_2eq$	$kgCO_2eq$	$kgCO_2eq/kW$
1,212.08	4.37	1,216.45	405.483

According to the simulations, the work hours of the PEMFC proposed for the Remote project are about 19,212 h. Regarding the lifetime of a PEM fuel cell, we refer to the European project STAYERS (Stationary PEM fuel cells with lifetimes beyond five years) that was dedicated to the goal of obtaining 40,000 hours of PEM fuel cell lifetime for power stationary applications employing the best technological and scientific means. According to the final report summary of the project, it was shown that extrapolated system lifetimes of 40,000 hours can be achieved [IV]. Then, a single fuel cell for the entire lifetime can be assumed. Multiplying the emissions per kW installed by the power rating of the Froan fuel cell (100 kW), we obtain the total emissions related to the fuel cell (40548.29 kgCO_2eq). The environmental impact of the 20-feet container already discussed in Section 4.2.4.2, dedicated to the electrolyser (11310 kgCO_2eq) is added to find the total emissions for the fuel cell system of our study (51858.29 kgCO_2eq). Dividing them by the total energy provided by the plant to the load we obtain the mass of CO_2eq emitted per MWh produced by the total plant (Table 4-49).

Table 4-49: Total GHG emissions rate (in functional unit) of the FC system in the Remote scenario.

GHG emissions per FC rated power [76]	FC rated power	Total FC GHG emissions	Container GHG emissions	Total GHG emissions	Total energy production	Total GHG emissions rate
$kgCO_2eq/kW$	kW	$kgCO_2eq$	$kgCO_2eq$	$kgCO_2eq$	MWh	$kgCO_2eq/MWh$
405.483	100	40,548.291	11,310	51,858.291	14,282.437	**3.631**

4.2.6.3 Comparison with the literature

In order to compare the results with the values in the literature, we divide the total GHG emissions by the energy provided only by the fuel cell system in the case of the real production simulated and in the case of the ideal production considering the lifetime of 40,000 h [IV] and a constant rated power of 100 kW (Table 4-50).

Table 4-50: Real and ideal GHG emissions rate per MWh delivered by the FC system in the Remote scenario.

Total energy delivered by the fuel cell	Real GHG emissions rate	Total energy deliverable by the fuel cell	Ideal GHG emissions rate
MWh	*kgCO₂ eq/MWh delivered by the fuel cell*	*MWh*	*kgCO₂ eq/MWh delivered by the fuel cell*
879.133	58.988	4,000.000	12.965

Study [43] assesses an emissions rate of 13.4 kgCO_2eq/MWh due to the manufacturing processes of a fuel cell system. The real GHG emissions of our study are more than four times the value of [43], but the ideal ones are very similar. In fact, the cited paper studies an uninterruptible power supply (UPS) system working and producing continuously during all the lifetime, while in our plant the fuel cell produces energy only in case the electricity from RES is not able to cover the load.

4.2.7 Diesel generator

4.2.7.1 Remote plant characteristics

The last part of the Remote plant is constituted by the diesel generator installed in order to cover the load in case of insufficient production from the RES and the storage system. It is useful also in case of damages or ruptures in the main renewable plant. It is assumed that the diesel should cover about 5% of the total energy required by the load, so about 28.6 MWh/y of the total 571.3 MWh/y. According to the simulation of the Froan plant, the maximum power needed is about 106 kW, but the required power exceeds 100 kW for only more or less 12 hours per year. This is why we assume a Diesel generator sized 100 kW, the HGM138 Googol Diesel Power Generator provided by Honny Power [96]. The genset prime output is 100 kW (125 kVA) with an average fuel consumption of 220 g/kWh (225 g/kWh at 75% of the genset prime output and 215 g/kWh at 100%). Table 4-51 resumes the main characteristics of the HGM138 Googol Diesel Power Generator.

Table 4-51: Main characteristics of the HGM138 Googol Diesel Power Generator provided by Honny Power [96].

Genset prime output		Rating power factor	Rating speed	Rating frequency	Rating voltage	Genset weight	Genset size (LxWxH)	Genset fuel consumption	
								At 75% of prime output	At 100% of prime output
kW	*kVA*	-	*rpm*	*Hz*	*V*	*kg*	*mm*	*g/kWh*	*g/kWh*
100	125	0.8	1500	50	400	1250	2300 x 850 x 1350	225	215

The total mass of diesel consumed by the Froan plant can be assessed multiplying the average fuel consumption (220 g/kWh) by the energy provided by the generator, obtaining a result of 157106.8 kg of Diesel (Table 4-52).

Table 4-52: Total diesel needed and consumed in the Remote scenario.

Average fuel consumption [96]	Total energy provided by the generator	Total diesel needed
g/kWh	*MWh*	*kg*
220	714.122	157,106.803

4.2.7.2 LCI from literature

In literature, some LCA on Diesel generators have already been assessed, especially in comparison with RES based plants. In [50], six case studies with the same load profile but different sizes of energy sources are compared in term of reliability, economic and environmental benefits. The objective is to minimize costs and emissions in the proposed microgrid system that consists of photovoltaic, wind turbine generator, electric storage system and diesel generator. Paper [43] compares the environmental impacts of an uninterruptible power supply (UPS) system based on an internal combustion engine (using unleaded gasoline instead of diesel) with the ones produced by a UPS system based on hydrogen technologies and RES. In [89], a multi-objective optimization is developed to minimize the levelized cost of energy and the equivalent carbon dioxide life cycle emissions of a stand-alone PV-wind-diesel system with battery storage. Study [95] compares greenhouse gases (GHG) emissions calculated over the life-cycle of two systems providing the same amount of energy: a stand-alone small wind turbine system and a single-home diesel generator system. A life cycle assessment to compare the environmental impacts of a Diesel/PV/wind microgrid on a Thai Island with the ones due to a grid extension or to the installation of home diesel generators cases is present in [117]. Study [124] investigates the LCA of two types of solar energy systems for rural households in developing countries in comparison with LCA of a small diesel generator, a battery charging station and kerosene lamps. Paper [135], instead, applies the LCA methodology to a diesel generator set to quantify the energy demands of each life cycle stage.

For our study, we assume different values from different sources. Regarding the manufacture of the generator, we take the value assumed in [89] and derived from [95]. In paper [95], the emissions related to the material production and manufacturing processes of two generators of 5 kVA with a lifetime of 10 years each are 1077 kgCO_2eq. In order to calculate the environmental impacts per kVA of generator, we divide the total value by the number of generators and their capacity, obtaining 107.7 kgCO_2eq/kVA. We estimate the operational hours of our diesel system assuming they are 5% of the total hours of the 25 years plant lifetime, so 10950 h. Assuming the lifetime of diesel generators within the range of 15,000-30,000 assessed by [137], only one generator is needed in the plant. The assumption is also in accordance with [119], which assesses that a diesel generator lifetime varies from 5,000 to 50,000 hours, depending on the proper installation, operation and maintenance and on the quality of the engine, with an average value of 20,000 h. Multiplying the value of emissions per kVA with the total capacity of the assumed diesel generator, we obtain 13,462.5 kgCO_2eq emitted in the manufacturing phase (Table 4-53).

Table 4-53: GHG emissions from the manufacture of the diesel generator (Remote scenario).

Generator manufacture [89, 95]			**Remote plant**	
GHG emissions	Size of each generator (2)	GHG emissions per generator power	Genset prime output	Total GHG manufacture emissions
$kgCO_2eq$	*kVA*	*$kgCO_2eq/kVA$*	*kVA*	*$kgCO_2eq$*
1077	5	107.7	125	13,462.5

The emissions related to the production of the diesel tank are assumed negligible, like in study [95]. Concerning the installation and maintenance processes, they are not considered in this study, as in [95], due to a lack of reliable data and because they are assumed small enough over the entire life cycle to be considered negligible [95]. Regarding the operational phase, the emissions related to the fuel combustion and production are accounted. For the fuel combustion, the value of 2.86 $kgCO_2eq$ per litre of diesel burnt, assumed in [95] and taken from [138] and [139], is used. This value is also in accordance with the range of emissions factor found in literature and assessed by [119] from 2.4 to 3.5 $kgCO_2eq/l$. Knowing the fuel density (0.84 kg/l) we can find the emissions per unit mass of diesel combusted, 3.405 $kgCO_2eq/kg$. Multiplying this value with the total mass of diesel consumed, the total GHG emissions result 534,911.3 $kgCO_2eq$ (Table 4-54).

Table 4-54: GHG emissions from the diesel combustion (Remote scenario).

Fuel combustion [95]			**Remote plant**	
GHG emissions per litre of diesel	Diesel density	GHG emissions per mass of diesel	Total diesel needed	Total GHG combustion emissions
$kgCO_2eq/l$	*kg/l*	*$kgCO_2eq/kg$*	*kg*	*$kgCO_2eq$*
2.86	0.84	3.405	157,106.803	534,911.258

Concerning the fuel production, we refer to paper [90] whose aim is to provide information about lifecycle GHG emissions of oil products based on collection of actual data as possible for different oil fields and fuel pathways. The lifecycle Carbon Intensity of petrol, diesel, kerosene and natural gas is assessed in a “well-to-tank” (WTT) approach, from extraction up to final consumers, including a chain of significant production stages such as exploration, exploitation, production, fuel recovery, upgrading, pipeline and maritime transportation, transmission, refining, distribution and dispersing, excluding the emissions resulting from the final combustion. We are interested in the production WWT of diesel and we assume as original oil field the one of Troll, located off-shore in Norway (latitude 60.646, longitude 3.726). The value of the environmental impact is 12.4 $kgCO_2eq$ per GJ of diesel produced, lower than the average value for EU (17.4 $kgCO_2eq/GJ$). Knowing from [95] the density (0.84 kg/l) and the energy content of diesel (10.72 kWh/l or 38.592 MJ/l), we can find the emissions per unit of mass of diesel produced, 0.570 $kgCO_2eq/kg$ for the Troll plant and 0.799 $kgCO_2eq/kg$ as average value for EU. Multiplying the value related to the production in the Troll plant by the total mass of diesel consumed, the total carbon dioxide emissions result 89,502.4 $kgCO_2eq$ for the diesel production (Table 4-55).

Table 4-55: GHG emissions from the diesel production (WTT) in the Remote scenario.

Fuel production [90]					**Remote plant**	
Troll WTT carbon intensity of diesel	Average EU WTT carbon intensity of diesel	Diesel energy content [95]	Troll WTT carbon intensity of diesel	Average EU WTT carbon intensity of diesel	Total diesel needed	Total GHG production emissions (Troll)
$kgCO_2eq/GJ$ of diesel produced	*$kgCO_2eq/GJ$ of diesel produced*	*MJ/kg*	*$kgCO_2eq/kg$ of diesel produced*	*$kgCO_2eq/kg$ of diesel produced*	*kg*	*$kgCO_2eq$*
12.4	17.4	45.943	0.570	0.799	157,106.803	89,502.399

The transports and the end of life phase are not considered. The following Figure 4-10 shows the system boundaries assumed.

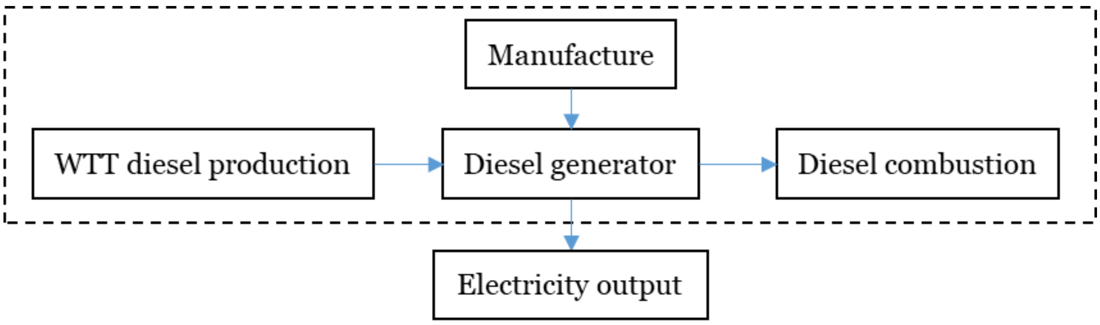

Figure 4-10: LCA boundaries assumed for the diesel generator system.

The total environmental impact related to the diesel part of the system is the summation of the three contributions studied, giving a final value of 637,876.2 $kgCO_2eq$. Dividing the total mass by the total energy delivered by the plant during its lifetime we obtain 44.662 $kgCO_2eq/MWh$. The following Table 4-56 sums up the results obtained.

Table 4-56: Total GHG emissions rate (in functional unit) of the diesel generator system in the Remote scenario.

Total GHG manufacture emissions	Total GHG combustion emissions	Total GHG production emissions (Troll)	Total GHG emissions	Total energy production	Total GHG emissions rate
$kgCO_2eq$	*$kgCO_2eq$*	*$kgCO_2eq$*	*$kgCO_2eq$*	*MWh*	*$kgCO_2eq/MWh$*
13,462.5	534,911.258	89,502.399	637,876.157	14282.437	**44.662**

A chart (Figure 4-11) shows also the relative contribution of the manufacturing phase of the generator, the combustion of the diesel and the production of the fuel to the total environmental impact. We can see that the emissions during the fuel combustion constitute the biggest part of the total environmental impacts (83.86%), followed by the fuel production phase (14.03%) and by the emissions related to the manufacture of the generator (2.11%). Similar results about the repartition of the environmental impacts are reported in paper [124].

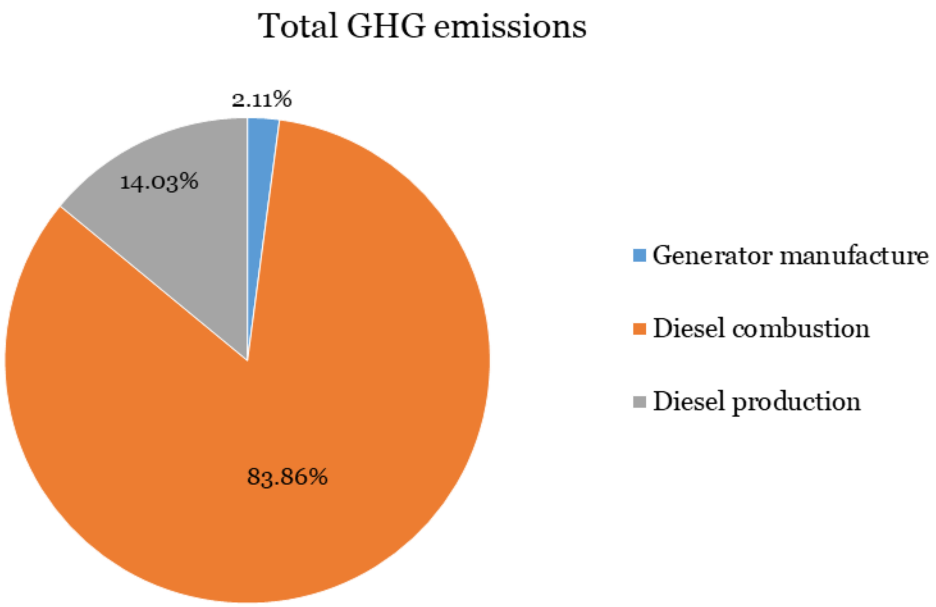

Figure 4-11: Relative contributions to the total GHG emissions of the diesel generator system (Remote scenario).

4.2.7.3 Comparison with the literature

In order to compare the results with the literature we divide the total GHG emissions by the energy delivered from the diesel generator, obtaining 893.2 $kgCO_2eq/MWh$ (Table 4-57).

Table 4-57: Total GHG emissions rate per electricity delivered by the diesel generator in the Remote scenario.

Total GHG emissions	Total energy provided by the diesel generator	Total GHG emissions rate	
$kgCO_2 eq$	*MWh*	*$kgCO_2 eq/MWh$ delivered by the diesel generator*	*$kgCO_2 eq/kWh$ delivered by the diesel generator*
637,876.157	714.122	893.232	0.893

Paper [43] presents in the introduction an average value of life-cycle CO_2eq emissions of electricity production from diesel equal to about 0.800 $kgCO_2$eq/kWh, taken from [125] which in turn uses as source the document [126]. The result value of [43] is instead 1.1912 $kgCO_2$eq/kWh, but the fuel considered is unleaded gasoline and not diesel, so a comparison cannot be made. In the study [89], a value of 1.27 $kgCO_2$eq/kWh is reported from study [123] which takes the value from paper [124], the same value also reported by [119] always from [124]. In the study presented in [124], the LCA of the diesel generator includes the manufacture of the generator, the fuel extraction, refining and transportation and the fuel combustion whose emissions are 3.13 $kgCO_2$eq per kg of diesel, a value similar and lower of the one assumed in our study (3.405 $kgCO_2$eq/kg). The final value is instead higher than the emissions per kWh of our plant (0.893 $kgCO_2$eq/kWh) because of the additional transport phase not accounted in our study and mostly because of the low efficiency of the small generator which consumes about 0.336 kg of diesel per kWh produced, while the generator assumed for the Froan plant has an average fuel consumption of 0.220 kg/kWh. In [95], the study from which we have taken the data of the manufacturing and fuel combustion phase, the obtained emissions by the generator are also higher than our study, 66,118 $kgCO_2$eq to produce 162.5 kWh every month for 20 years (39,000 kWh in total), i.e. 1.695 $kgCO_2$eq/kWh. The higher value is again mostly due to the higher fuel consumption of the generator, 0.53 l/kWh (0.445 kg/kWh), and slightly because of the additional transport phase accounted in the total result. In paper [117], instead, the environmental impact of the 65-kW diesel generator in the microgrid is lower than the Remote plant output. The emissions are 1,030,000 $kgCO_2$eq, including raw materials extraction, energy inputs from manufacturing, transportations, use phase (only diesel combustion and lubrification oil production) and disposal phase. Given the energy produced by the generator, 212 kWh per day for 20 years (1,547,600 kWh in total), an emission rate of 0.666 $kgCO_2$eq/kWh can be found. The lower value is probably caused by the exclusion of the impacts due to the diesel production and by the lower fuel consumption rate of the generator, 0.23 l/kWh (0.193 kg/kWh), instead of 0.220 kg/kWh. Finally, the value found in our study is within the range assessed in paper [119], which estimates the amount of carbon footprints emitted from diesel generators in terms of carbon dioxide at various rated power (from 2 to 5 kW) and emissions factor (from 1 to 5 $kgCO_2eq/l$). The results of [119] show a range between 0.41 and 3.24 $kgCO_2eq/kWh$. Table 4-58 resumes the comparison of the value of the Remote diesel generator with the literature.

Table 4-58: Comparison of the total GHG emissions rate of the diesel generator system in the Remote scenario with literature results.

Sources	Infos	GHG combustion emissions	Diesel consumption	Total GHG emissions per energy delivered by the diesel generator
-	-	*$kgCO_2 eq/kg$*	*kg/kWh*	*$kgCO_2 eq/kWh$*
Remote	-	3.405	0.220	0.893
[43, 125, 126]	-	-	-	0.800
[89, 119, 123, 124]	Transports included	3.130	0.336	1.270
[95]	Transports included	3.405	0.445	1.695
[117]	Transports, lubrification oil production and EOL included, no diesel production	-	0.193	0.666
[119]	Ranges of rated power and diesel emission factors	-	-	0.410 - 3.240

4.2.8 Remote scenario results

Figure 4-12 (modified from [21]) resumes in a schematic way the components considered in the LCA of the Remote plant.

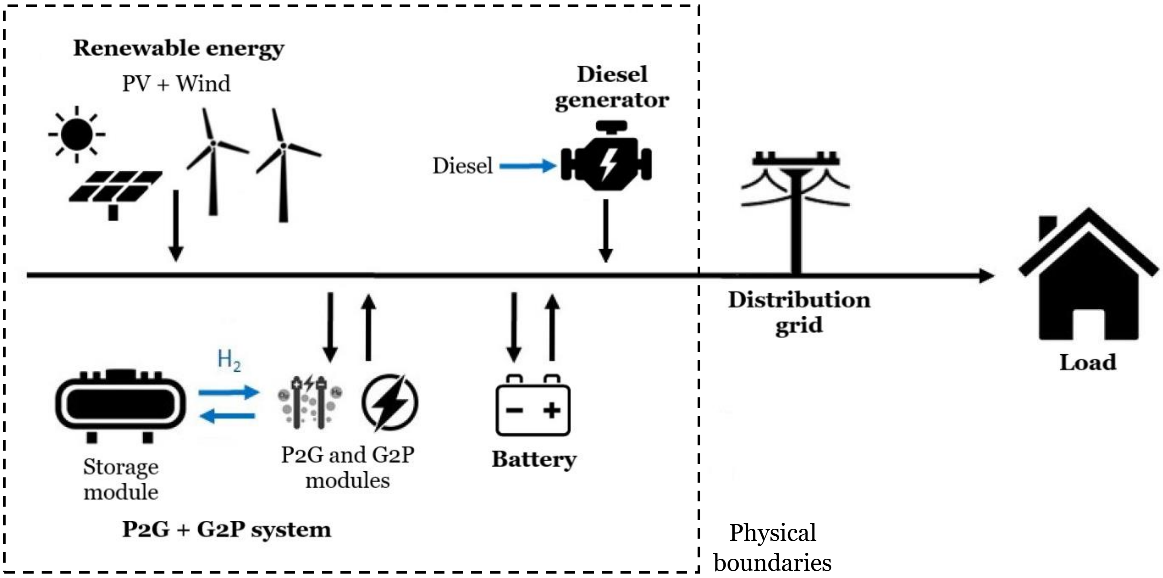

Figure 4-12: LCA physical system boundaries of the Remote scenario [21].

The relative contributions of each component to the total impact are shown in Figure 4-13 and the obtained results for each component, with the total GHG emissions rate of the Remote scenario, are summarized in Table 4-59.

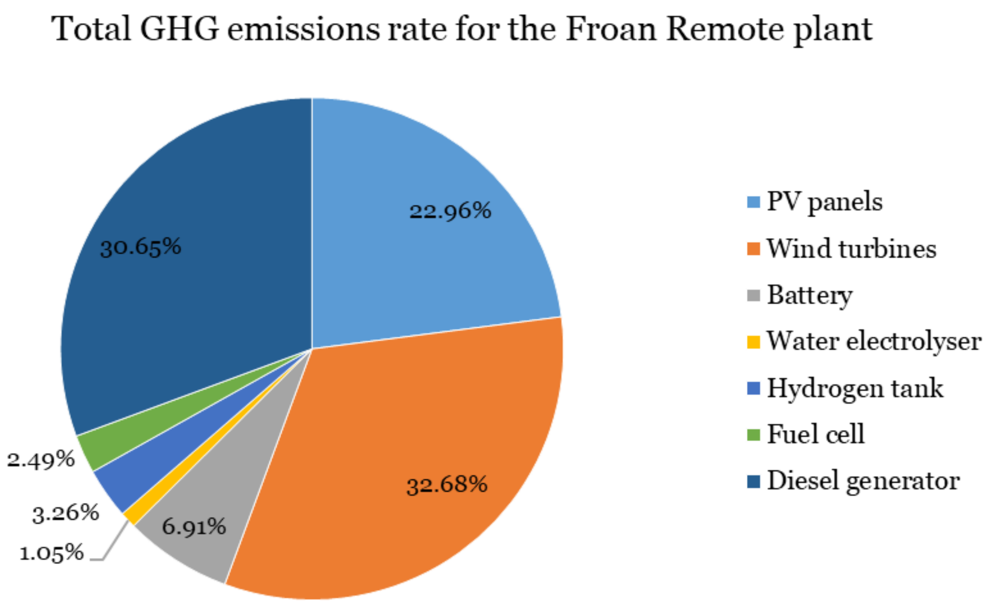

Figure 4-13: Relative contributions of each subsystem to the total GHG emissions of the Remote scenario.

Table 4-59: Relative contributions of each subsystem and total GHG emissions rate of the Remote scenario.

GHG emissions rate for each component							Total GHG emissions rate
$kgCO_2 eq/MWh$							*$kgCO_2 eq/MWh$*
PV panels	Wind turbines	Battery	Water electrolyser	Hydrogen tank	Fuel cell	Diesel generator	Froan Remote plant
33.455	47.627	10.069	1.525	4.749	3.631	44.662	**145.716**

The three energy production systems have the biggest impacts (86.29%) with, in decreasing order, 32.68% due to the wind turbine, 30.65% accounted for the diesel generator and 22.96% caused by the PV installation. Even if the diesel generator produces only 5% of the total energy, it has the second highest share of environmental impacts, strongly because of the emissions due to the combustion phase. The storage systems have instead a lower environmental impact (13.71%). Battery has a share of 6.91%, slightly higher than the 6.80% of the hydrogen system composed by the electrolyser (1.05%), the storage tank (3.26%) and the fuel cell (2.49%).

4.3 Cable scenario

One of the alternatives to the renewable plant is the substitution of the existing submarine cables connecting the islands to the mainland. In this scenario, almost all the electricity is assumed provided by the sea cables from the grid except for a small part generated by a diesel generator in case of interruptions or malfunctions of the electric connection to the mainland. Figure 4-14, modified from [21], offers a schematic view of the described scenario, including its components and the physical boundaries of the LCA analysis.

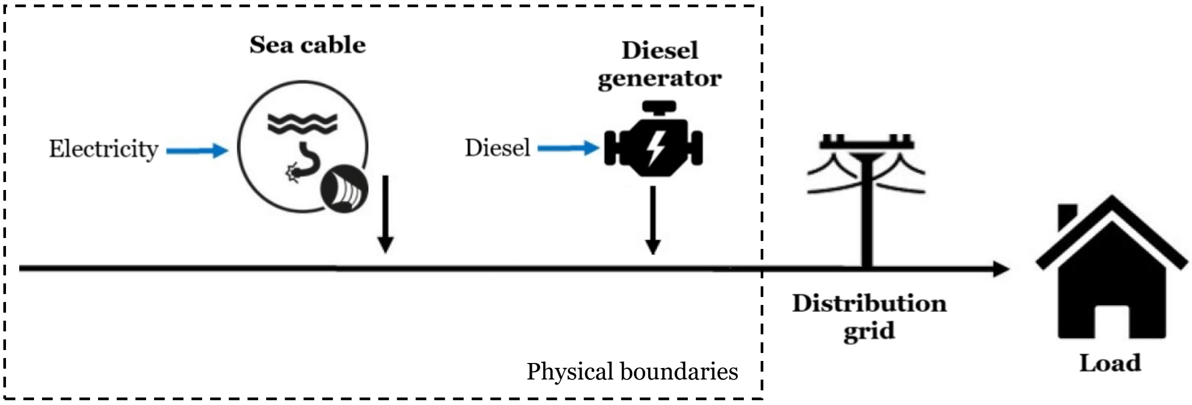

Figure 4-14: LCA physical system boundaries of the Cable scenario [21].

Assuming the annual energy required by the load equal to the one of the Remote scenario (571.3 MWh/y) and the same lifetime of 25 years, we can find the annual and total energy provided by the sea cable (98%) and by the generator (2%), summarized in Table 4-60. The percentage of electricity not provided by the cable is assessed according to failure rates and repair times found in literature. A more detailed explanation is present in Section 4.3.1.2, regarding the LCI of the sea cable.

Table 4-60: Annual and total energy exchanges in the Cable scenario.

Annual energy from the sea cable	Total energy from the sea cable	Annual energy from the diesel generator	Total energy from the diesel generator	Annual energy to the load	Total energy to the load
MWh/y	*MWh*	*MWh/y*	*MWh*	*MWh/y*	*MWh*
559.872	13,996.788	11.426	285.649	571.297	14,282.437

A detailed analysis of the scenario is provided in the next sections.

4.3.1 Submarine cable

4.3.1.1 Characteristics

The actual electrical connection is composed by two sea cables with a nominal voltage of 11 kV, owned by TrønderEnergi Nett AS and orange-highlighted in Figure 4-15 (modified from [VI]). The first one (FRØ030) has been installed in 1986 between Rottingen, reached by the mainland distribution system (green-coloured in Figure 4-15), and Gjæsingen, for a total length of 13.629 km according to the Norwegian Water Resources and Energy Directorate (NVE) [V]. The second one (FRØ031), installed in 1991 and 9.806 km long [V], connects instead Gjæsingen with Sørburøy, where the distribution system starts again covering all the Froan islands.

Table 4-61: Characteristics of the sea cables connecting the Froan Islands to the mainland [V].

Cable name	Installation year	Rated voltage	Length
-	-	*kV*	*km*
FRØ030 (Rottingen-Gjæsingen)	1986	11	13.629
FRØ031 (Gjæsingen-Sørburøy)	1991	11	9.806
FRØ030 + FRØ031	1986-1991	11	23.435

Figure 4-15: Sea cables electrically connecting the Froan Islands to the mainland [VI].

4.3.1.2 LCI and comparison with the literature

In this scenario both the sections are substituted for the total length of 23.435 km. The installation and dismantling of the new sea cables are included in our analysis, while the dismission of the old cables is not considered, since they must be removed also in the other scenarios. The maintenance and the manufacturing phase are also included. Figure 4-16 shows the boundaries of our study.

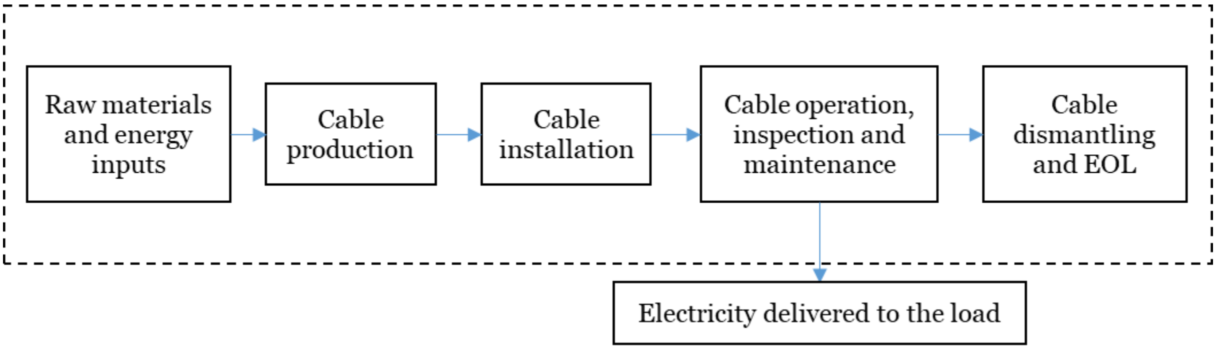

Figure 4-16: LCA boundaries assumed for the submarine cables system.

In literature there are no studies regarding the precise LCA of the single sea cable, while in general the analysis is present in a more general LCA of energy plants. This is the case of papers [92], [140], [94], [129] that consider the LCA of offshore wind power systems where sea cables are also present. In particular, studies [92] and [94] calculate the life-cycle energy, emissions and cost-benefits of an offshore wind farm based in China and paper [140] evaluates the environmental impacts and energy benefits of offshore wind power systems using the LCA and a net energy analysis. Document [129] presents instead the environmental impacts regarding the offshore wind power production and the development of an offshore grid in the North Sea. In this paper, four LCA's are conducted, one about an entire offshore wind farm and three analysing different submarine cables. High voltage cables in alternating current (HVAC) used internally in the plant (33 kV) or to transmit power from the wind farm (132 kV) and in direct current (HVDC) for long-distance submarine power transmission (450 kV) are studied.

Since in our study the cables voltage (11 kV) and lengths (13.629 km and 9.806 km) are relatively small, the best option is the alternating current. HVDC technology is preferred for long distance and high voltage power transmission because of the lower losses of capacity and power, the fewer cables required, the lower charging current and reactive power needed and the absence of skin effect, but it requires extra converters since the mainland transmission and distribution grid works with AC. Then, despite the higher losses and the length and voltage limitations, the AC cable systems have a more mature technology and they are the most cost-effective alternative for limited voltage and lengths [129]. According to paper [141], cited in [129], the point when DC technology become cheaper than AC is estimated to be between 30 and 250 km, values higher than our cable length. The solution chosen is then a medium-voltage AC submarine cable, in particular a three-core cable (including a fibre optic cable not relevant for our study) provided by Nexans, the 2XS(FL)2YRAA 6/10 (12) kV cable, with a nominal voltage of 10 kV. The conductor material is Copper and the insulation is composed by cross-linked polyethylene (XLPE). Figure 4-17, taken from [129], represents the selected cable technology with the different construction layers.

Figure 4-17: Construction layers of the XLPE three-core cable provided by Nexans [129].

Besides the conductor (1) and the insulation (2) layers, there are others important parts composing the cable, such as the semi-conductive screening layer (2,4,5), which smooths the electric field and reduces electrical stress concentrations and the metallic laminated sheath (6), which carries the eventual fault currents in case of damage and helps in grounding the cable. The final layers of the cable, the armor (11) and the external protection (12), have instead the function of protecting the cable from the external environment [129].

Among the different possible conductor sections, we assume the size of 70 mm^2 for each core of Copper. The reasons for this assumption are described in detail in Section 4.3.2, regarding the electricity and they concern the power losses in the cable. Some of the main data of the selected cable, found in the datasheet [142] provided by Nexans, are summarised in Table 4-62 and Table 4-63.

Table 4-62: Main characteristics of the assumed 2XS(FL)2YRAA 6/10 (12) kV sea cable (a) [142].

Name	Insulation	Nominal insulation thickness	Conductor	Number of conductors (cores)	Conductor section	External diameter	Approximative weight
-	-	*mm*	-	-	*mm²*	*mm*	*kg/m*
2XS(FL)2YRAA	XLPE	3.4	Copper	3	70	77	9.9

Table 4-63: Main characteristics of the assumed 2XS(FL)2YRAA 6/10 (12) kV sea cable (b) [142].

Nominal voltage	Maximum operational voltage	Electrical resistance (1 core, 50 Hz, 90°C)	Total electrical resistance (3 cores, 50 Hz, 90°C)	Maximum current	Permissible transmission capacity (buried)
kV		*Ω/km*	*Ω/km*	*A*	*MVA*
10	12	0.34	1.02	241	4

Regarding the reliability of the subsea power cable, we can find in literature the failure rates and the repair times related to this technology. Reports [143] and [144], published in 2009 by the International Council on Large Electric Systems (CIGRE), study the submarine faults reported from 1990 to 2005 and state for AC-XLPE cables (60-220 kV) an average failure rate of 0.0705 failures per year and per 100 km of length. This value is significantly lower than the failure rates of MVAC cables (10-66 kV) reported in paper [133], which presents a review of European offshore wind farm transmission failures regarding the subsea cables. The mean AC failure rate assessed by [133], concerning European wind farm connections, is equal to 0.00299 failures/km/year, a value more than four times higher. Concerning the repair times, we take the information from paper [136] that analyses subsea power cable projects in Europe with main focus on technology, reliability and environmental impact in order to evaluate the suitable technology in Icelandic conditions. The activities required to repair the subsea cable damage are several and require different durations. In particular, the waiting on weather (WOW) window, which is the time spent to wait for acceptable weather to work, is the most

Table 4-64: Waiting on weather windows [136].

Period of the year	WOW time
-	*days*
October-January	40-45
February-March	25
April-May	5
August-September	5
June-July	2

variable. According to [136] that cites [145], the WOW time of the North Sea in function of the period of the year is shown in Table 4-64, where the average value between the large range of 2-45 days is 17 days.

Table 4-65, presented by [136], which refers to [143] and [146], shows the duration time of the different activities required to repair the cable.

Table 4-65: Sea cable repairing time (total and subdivided for each activity required) [136].

Activity	Duration time
-	*days*
Fault location	5
Mobilisation to uncover cable	10
Uncover the cable	3
Mobilisation to perform repair	12
Wait for weather window (average)	17
Wait for weather window (maximum)	45
Time for repair itself	10
Total repair time (average WOW)	57
Total repair time (maximum WOW)	85

In order to be conservative, we assume for our analysis the average failure rate of paper [133] and the highest repair time assessed in [136]. Considering the 25 years lifetime assumed and the total cable length of 23.345 km, we can calculate the number of failures during lifetime. The found value is then rounded up in order to obtain an integer value. Knowing the value of failures and the total repair time for each failure, we obtain the total repair time during lifetime and the percentage of unavailability of the cable system. This value is then rounded up in order to be more conservative and a 2% of unavailability is assumed for our analysis. Table 4-66 and Table 4-67 resume the results.

Table 4-66: Expected sea cables number of failures during lifetime.

Average failure rate [133]	Considered lifetime	Cable length	Number of failures during lifetime	Rounded up number of failures during lifetime
failures/km/year	*years*	*km*	*failures*	*failures*
0.00299	25	23.435	1.752	2

Table 4-67: Expected sea cables unavailability during lifetime.

Total repair time [136]	Total repair time during lifetime	Percentage of unavailability during lifetime	Rounded up percentage of unavailability during lifetime
days/failure	*days*	*%*	*%*
85	170	1.863	2

We are now interested in the LCA of the 33-kV submarine cable presented by paper [129]. The inventories are based on the project of the offshore wind farm Havsul 1 located in Norway, in which the 33-kV cables constitute the internal connections. The studied cables have a three-core copper conductor, a XLPE insulation, the sheath composed by lead and a layer of galvanized steel armor. Different conductor cross-sections are assumed for the internal connections that compose a total length of 63.3 km with a required transmission capacity of 390 MW and a lifetime expectancy of 40 years [129], [147]. Since this lifetime is higher than the 25 years assumed in our scenario, only one cable is needed for each section of the total length. Table 4-68 resumes the main characteristics.

Table 4-68: Main characteristics of the submarine cable studied in paper [129].

Source	Year	Cable type	Voltage	Insulation	Conductor	Total length	Required transmission capacity	Lifetime expectancy
-	-	-	*kV*	-	-	*km*	*MW*	*years*
129	2011	HVAC	33	XLPE	Three-core Copper	63.3	390	40

The analysis includes the manufacturing phase, the installation of the cables (laid and buried one meter into the seabed), their inspection and maintenance during operation, the dismantling and EOL phase and the transports needed during all the life-cycle phases, both by land and by sea. According to the system boundaries assumed in our analysis, the contribution of the transports is not considered. The functional unit assumed is 1 MW*km, considering 1 MW of transmission capacity needed in the cable and 1 km of cable length.

Regarding the manufacture, the material amount required for the cables are calculated from the data presents in the technical product sheets. The total values found are then divided by the total length of 63.3 km, obtaining the average percentages and amounts of material required (t/km) (Table 4-69).

Table 4-69: Percentages and normalized amounts (per sea cables length) of materials needed in the sea cables manufacture [129].

Average amounts and percentages of materials needed [129]										
Copper		Polyethylene (XLPE)		Polypropylene		Lead		Steel (galvanized)		Total
t/km	*%*	*t/km*	*%*	*t/km*	*%*	*t/km*	*%*	*t/km*	*%*	*t/km*
6	20.69	2	6.90	1	3.45	8	27.59	12	41.38	29

The relative percentages of each material are similar to the ones stated in studies [94] and [92] as we can see in Table 4-70.

Table 4-70: Percentages and normalized amounts (per sea cables length) of materials needed in the sea cables manufacture [94] [92].

Average amounts and percentages of materials needed [94, 92]										
Copper		Polyethylene		Polypropylene		Lead		Steel		Total
t/km	*%*	*t/km*	*%*	*t/km*	*%*	*t/km*	*%*	*t/km*	*%*	*t/km*
8.12	22.55	2.29	6.36	1.54	4.28	9.65	26.80	14.41	40.02	36.01

Concerning the installation, the operation and the dismantling phases, the information about vessels and work time presented in [129] are shown in Table 4-71.

Table 4-71: Technical information about the installation, operation and EOL phases [129].

LCA phase (vessel type)	Number of vessels	Fuel type	Work time	Fuel consumption
-	-	-	*days*	*l/h*
Installation (cable lay vessel with plough)	1	Diesel	8	572.9
Inspection and maintenance during 40 years operation	1	Diesel	156	150
Dismantling and EOL (cable lay vessel with plough)	1	Diesel	6.8	572.9

The results of the analysis are presented in the Table 4-72. The maintenance phase of 40 years operation is scaled down to the assumed 25 years operation of our plant through a simple proportion.

Table 4-72: Total GHG emissions rate and contributions of each LCA phase according to [129] (a).

GHG emissions rates through the different LCA phases [129]					
Manufacture	Installation	Maintenance and inspection (40 y)	Maintenance and inspection (25 y)	Dismantling and EOL	Total (25 years and without transports)
$kgCO_2eq/MW/km$					
129.540	13.142	72.202	45.126	12.065	199.874

Knowing the total transmission capacity of the cables, 390 MW, we can calculate the emissions produced by each km of the cable (Table 4-73).

Table 4-73: Total GHG emissions rate and contributions of each LCA phase according to [129] (b).

GHG emissions rates through the different LCA phases [129]				
Manufacture	Installation	Maintenance and inspection (25 y)	Dismantling and EOL	Total (25 years and without transports)
$kgCO_2eq/km$				
50,520.670	5,125.466	17,599.213	4,705.346	77,950.695

Concerning the phases related to the installation, the operation and the dismantling, we assume for our analysis the same values of paper [129]. Regarding the manufacturing phase instead, since the mass of our 10-kV cable (9.9 t/km) is lower than the mass of the 33-kV cable studied in [129] (29 t/km), we scale down the emissions rate, assuming the same relative percentages of needed materials already shown in Table 4-69. Firstly, we divide the resulting value of the manufacturing phase by the 33-kV cable mass obtaining the GHG emissions related to the manufacture of one kg of cable, a value very similar to the ones obtainable from studies [92] and [94] and reported in Table 4-74. Then, in order to find the GHG emissions per km of our 10-kV cable, we multiply its mass by the emissions per kg of cable found in [129].

Table 4-74: Manufacturing GHG emissions per cable mass and length from literature.

Source	GHG emissions per cable mass manufacture	GHG emissions per cable length manufacture (10 kV)
-	*$kgCO_2eq/kg$ of cable*	*$kgCO_2eq/km$*
[129]	1.742	17,246.712
[92]	1.658	-
[94]	1.665	-

The following Table 4-75 resumes the assumed emissions per cable length assumed for our Froan scenario.

Table 4-75: Total GHG emissions per cable length and contributions of each LCA sea cables phase in the Cable scenario.

Froan GHG emissions per cable length through the different LCA phases [129]				
Manufacture (10-kV cable)	Installation	Maintenance and inspection (25 y)	Dismantling and EOL	Total (25 years and without transports)
$kgCO_2 eq/km$				
17,246.712	5,125.466	17,599.213	4,705.346	44,676.737

Knowing the total length of the 10-kV cable (23.435 km), we can find the total environmental impacts of each phase and for the entire life-cycle (Table 4-76).

Table 4-76: Total GHG emissions and contributions of each LCA sea cables phase in the Cable scenario.

Froan GHG emissions through the different LCA phases [129]				
Manufacture (10-kV cable)	Installation	Maintenance and inspection (25 y)	Dismantling and EOL	Total (25 years and without transports)
$kgCO_2 eq$				
404,180.335	120,116.376	412,441.284	110,270.782	1,047,008.776

Figure 4-18 shows also the relative contribution of each phase to the total life-cycle GHG emissions.

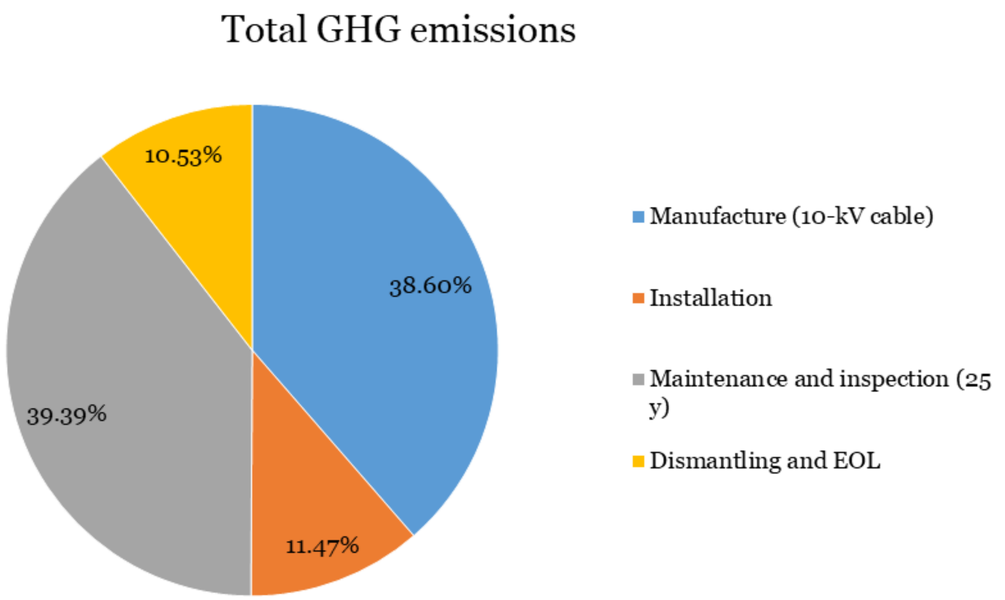

Figure 4-18: Relative contributions to the total GHG emissions of the submarine cable system.

As we can see, the operation of the cable including maintenance and inspection with vessels is the most impacting phase (39.4%), closely followed by the 38.6% of the manufacture. Installation and dismantling have similar and lower impacts since they required similar operations required only once during the life cycle of the cables.

Knowing the total GHG emissions related to the submarine cables and the total energy delivered to the Froan load, we can calculate the environmental impacts per MW of electricity delivered. Results are shown in Table 4-77.

Table 4-77: Total GHG emissions rate (in functional unit) of the submarine cable system in the Cable scenario.

Total GHG emissions	Total energy delivered	Total GHG emissions rate
$kgCO_2eq$	*MWh*	*$kgCO_2eq/MWh$*
1,047,008.776	14,282.437	**73.307**

4.3.2 Electricity

The emissions related to the production and distribution of the mainland electricity delivered by the cable must be taken into account. We know the net electricity delivered to the Froan load, but we should find the electrical losses in the cables in order to know the total electricity withdrawn from the grid to cover the load. In order to calculate the losses, we use the electrical resistance per cable length assessed in the datasheet of cables "2XS(FL)2YRAA 6/10 (12) kV" provided by Nexans [142]. Knowing the resistance per metre of cable and the total length required, we can calculate the total electrical resistance (R_{el}) of the cables. According to the 2-years simulations of the Froan load, we know the average power (P_{el}) required each hour and we can calculate the average current flowing each hour in the cable with rated voltage V equal to 10 kV (equation (11)).

$$I = \frac{P_{el}}{V} \tag{11}$$

In order to find the power losses (P_{loss}), we use instead the equation (12).

$$P_{loss} = R_{el} \cdot I^2 \tag{12}$$

Knowing the hourly average power losses, we can calculate the total energy losses of the 2-years simulation and the yearly average energy losses. We repeat this methodology for different conductor sections having different electrical resistance per cable length in order to find all the possible energy losses. We assume to select the smallest conductor section having the electrical losses lower than 2% of the total energy delivered by the cable. The conductor section of 70 mm² is then assumed according to the results shown in Table 4-78.

Table 4-78: Yearly electricity lost and withdrawn in the submarine cables for various conductor sizes.

Conductor size	Electrical resistance per cable length	Cable length	Total electrical resistance	Average energy losses	Electricity delivered by the cable to the load	Relative energy losses	Electricity withdrawn by the cable from the mainland grid
mm²	*Ω/km*	*km*	*Ω*	*MWh/y*	*MWh/y*	*%*	*MWh/y*
50	1.47	23.435	34.450	12.206	559.872	2.180	572.077
70	1.02	23.435	23.904	8.469	559.872	1.513	568.341
95	0.75	23.435	17.576	6.227	559.872	1.112	566.099
120	0.6	23.435	14.061	4.982	559.872	0.890	564.853
150	0.48	23.435	11.249	3.985	559.872	0.712	563.857
185	0.39	23.435	9.140	3.238	559.872	0.578	563.110
240	0.3	23.435	7.031	2.491	559.872	0.445	562.362

Knowing the total electricity needed to be carried by the cable from the mainland grid, we can calculate the environmental impacts related to the electricity of the main grid. The average equivalent carbon dioxide intensity of the Norwegian electricity is taken from Ecoinvent 3. It is equal to about 29.2 $kgCO_2eq/MWh$, a value very small thanks to the very high renewable contribution to the Norwegian electricity production, 98% of the total, according to the "Electricity disclosure 2018" provided by NVE [V]. Multiplying this value by the total electricity withdrawn from the mainland grid, we obtain the total GHG emissions related to the electricity and the environmental impacts per MWh of energy delivered, dividing the total emissions by the total energy required by the load. Table 4-79 resumes the results.

Table 4-79: Total GHG emissions rate (in functional unit) of the electricity system in the Cable scenario.

Electricity withdrawn by the cable from the mainland grid	Total electricity withdrawn by the cable from the mainland grid	GHG emissions rate per MWh_{el} (Norway) [Ecoinvent 3]	Total electricity GHG emissions (Norway)	Total energy delivered	Total GHG emissions rate
MWh/y	*MWh*	*$kgCO_2eq/MWh$*	*$kgCO_2eq$*	*MWh*	*$kgCO_2eq/MWh$*
568.341	14,208.517	29.181	414,619.727	14,282.437	**29.030**

The resulting value is obviously very similar to the carbon intensity of the Norwegian electricity. It is a little smaller since we divide the total emissions by the total energy delivered that is a little higher than the total electricity withdrawn from the mainland grid.

4.3.3 Diesel generators

4.3.3.1 *Characteristics*

The purpose of the diesel generator is to cover the load in case no electricity is delivered by the cables. Since the cable unavailability is assumed equal to 2%, the generator should provide an amount of energy equal to 2% of the total load, so about 11.43 MWh per year and 285.65 MWh during the lifetime. According to the simulations of the Froan load, we assume the same diesel generator chosen in the Remote plant scenario, the HGM138 Googol Diesel Power Generator provided by Honny Power [96]. The reasons of the choice are related to the maximum power required and they are the ones already assessed in Section 4.2.7.1. The main characteristics of the assumed generator are resumed in Table 4-80.

Table 4-80: Main characteristics of the HGM138 Googol Diesel Power Generator (by Honny Power) [96].

Genset prime output		Rating power factor	Rating speed	Rating frequency	Rating voltage	Genset weight	Genset size (LxWxH)	Genset fuel consumption	
								At 75% of prime output	At 100% of prime output
kW	*kVA*	-	*rpm*	*Hz*	*V*	*kg*	*mm*	*g/kWh*	*g/kWh*
100	125	0.8	1500	50	400	1250	2300 x 850 x 1350	225	215

We can then calculate the total mass of diesel consumed, multiplying the average fuel consumption (220 g/kWh) by the generator energy production (Table 4-81).

Table 4-81: Total diesel needed and consumed in the Cable scenario.

Average fuel consumption [96]	Total energy provided by the generator	Total diesel needed
g/kWh	*MWh*	*kg*
220	285.649	62,842.721

4.3.3.2 *LCI and comparison with the literature*

Regarding the literary review on previous LCA of diesel generators we refer to Section 4.2.7.2. In order to calculate the environmental impacts of the diesel generator we consider the same analysis, calculations, assumptions and literature data assumed in Section 4.2.7.2. The only differences are the total amount of diesel consumed and the estimated operational hours, being 2% instead of 5% of the total hours of the 25 years lifetime. The resulting value of 4,380 operational hours is however lower than the lifetime range of 15,000-30,000 assessed by [137], meaning that also in this scenario only one generator is needed. Then, the total GHG manufacture emissions remain unchanged, while the impacts related to the diesel combustion and production change according to the different amount of diesel consumed. The following Table 4-82 and Table 4-83 present the modified results of this scenario.

Table 4-82: GHG emissions from the diesel combustion and production (Cable scenario).

Total diesel needed	**Fuel combustion**		**Fuel production**	
	GHG emissions per mass of diesel [95]	Total GHG combustion emissions	Troll WTT carbon intensity of diesel [90, 95]	Total GHG production emissions (Troll)
kg	*$kgCO_2eq/kg$*	*$kgCO_2eq$*	*$kgCO_2eq/kg$ of diesel produced*	*$kgCO_2eq$*
62,842.721	3.405	213,964.503	0.570	35,800.960

Table 4-83: Total GHG emissions rate (in functional unit) of the diesel generator system in the Cable scenario.

Total GHG manufacture emissions	Total GHG combustion emissions	Total GHG production emissions (Troll)	Total GHG emissions	Total energy production	Total GHG emissions rate
$kgCO_2eq$	*$kgCO_2eq$*	*$kgCO_2eq$*	*$kgCO_2eq$*	*MWh*	*$kgCO_2eq/MWh$*
13,462.5	213,964.503	35,800.960	263,227.963	14282.437	**18.430**

Figure 4-19 represents the relative contributions of each subsystem to the total environmental impacts. Compared to the chart of Section 4.2.7.2, we can see a similar repartition, even if the manufacturing phase is larger because of the lower amount of diesel consumed.

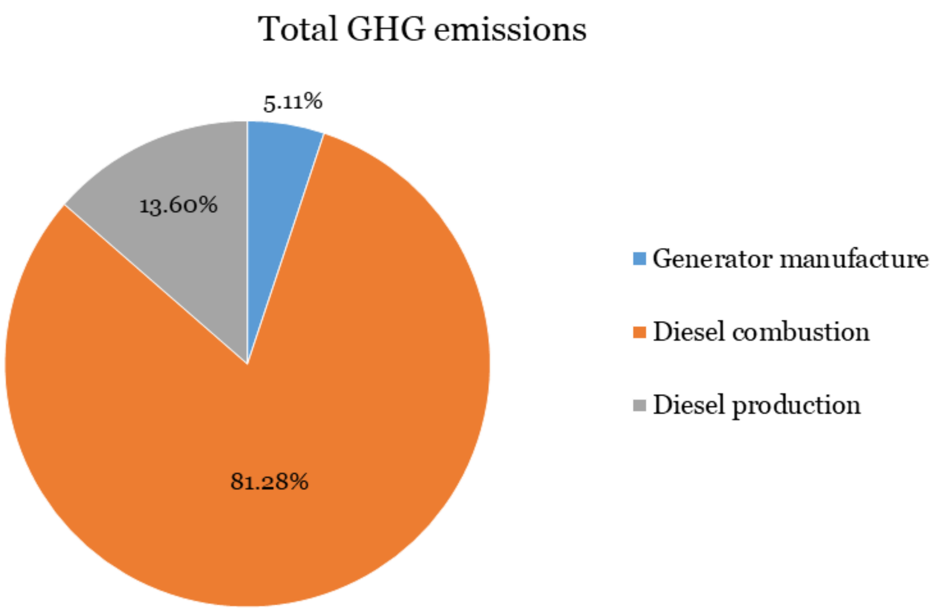

Figure 4-19: Relative contributions to the total GHG emissions of the diesel generator system (Cable case).

The equivalent carbon dioxide emissions per kWh delivered by the diesel generator are also calculated in order to make a comparison with the literature results (Table 4-84).

Table 4-84: Total GHG emissions rate per electricity delivered by the diesel generator in the Cable scenario.

Total GHG emissions	Total energy provided by the diesel generator	Total GHG emissions rate	
$kgCO_2eq$	*MWh*	*$kgCO_2eq/MWh$ delivered by the diesel generator*	*$kgCO_2eq/kWh$ delivered by the diesel generator*
263,227.963	285.649	921.509	0.922

The resulting value of 0.922 $kgCO_2eq/kWh$ is similar and higher to the one of the Remote scenario because of the lower energy production of the diesel generator. However, the found GHG emission rate is in accordance with the literature results discussed in Section 4.2.7.3, as we can see from Table 4-85, modified from Section 4.2.7.3.

Table 4-85: Comparison of the total GHG emissions rate of the diesel generator system in the Cable scenario with the previous scenario and literature results.

Sources	Infos	GHG combustion emissions	Diesel consumption	Total GHG emissions per energy delivered by the diesel generator
-	-	*$kgCO_2eq/kg$*	*kg/kWh*	*$kgCO_2eq/kWh$*
Cable scenario	-	3.405	0.220	0.922
Remote scenario	-	3.405	0.220	0.893
[43, 125, 126]	-	-	-	0.800
[89, 119, 123, 124]	Transports included	3.130	0.336	1.270
[95]	Transports included	3.405	0.445	1.695
[117]	Transports, lubrification oil production and EOL included, no diesel production	-	0.193	0.666
[119]	Ranges of rated power and diesel emission factors	-	-	0.410 - 3.240

4.3.4 Cable scenario results

The results previously assessed are summarized in Table 4-86, where we calculate also the total environmental impact of this scenario. Figure 4-20 shows the relative contribution of each subsystem considered.

Table 4-86: Relative contributions of each subsystem and total GHG emissions rate of the Cable scenario.

GHG emissions rate for each subsystem			Total GHG emissions rate
$kgCO_2 eq/MWh$			$kgCO_2 eq/MWh$
Submarine cable	Electricity	Diesel generator	Cable scenario
73.307	29.030	18.430	**120.768**

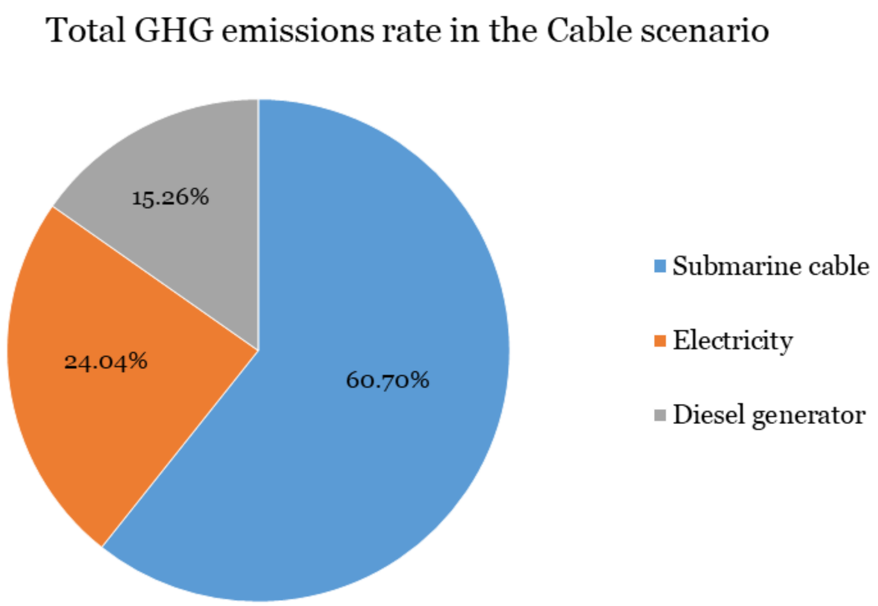

Figure 4-20: Relative contributions of each subsystem to the total GHG emissions of the Cable scenario.

The biggest contribution is related to the installed submarine cable (60.70%), followed by the electricity subsystem (24.04%) having a low impact mainly thanks to the low carbon intensity of the Norwegian electricity generated in the mainland. The emissions related to the diesel generator, including diesel production and combustion, have the smallest contribution (15.26%) in this scenario, but only because the diesel system should generate a very small part of the total load (2%).

4.4 Diesel scenario

4.4.1 Characteristics

The installation of diesel generators is the third scenario taken into account in order to cover the load of the Froan Islands. The electricity would be provided entirely by the generators placed on the islands. Figure 4-21, modified from [21], shows a simple scheme of the scenario, including its components and the physical boundaries of the LCA analysis.

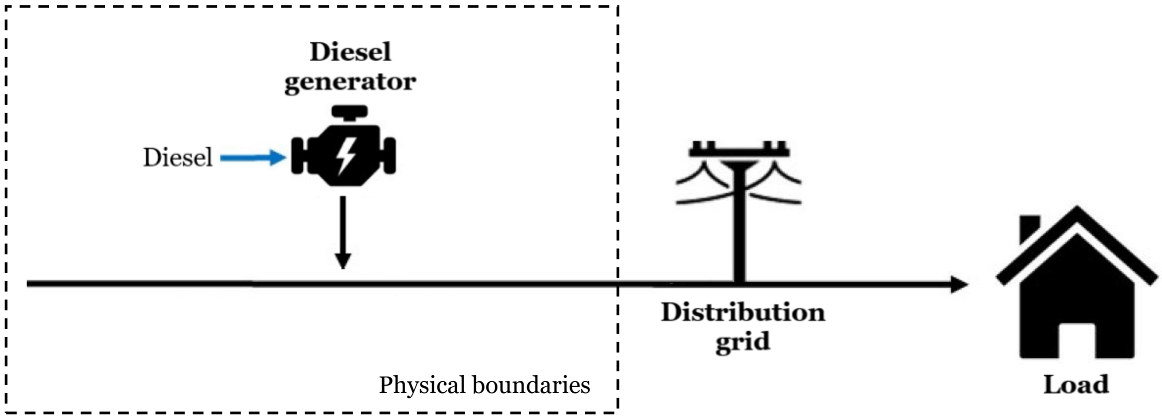

Figure 4-21: LCA physical system boundaries of the Diesel scenario [21].

Assuming the lifetime of 25 years and the annual load (571.3 MWh/y) already assessed in the Remote scenario, we can find the total electricity generated (Table 4-87).

Table 4-87: Annual and total energy exchanges in the Diesel scenario.

Annual energy provided by the diesel generators to the load	Total energy provided by the diesel generators to the load
MWh/y	*MWh*
571.297	14,282.437

Knowing the maximum power required according to the simulations (about 106 kW), we assume two diesel generators rated 54 kW, the generators model KD66W provided by Kohler Company [148], for a total capacity of 108 kW. In this scenario, we don't consider only one generator sized 100 kW, as in the previous ones, because the load is fully provided by the generators that are required to work continuously, differently from the other scenarios where the diesel generators provide electricity only on demand in case of malfunctions of the main energy system. Since they must work continuously at variable load, it is better having two small generators instead of a big one for different reasons. Firstly, the efficiency and the relative fuel consumption of a diesel generator depend not only on the size, but also on the real power production. In particular, the efficiency at partial load is lower than the one at full load [119], so having two small generators working at higher load is better than having a big one at lower load. Secondly, if one generator breaks or needs maintenance, the second one can momentarily supply to the load the total or at least a part of the required electricity.

The main characteristics of the chosen generators are summarized in Table 4-88.

Table 4-88: Main characteristics of the diesel generator model KD66W provided by Kohler Company [148].

Genset prime output		Rating speed	Rating frequency	Rating voltage	Genset dry weight	Genset size (LxWxH)	Genset fuel consumption		
							At 50% of prime output	At 75% of prime output	At 100% of prime output
kW	*kVA*	*rpm*	*Hz*	*V*	*kg*	*mm*	*l/h*	*l/h*	*l/h*
54	67	1500	50	400	980	1870 x 994 x 1360	8.5	12.0	16.0

Concerning the fuel consumption, even if its relationship with the power production is not necessarily linear [51], we assume three different linear relationships in order to approximate the real behaviour, since we know only three points of operation (four counting the no-load condition). Figure 4-22 represent graphically the linear approximations and the data of the fuel consumption, which are also resumed in Table 4-89 (assuming the diesel density equal to 0.84 kg/l according to [95]).

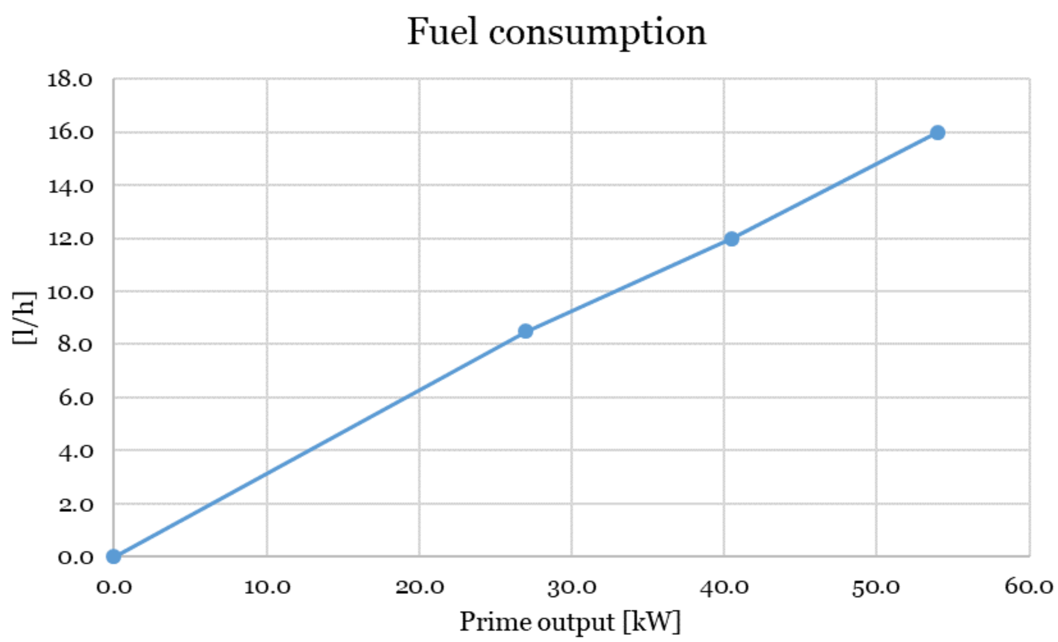

Figure 4-22: Fuel consumption of the diesel generator in function of the prime output.

Table 4-89: Fuel consumption of the diesel generator for different points of operation and prime output values.

Prime output		Fuel consumption	
%	*kW*	*l/h*	*kg/kWh*
100	54	16.0	0.249
75	40.5	12.0	0.249
50	27	8.5	0.264
0	0	0	0

The three linear approximations, shown in Figure 4-22, are used to calculate the hourly fuel consumption, according to the hourly simulation of the Froan load that assesses the hourly power required to the diesel generator. We take into account one year of simulation and we build the cumulative curve of the hourly average required power (Figure 4-23). The resulting total energy production of the one-year simulation is about 543.2 MWh/y, while the assumed annual load covered by the generators is 571.3 MWh/y. Then, the results obtained from the one-year simulation must be scaled-up to the assumed energy generation.

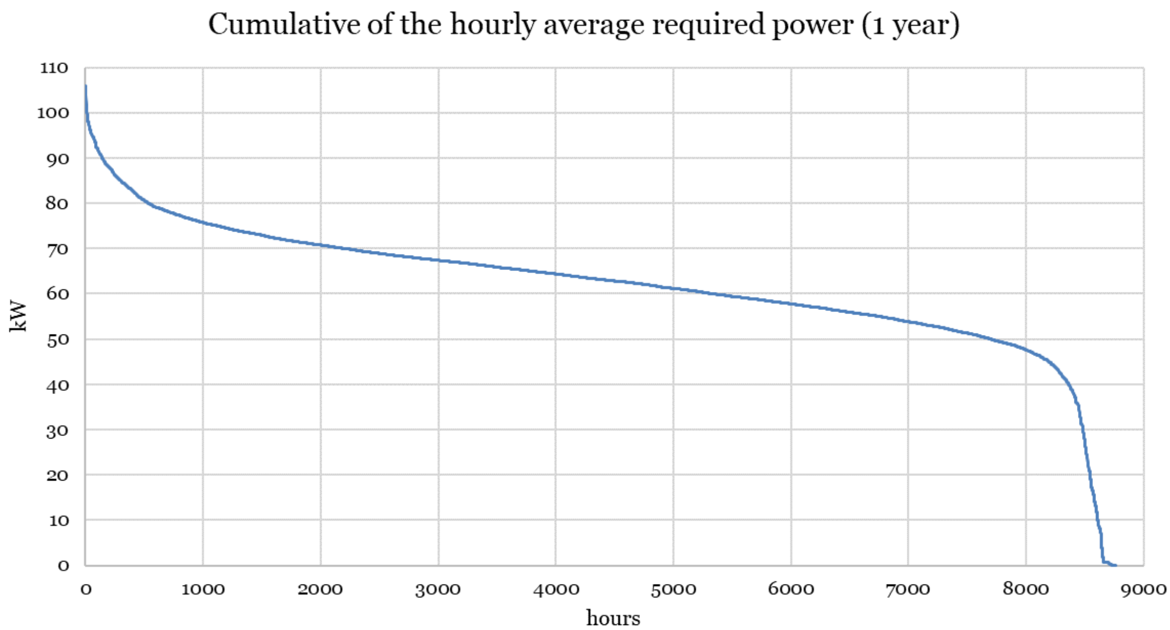

Figure 4-23: Cumulative curve of the hourly average power required by the Froan load (1-year simulation).

Now, according to this cumulative curve, we assume different load scenarios for the two working generators in order to cover the total load. In the first and in the second model, one motor is always kept at, respectively, 50% and 75% of its rated power (when possible), while the second follows the load. In the third one, we try to keep, as long as possible, one generator at 75% and the other at 50% of their rated power. In the last one, instead, we consider the power equally generated from the two motors that follow exactly the load. The following figures (Figure 4-24, Figure 4-25, Figure 4-26, Figure 4-27) report the four cumulative curves of the working points, expressed in percentage of rated power, corresponding to the four explained models.

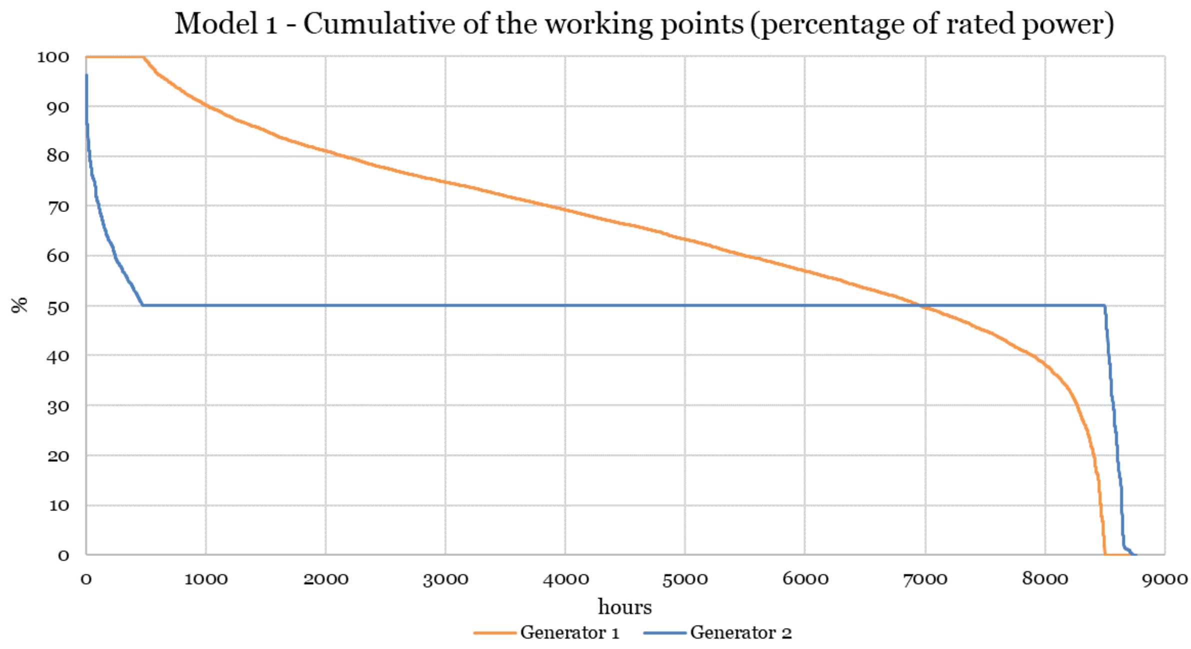

Figure 4-24: Cumulative curve of the generators working points (load model 1).

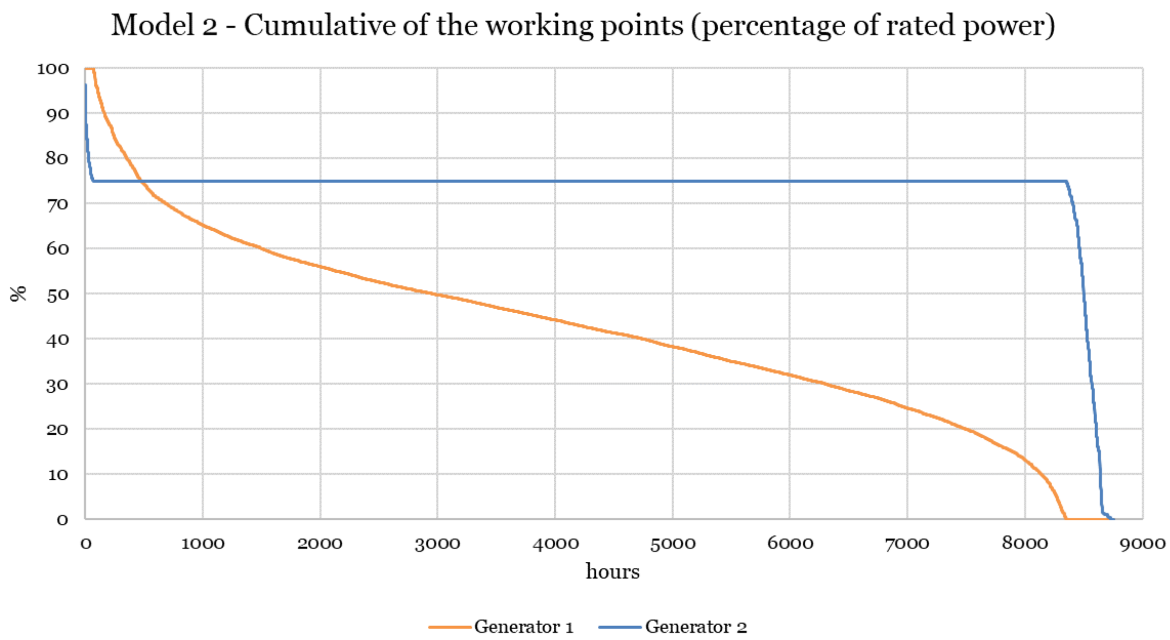

Figure 4-25: Cumulative curve of the generators working points (load model 2).

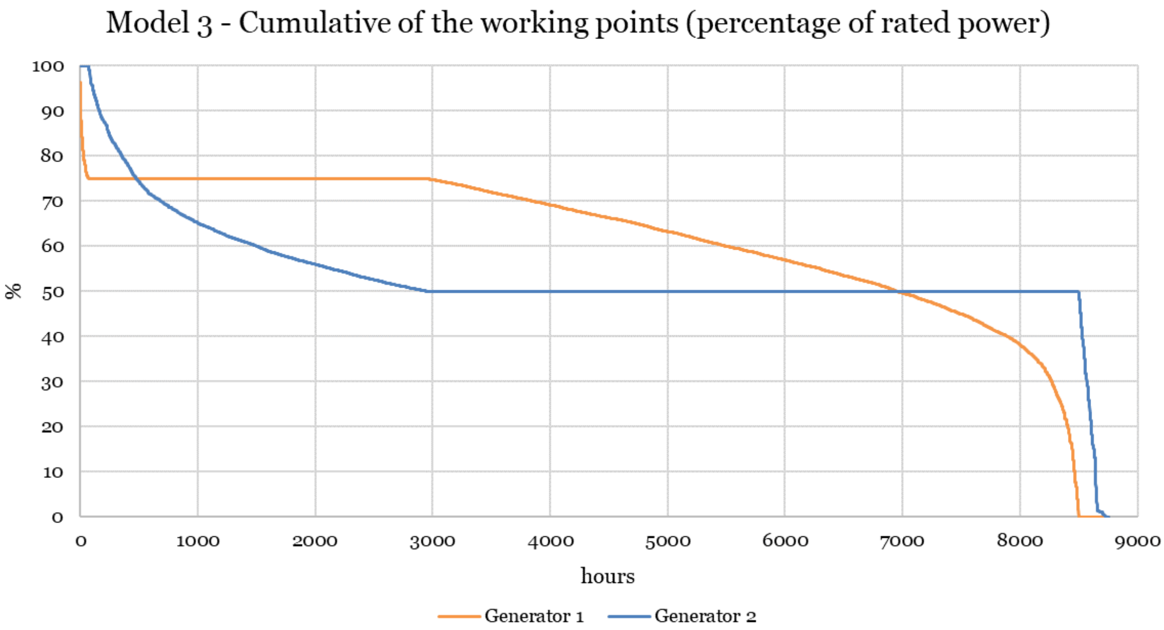

Figure 4-26: Cumulative curve of the generators working points (load model 3).

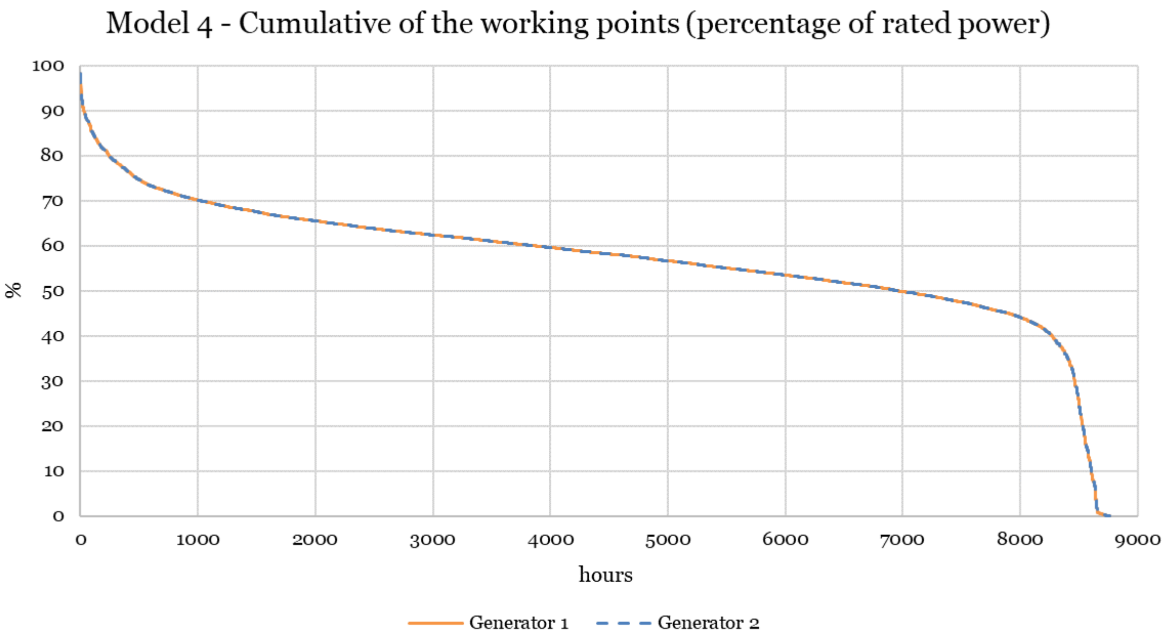

Figure 4-27: Cumulative curve of the generators working points (load model 4).

In order to select the most suitable model, we look at two interesting parameters. The first is the average annual fuel consumption, calculated summing all the hourly consumptions of the one-year simulation and aimed to be as low as possible. The second interesting value resulting from the analyses is the number of hours during which the generators are below the 50% of the rated power, excluding the no-load operation. We want to have this parameter as low as possible, in order to maintain the generator efficiency at reasonable values and because we have no data about the fuel consumption and the efficiency below 50%, but only the linear approximation until the no-load operation. Table 4-90, Figure 4-28 and Figure 4-29 show the results.

Table 4-90: Relevant parameters resulting from the load models.

Model	Annual fuel consumption	Total working hours below 50% of prime output
-	*l/y*	*h*
1	166,669.640	1,778
2	163,558.727	5,635
3	166,084.763	1,778
4	166,084.763	3,556

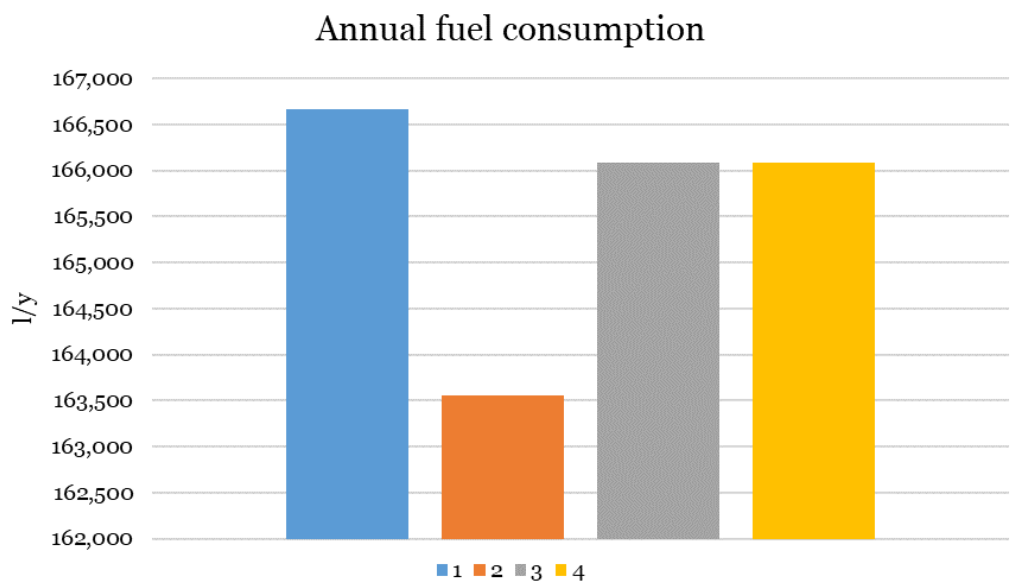

Figure 4-28: Annual fuel consumption resulting from the different load models.

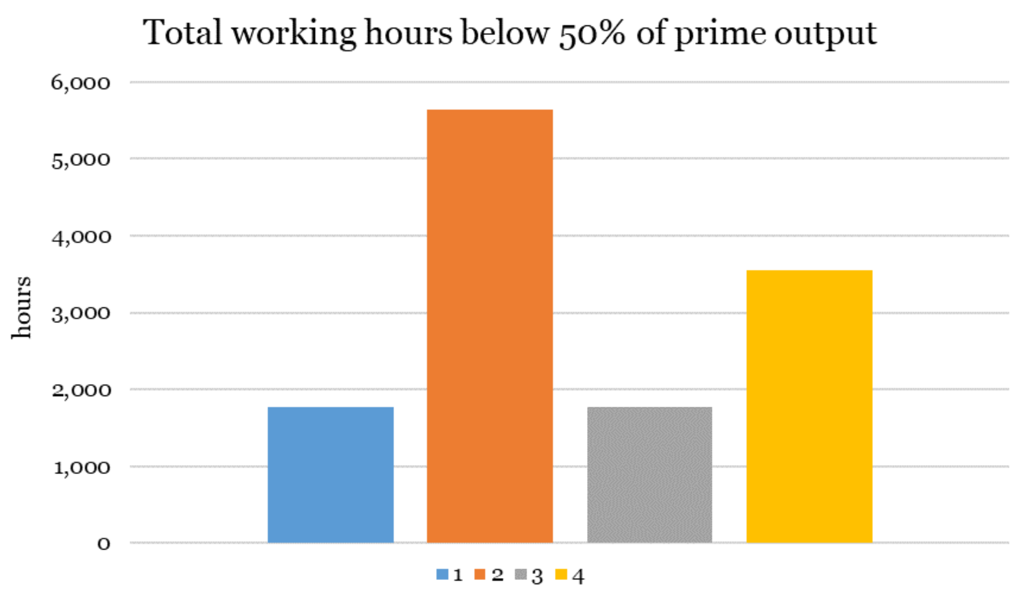

Figure 4-29: Working hours below 50% of prime output resulting from the different load models.

The second model has the lowest annual fuel consumption, but also the highest value of working hours below 50% of prime output. On the contrary, the first model has the highest consumption even if it has one of the lowest values for the second parameter. The third and fourth scenarios has instead an equal annual fuel consumption, but a very different number of working hours below 50% of rated power. Combining these parameters, we chose the third model and its annual fuel consumption as input values for our analysis of the diesel scenario. The average yearly working hours of this model are 8,498 and 8,733 for the two generators, for an average value of about 8,616 h/y and for a total of about 215400 h in the 25-years lifetime considered. The total fuel consumption can be also calculated, both in litres and in kilograms (with a diesel density of 0.84 kg/l according to [95]). Table 4-91 sums up the results for the one-year simulation and Table 4-92 shows the scaled-up values of fuel consumption, according to the assumed total load.

Table 4-91: Annual and total fuel consumption and working hours for the load model 3.

Model	Annual energy provided by the diesel generators to the load	Annual fuel consumption	Total fuel consumption		Yearly average working hours	Total average working hours
-	*MWh/y*	*l/y*	*l*	*kg*	*h/y*	*h*
3	543.180	166,084.8	4,152,119.1	3,487,780.0	8,616	215,400

Table 4-92: Annual and total fuel consumption and working hours scaled-up for the total Froan load.

Annual energy provided by the diesel generators to the load	Annual fuel consumption	Total fuel consumption		Yearly average working hours	Total average working hours
MWh/y	*l/y*	*l*	*kg*	*h/y*	*h*
571.297	174,682.2	4,367,054.2	3,668,325.5	8,616	215,400

4.4.2 LCI from literature

Concerning the review of previous LCA on diesel generators present in literature we refer to Section 4.2.7.2. From this section we use also the same assumptions, analysis, calculations and literature data. As in Section 4.3.3.2, the only differences are the estimated operational hours and the total amount of diesel consumed. The lifetime of diesel generators depends on various factors, such as the proper installation, the operation and maintenance, the quality of the engine and the atmospheric conditions. This is why the lifetime range is very wide, 5,000-50,000 h with an average value of 20,000 h according to paper [119] and 15,000-30,000 h in accordance with [137]. Assuming the average lifetime of 20,000 h assessed in [119], the two assumed generators should be changed about 10 times during the 25-years lifetime in order to work the total amount of working hours (215,400 h), for a total of 22 required diesel generators. The following tables (Table 4-93, Table 4-94, Table 4-95) show the results of the different life-cycle phases.

Table 4-93: GHG emissions from the manufacture of the diesel generators (Diesel scenario).

Generators manufacture			
GHG emissions per generator power [89, 95]	Size of each generator (22)	GHG manufacture emissions of one generator	Total GHG manufacture emissions (22 generators)
$kgCO_2eq/kVA$	*kVA*	*$kgCO_2eq$*	*$kgCO_2eq$*
107.7	67	7,215.9	158,749.8

Table 4-94: GHG emissions from the diesel combustion (Diesel scenario).

Fuel combustion		
GHG emissions per mass of diesel [95]	Total diesel needed	Total GHG combustion emissions
$kgCO_2eq/kg$	*kg*	*$kgCO_2eq$*
3.405	3,668,325.5	12,489,775.079

Table 4-95: GHG emissions from the diesel production (WTT) in the Diesel scenario.

Fuel production		
Troll WTT carbon intensity of diesel [90, 95]	Total diesel needed	Total GHG production emissions (Troll)
$kgCO_2eq/kg$ of diesel produced	*kg*	*$kgCO_2eq$*
0.570	3,668,325.5	2,089,813.622

4.4.3 Diesel scenario results and comparison with the literature

In the following Table 4-96, we can see the final results of this scenario, summing all the contributions previously studied.

Table 4-96: Total GHG emissions rate (in functional unit) of the diesel generators system in the Diesel scenario.

Total GHG manufacture emissions	Total GHG combustion emissions	Total GHG production emissions (Troll)	Total GHG emissions	Total energy production	Total GHG emissions rate
$kgCO_2eq$	*$kgCO_2eq$*	*$kgCO_2eq$*	*$kgCO_2eq$*	*MWh*	*$kgCO_2eq/MWh$*
158,749.8	12,489,775.079	2,089,813.622	14,738,338.500	14,282.437	**1,031.920**

Figure 4-30 shows instead the relative contribution of the different phases to the total GHG emissions. As in the previous sections about the diesel generators (Section 4.2.7.2 and 4.3.3.2), the impact caused by the fuel combustion constitutes the biggest part of the total (84.74%), followed by the diesel production phase (14.18%) and by the manufacturing step (1.08%), which has a lower value than the previous sections (Section 4.2.7.2 and 4.3.3.2) because of the higher production and diesel consumption.

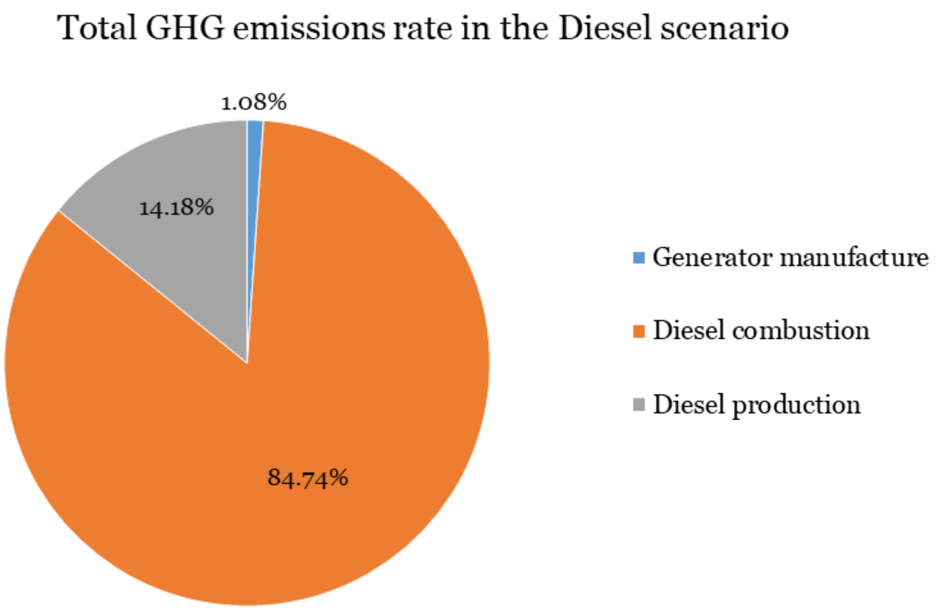

Figure 4-30: Relative contributions to the total GHG emissions of the diesel generator system (Diesel scenario).

The final value of 1.032 $kgCO_2eq/kWh$ is similar to the ones of the previous scenarios, even if it is a little higher because of the higher fuel consumption. The resulting environmental impact is however in accordance with the literature results shown in Section 4.2.7.3 and resumed in Table 4-97 modified from Section 4.3.3.2.

Table 4-97: Comparison of the total GHG emissions rate of the diesel generators system in the Diesel scenario with the previous scenarios and literature results.

Sources	Infos	GHG combustion emissions	Diesel consumption	Total GHG emissions per energy delivered by the diesel generator
-	-	*$kgCO_2eq/kg$*	*kg/kWh*	*$kgCO_2eq/kWh$*
Diesel scenario	-	3.405	0.249 - 0.264	1.032
Cable scenario	-	3.405	0.220	0.922
Remote scenario	-	3.405	0.220	0.893
[43, 125, 126]	-	-	-	0.800
[89, 119, 123, 124]	Transports included	3.130	0.336	1.270
[95]	Transports included	3.405	0.445	1.695
[117]	Transports, lubrification oil production and EOL included, no diesel production	-	0.193	0.666
[119]	Ranges of rated power and diesel emission factors	-	-	0.410 - 3.240

5 Comparison of the scenarios results

The results of the three scenarios are summarized in Table 5-1, which shows also the relative variation of the Cable and Diesel scenarios in comparison with the base case of the Remote scenario. A visive comparation is also shown in Figure 5-1.

Table 5-1: Total GHG emissions rates of the three scenarios (Remote, Cable, Diesel) and relative variation in comparison with the Remote scenario.

Scenario	Total GHG emissions rate	Relative variation from the base scenario
-	*$kgCO_2 eq/MWh$*	*%*
Remote	145.716	-
Cable	120.768	-17.1
Diesel	1,031.920	608.2

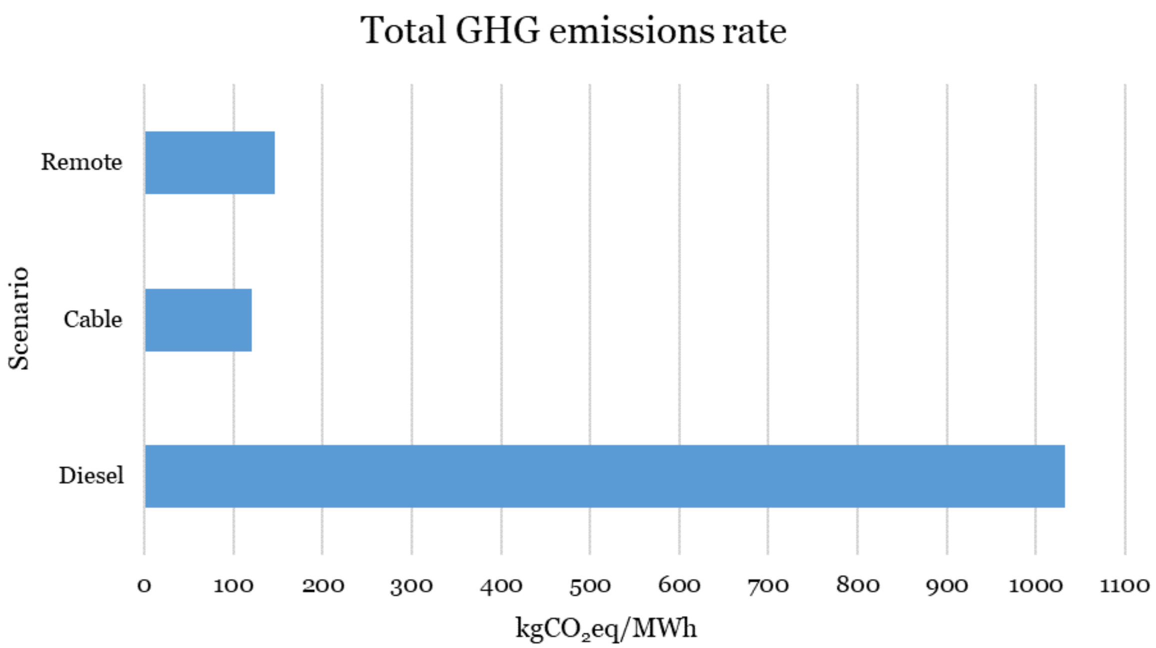

Figure 5-1: Comparison of the total GHG emissions rates of the three scenarios (Remote, Cable, Diesel).

The Diesel case, as expected, has very high GHG emissions in comparison with the other two scenarios, more or less 7 times the emissions of Remote case and more than 8 times the ones of the Cable case. In the entire lifetime (25 years), with the installation of the Remote P2P plant instead of diesel generators, the total GHG emissions avoidable are 12,657.2 tons of CO_2 equivalent, as shown in Table 5-2.

Table 5-2: Total lifetime GHG emissions avoidable in the Remote scenario in comparison with the Diesel case.

Total lifetime (25 y) energy to load	Total Remote GHG emissions rate	Total Diesel GHG emissions rate	Total lifetime (25 y) GHG emissions avoidable Remote Vs Diesel
MWh	*kgCO₂eq/MWh*	*kgCO₂eq/MWh*	*t CO₂eq*
14,282.437	145.716	1,031.920	12,657.157

The cable scenario, instead, is an environmentally friendly solution and it presents unexpectedly a lower impact than the Remote scenario. The possible reasons are multiple. In the renewable scenario, the assumed contribution of the diesel generators to the energy production (5%) is higher than the one calculated in the cable case (2%). The distance of the Froan islands from the mainland is also a parameter influencing a lot the environmental impact of the submarine cables. In fact, a longer cable would have meant higher GHG emissions. Last but not least, the mix of the energy sources used to produce the electricity transmitted by the cable has a relevant impact to the final results. Since the Norwegian electricity production is almost totally renewable, 98% according to the "Electricity disclosure 2018" provided by NVE [V], the resulting GHG emissions related to the electricity are very low. Concerning these considerations, we develop further scenarios in order to better evaluate the relative impacts of the different parameters discussed. Regarding the Remote scenario, the contribution of the generators is reduced from 5% to 2% in order to compare the results with the cable scenario. Concerning the cable case, instead, the length of the submarine connection and the carbon intensity of the electricity produced are modified in different scenarios.

6 Additional scenarios

6.1 Remote-2% scenario

This scenario is equal to the Remote scenario, but we assume to reduce the contribution of the diesel generators in the Remote case production from 5% to 2%, the same unavailability of the Cable scenario covered by the generators. Since the two scenarios have also the same assumptions for the diesel motors, their contribution in the Remote-2% scenario become the same of the Cable one, making the diesel part unconcerned in the comparison. The resulting GHG emissions, related to the generators of the Remote-2% case, are in fact the same already assessed in Section 4.3.3.2. The final environmental impacts of this scenario are presented in Table 6-1 and Figure 6-1.

Table 6-1: Relative contributions of each subsystem and total GHG emissions rate of the Remote-2% scenario.

GHG emissions rate for each component							Total GHG emissions rate
$kgCO_2eq/MWh$							*$kgCO_2eq/MWh$*
PV panels	Wind turbines	Battery	Water electrolyser	Hydrogen tank	Fuel cell	Diesel generator	Remote-2% scenario
33.455	47.627	10.069	1.525	4.749	3.631	18.430	**119.485**

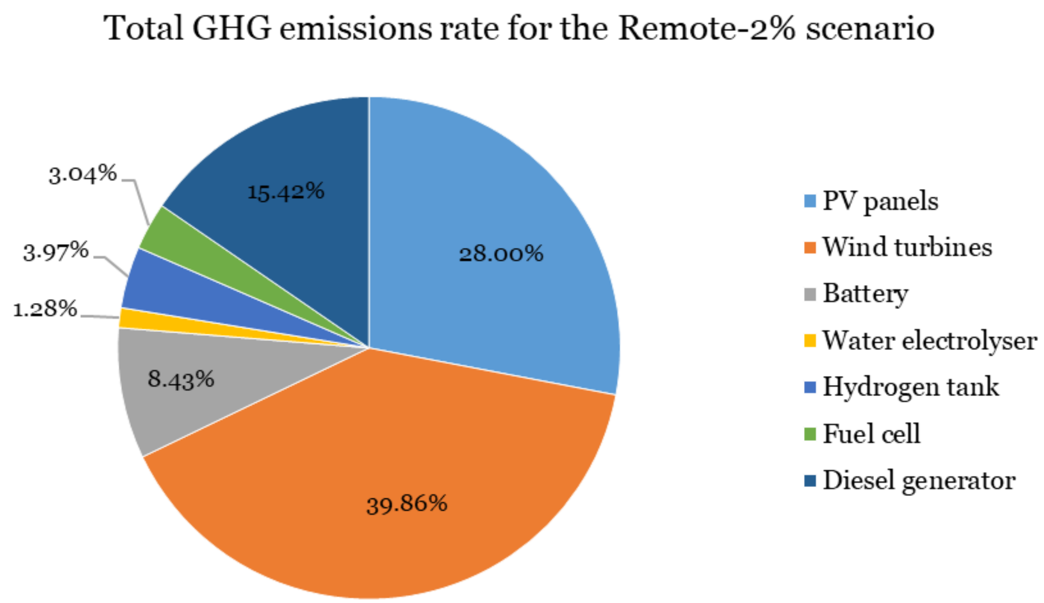

Figure 6-1: Relative contributions of each subsystem to the total GHG emissions of the Remote-2% scenario.

As expected, compared to the Remote scenario, the impact of the diesel generator has decreased from 44.66 to 18.43 $kgCO_2eq/MWh$ and the total emissions are lower than the ones of the base case (145.716 $kgCO_2eq/MWh$). This causes the different percentage contributions of each subsystem, with a decrease of the generator part (from 30.65% to 15.42%) and a subsequent increase of the other parts. Moreover, equalizing in the two scenarios the contribution of the diesel generators, the environmental impacts of the Remote-2% scenario are also slightly lower than the ones of the Cable case (120.768 $kgCO_2eq/MWh$). Figure 6-2 shows the comparison of the cited scenarios.

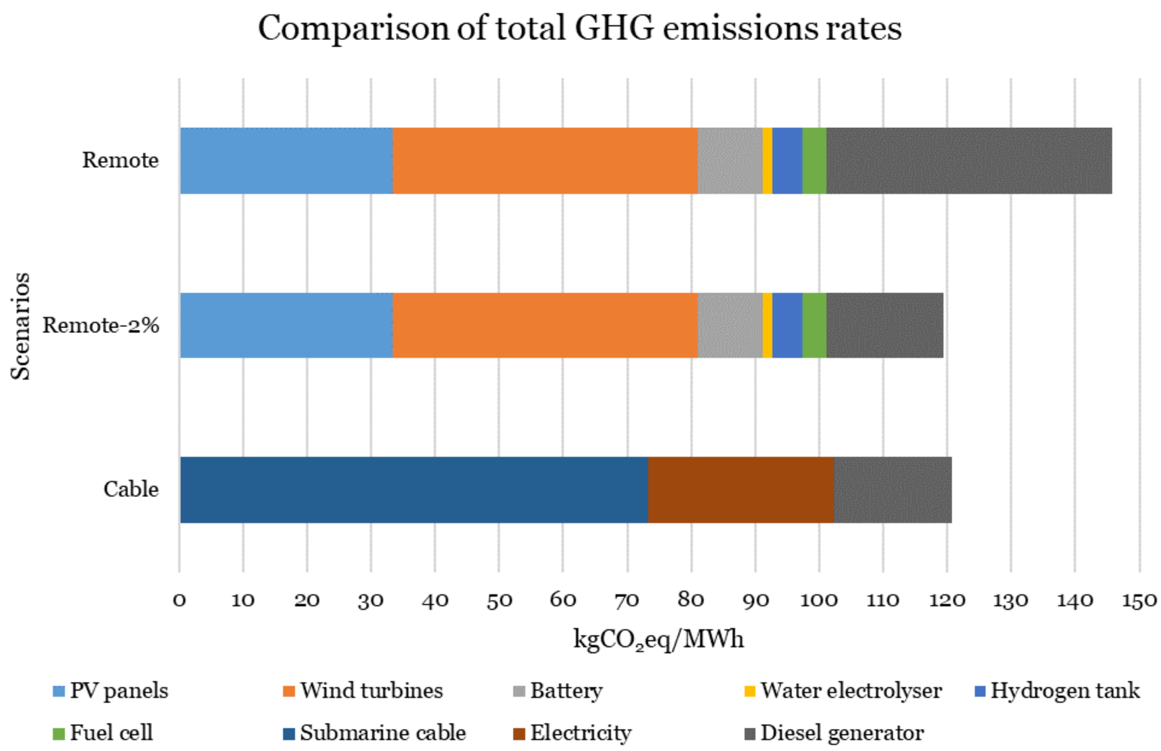

Figure 6-2: Comparison of the total GHG emissions rate (subdivided in each contribution) of the Remote-2% scenario with the Remote and Cable cases.

From this analysis, we can conclude that the unavailability of the main power plant solution, covered by diesel generators, is a very important parameter.

6.2 Cable-2x scenario

The analysis of this case is the same of the Cable scenario, but we assume a double cable length (46.870 km). This parameter influences all the parts considered in the calculations. Firstly, the emissions strictly related to the submarine cable are doubled, since they are calculated by each km of length (Table 6-2).

Table 6-2: Total GHG emissions rate (in functional unit) and contributions of each LCA phase of the submarine cable system in the Cable-2x scenario.

Cable-2x GHG emissions through the different LCA phases [129]					Total energy delivered	Total GHG emissions rate
Manufacture (10-kV cable)	Installation	Maintenance and inspection (25 y)	Dismantling and EOL	Total (25 years and without transports)		
$kgCO_2eq$					*MWh*	*$kgCO_2eq/MWh$*
808,360.670	240,232.751	824,882.568	220,541.563	2,094,017.552	14,282.437	**146.615**

Secondly, it influences the probable number of failures and the unavailability of the submarine cable, doubling also these parameters (Table 6-3 and Table 6-4).

Table 6-3: Expected sea cables number of failures during lifetime (Cable-2x scenario).

Average failure rate [133]	Considered lifetime	Cable length	Number of failures during lifetime	Rounded up number of failures during lifetime
failures/km/year	*years*	*km*	*failures*	*failures*
0.00299	25	46.870	3.504	4

Table 6-4: Expected sea cables unavailability during lifetime (Cable-2x scenario).

Total repair time [136]	Total repair time during lifetime	Percentage of unavailability during lifetime	Rounded up percentage of unavailability during lifetime
days/failure	*days*	*%*	*%*
85	340	3.726	4

The diesel generator would then cover 4% of the load and not the previous 2% of the normal Cable case, which means a higher environmental impact related to the diesel motors. While the manufacturing phase is unchanged since only one generator is still needed, the diesel production and consumption phases have higher carbon dioxide emissions caused by the higher amount of diesel required (Table 6-5, Table 6-6, Table 6-7).

Table 6-5: Total diesel needed and consumed in the Cable-2x scenario.

Average fuel consumption [96]	Total energy provided by the generator	Total diesel needed
g/kWh	*MWh*	*kg*
220	571.297	125,685.443

Table 6-6: GHG emissions from the diesel combustion and production (Cable-2x scenario).

Fuel combustion		**Fuel production**	
GHG emissions per mass of diesel [95]	Total GHG combustion emissions	Troll WTT carbon intensity of diesel [90, 95]	Total GHG production emissions (Troll)
$kgCO_2eq/kg$	$kgCO_2eq$	$kgCO_2eq$/kg of diesel produced	$kgCO_2eq$
3.405	427,929.007	0.570	71,601.919

Table 6-7: Total GHG emissions rate (in functional unit) of the diesel generator system in the Cable-2x scenario.

Total GHG manufacture emissions	Total GHG combustion emissions	Total GHG production emissions (Troll)	Total GHG emissions	Total energy delivered	Total GHG emissions rate
$kgCO_2eq$	$kgCO_2eq$	$kgCO_2eq$	$kgCO_2eq$	*MWh*	$kgCO_2eq/MWh$
13,462.5	427,929.007	71,601.919	512,993.426	14,282.437	**35.918**

Finally, also the electricity part of the analysis is modified. Since the availability is now reduced to 96%, the electricity provided by the cable is lower, but a doubled length means also doubled losses through the cable, so more surplus energy required from the mainland grid. In total, the electricity withdrawn from the grid is a little lower than the one of the normal Cable cases, because the effect of the reduction of availability prevails (Table 6-8). The new GHG emissions are shown in Table 6-9.

Table 6-8: Yearly electricity lost and withdrawn in the submarine cables in the Cable-2x scenario.

Conductor size	Electrical resistance per cable length	Cable length	Total electrical resistance	Average energy losses	Electricity delivered by the cable to the load	Relative energy losses	Electricity withdrawn by the cable from the mainland grid
mm^2	Ω/km	*km*	Ω	*MWh/y*	*MWh/y*	*%*	*MWh/y*
70	1.02	46.870	47.808	16.938	548.446	3.088	565.384

Table 6-9: Total GHG emissions rate (in functional unit) of the electricity system in the Cable-2x scenario.

Electricity withdrawn by the cable from the mainland grid	Total electricity withdrawn by the cable from the mainland grid	GHG emissions rate per MWh_{el} (Norway) [Ecoinvent 3]	Total electricity GHG emissions (Norway)	Total energy delivered	Total GHG emissions rate
MWh/y	*MWh*	*$kgCO_2eq/MWh$*	*$kgCO_2eq$*	*MWh*	*$kgCO_2eq/MWh$*
565.384	14,134.597	29.181	412,462.672	14,282.437	**28.879**

The final results of the scenario are presented in Table 6-10 and Figure 6-3.

Table 6-10: Relative contributions of each subsystem and total GHG emissions rate of the Cable-2x scenario.

GHG emissions rate for each subsystem			Total GHG emissions rate
$kgCO_2eq/MWh$			*$kgCO_2eq/MWh$*
Submarine cable	Electricity	Diesel generator	Cable-2x scenario
146.615	28.879	35.918	**211.412**

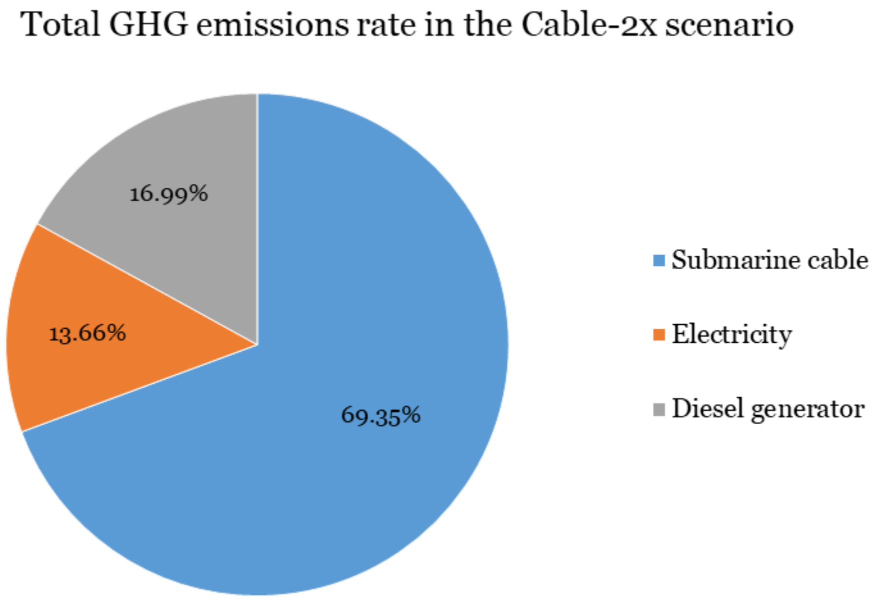

Figure 6-3: Relative contributions of each subsystem to the total GHG emissions of the Cable-2x scenario.

As expected, compared to the Cable scenario, the total impact increases. The final value (211.4 $kgCO_2eq/MWh$) is almost the double (75.1% more) of the resulting impact of the original Cable case (120.8 $kgCO_2eq/MWh$), because of the great increment in the emissions related to the submarine cable, doubled from 73.3 to 146.6 $kgCO_2eq/MWh$, and of the emissions related to the diesel generators, almost doubled from 18.4 to 35.9 $kgCO_2eq/MWh$. The impact caused by the electricity generation, instead, slightly decreases from 29.0 to 28.9 $kgCO_2eq/MWh$, because of the slightly lower electricity delivered by the cable. Figure 6-4 shows the comparison of the cited scenarios.

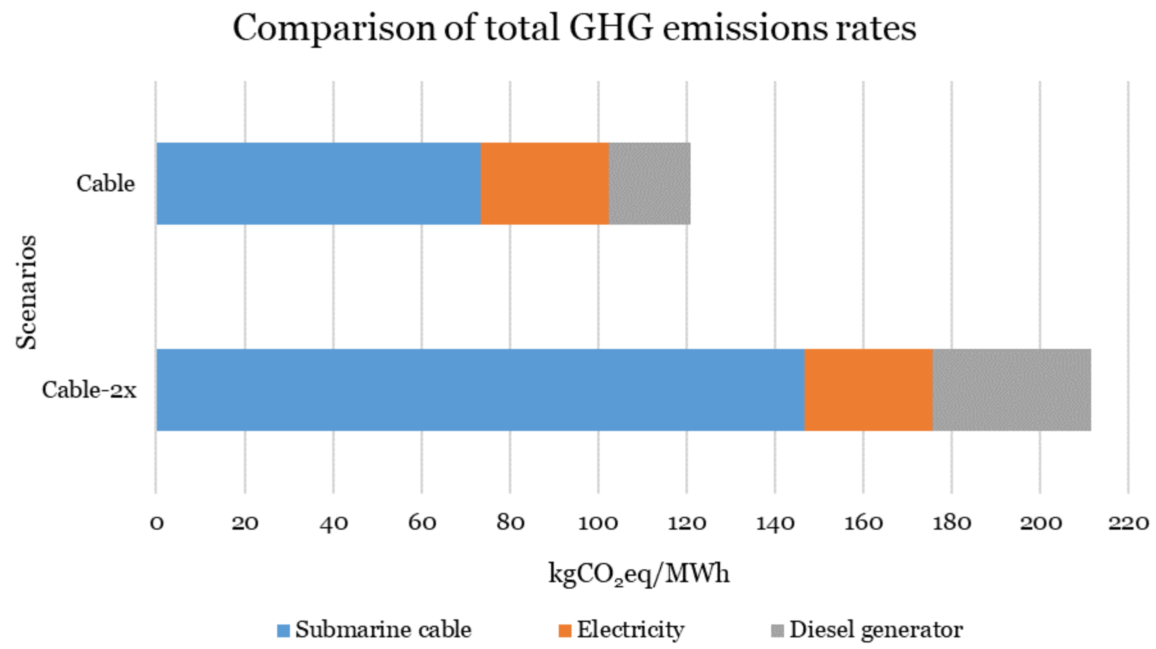

Figure 6-4: Comparison of the total GHG emissions rates of the Cable and Cable-2x scenarios.

Regarding the relative impacts, the percentages of the submarine cable and of the diesel generators increases, at the expense of the electricity contribution (Figure 6-5).

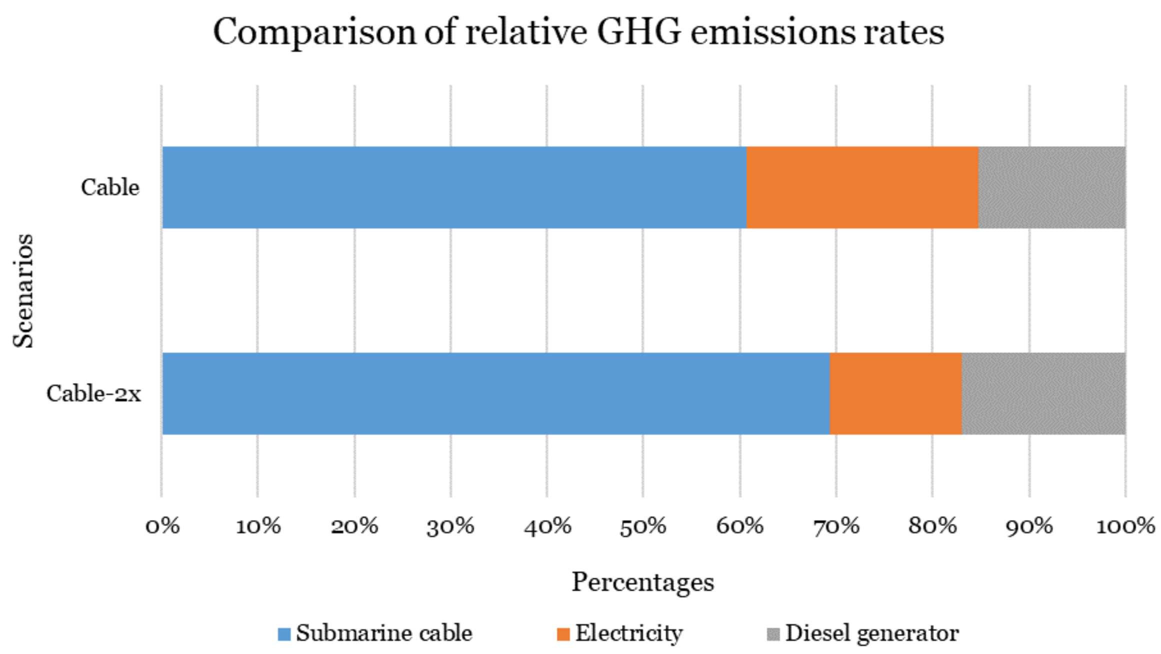

Figure 6-5: Comparison of the relative impacts to the total GHG emissions rate of the Cable and Cable-2x cases.

In conclusion, this additional scenario shows how much the sea cables length impacts the final GHG emissions per energy delivered.

6.3 Cable-Italy and Cable-2x-Italy scenarios

In these additional scenarios, we assume the identical data, analysis and considerations of the Cable and Cable-2x cases, but with the GHG intensity of the electricity produced in Italy, in order to see the effects on the final GHG emissions rate. According to paper [88], the emissions related to electricity consumed at MV (with upstream) in Italy are equal to 417 gCO_2eq/kWh_{el}, a value similar to the EU-28 average one (432 gCO_2eq/kWh_{el}) and really higher than the environmental impact of the Norwegian electricity (29.2 gCO_2eq/kWh_{el}). Regarding the Cable-Italy scenario, the final results are summarized in Table 6-11, Table 6-12 and in Figure 6-6.

Table 6-11: Total GHG emissions rate (in functional unit) of the electricity system in the Cable-Italy scenario.

Electricity withdrawn by the cable from the mainland grid	Total electricity withdrawn by the cable from the mainland grid	GHG emissions rate per MWh_{el} (Italy) [88]	Total electricity GHG emissions (Italy)	Total energy delivered	Total GHG emissions rate
MWh/y	*MWh*	*$kgCO_2eq/MWh$*	*$kgCO_2eq$*	*MWh*	*$kgCO_2eq/MWh$*
568.341	14,208.517	417	5,924,951.571	14,282.437	**414.842**

Table 6-12: Relative contributions of each subsystem and total GHG emissions rate of the Cable-Italy scenario.

GHG emissions rate for each subsystem			Total GHG emissions rate
$kgCO_2eq/MWh$			*$kgCO_2eq/MWh$*
Submarine cable	Electricity	Diesel generator	Cable-Italy scenario
73.307	414.842	18.430	**506.579**

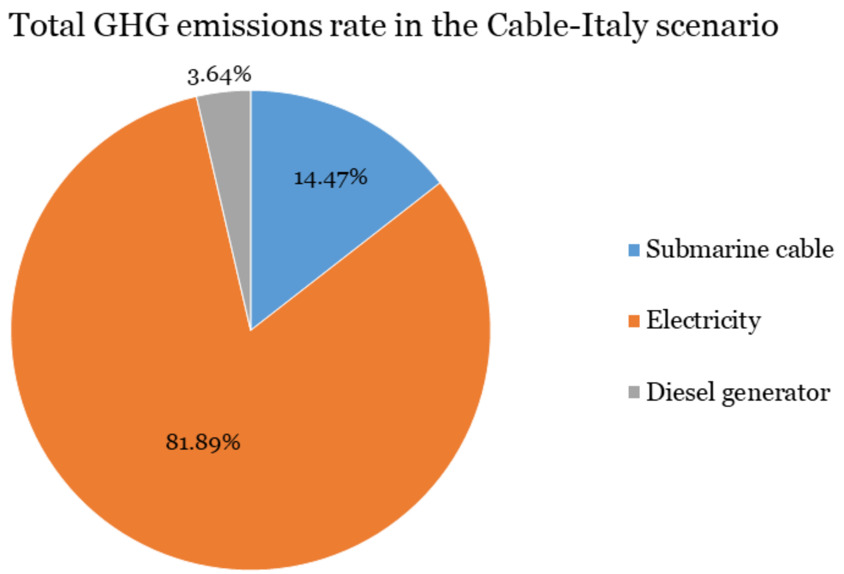

Figure 6-6: Relative contributions of each subsystem to the total GHG emissions of the Cable-Italy scenario.

The GHG emissions rate related to the electricity generation is obviously similar to the carbon intensity assumed and much higher than the one of the Cable case, where the Norwegian electricity is used. The final emissions are also much higher (more than four times) than the Cable scenario, but it is interesting to see how much varies the relative contribution of each subsystem in the two scenarios proposed. In the Italian case, the electricity dominates the final impacts (81.89%), followed by the lower percentages caused by the submarine cables (14.47%) and by the diesel generators (3.64%). This is a very different framework in comparison with the initial Cable scenario where the biggest part is caused by the submarine cable (60.70%). These variations are entirely produced by the different assumed carbon intensity of the electricity generated in the mainland grid, showing how much this parameter is important for the analysis. Figure 6-7 shows the comparison of the cited scenarios.

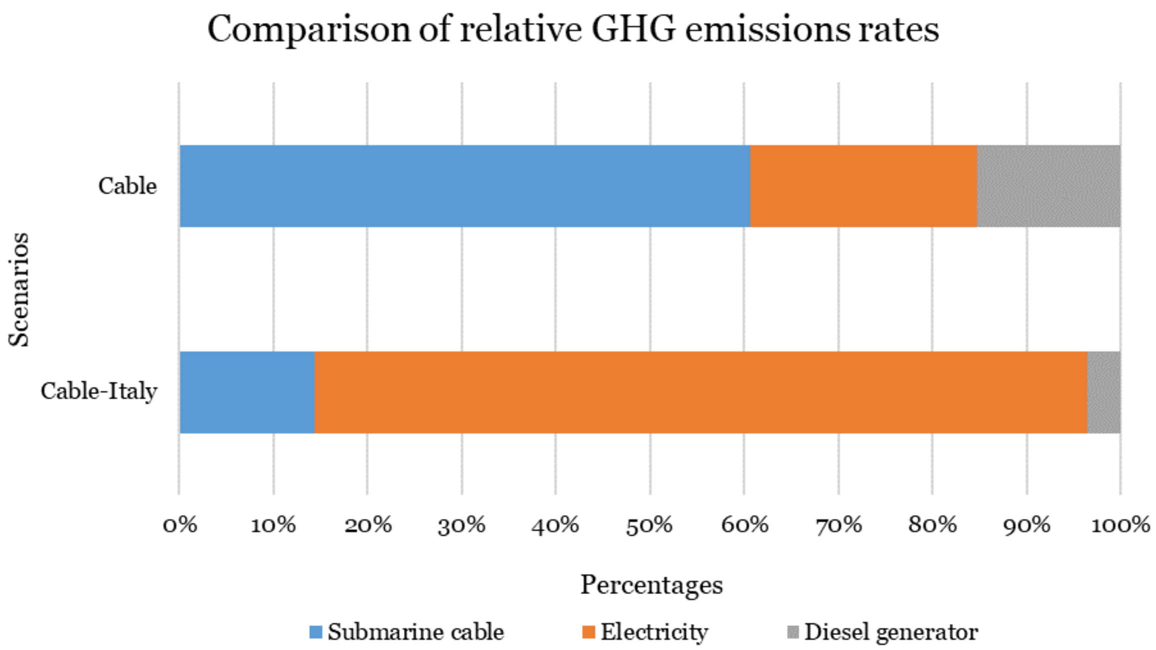

Figure 6-7: Comparison of the relative impacts to the total GHG emissions rate of the Cable and Cable-Italy scenarios.

Concerning the Cable-2x-Italy scenario, the final results are summarized in Table 6-13, Table 6-14 and in Figure 6-8.

Table 6-13: Total GHG emissions rate (in functional unit) of the electricity system in the Cable-2x-Italy scenario.

Electricity withdrawn by the cable from the mainland grid	Total electricity withdrawn by the cable from the mainland grid	GHG emissions rate per MWh_{el} (Italy) [88]	Total electricity GHG emissions (Italy)	Total energy delivered	Total GHG emissions rate
MWh/y	*MWh*	*$kgCO_2eq/MWh$*	*$kgCO_2eq$*	*MWh*	*$kgCO_2eq/MWh$*
565.384	14,134.597	417	5,894,127.059	14,282.437	**412.684**

Table 6-14: Relative contributions of each subsystem and total GHG emissions rate of the Cable-2x-Italy scenario.

GHG emissions rate for each subsystem			Total GHG emissions rate
$kgCO_2eq/MWh$			*$kgCO_2eq/MWh$*
Submarine cable	Electricity	Diesel generator	Cable-2x-Italy scenario
146.615	412.684	35.918	**595.216**

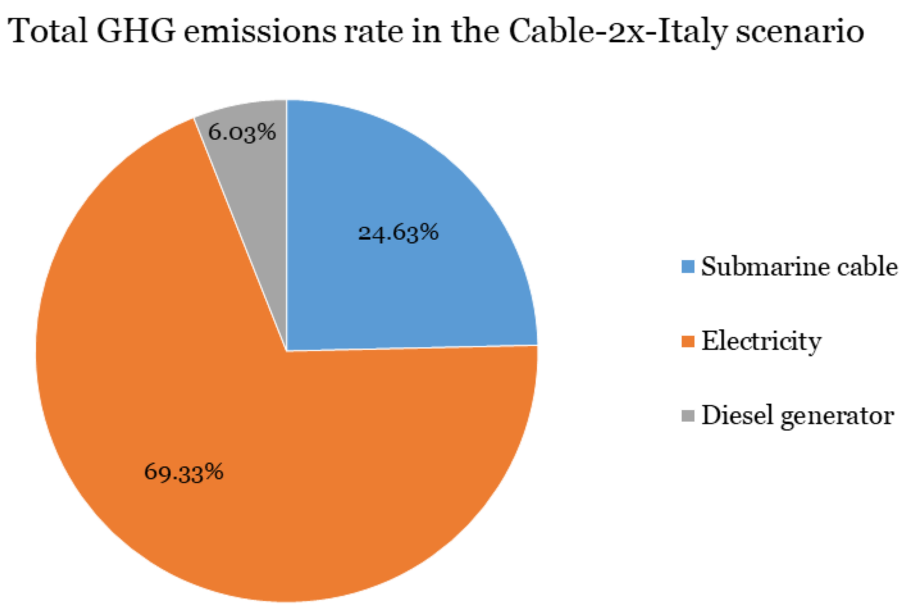

Figure 6-8: Relative contributions of each subsystem to the total GHG emissions of the Cable-2x-Italy scenario.

For this scenario, the same considerations, already explained above, are valid in comparison to the initial Cable-2x case. The interesting fact of this scenario, involving a double cable length, is that the final emissions are higher than the Cable-Italy case but not so much in percentage (17.5% higher), contrary to the Cable-2x case whose emissions are almost the double (75.1% higher) than the emissions of the initial Cable scenario (Figure 6-9). This is due to the already large environmental impact of the Cable-Italy scenario mainly caused by the electricity production (the most impacting subsystem of the scenario), contrary to the original Cable case in which the low impact is mainly due to the submarine cable that is instead the most sensible parameter in that case.

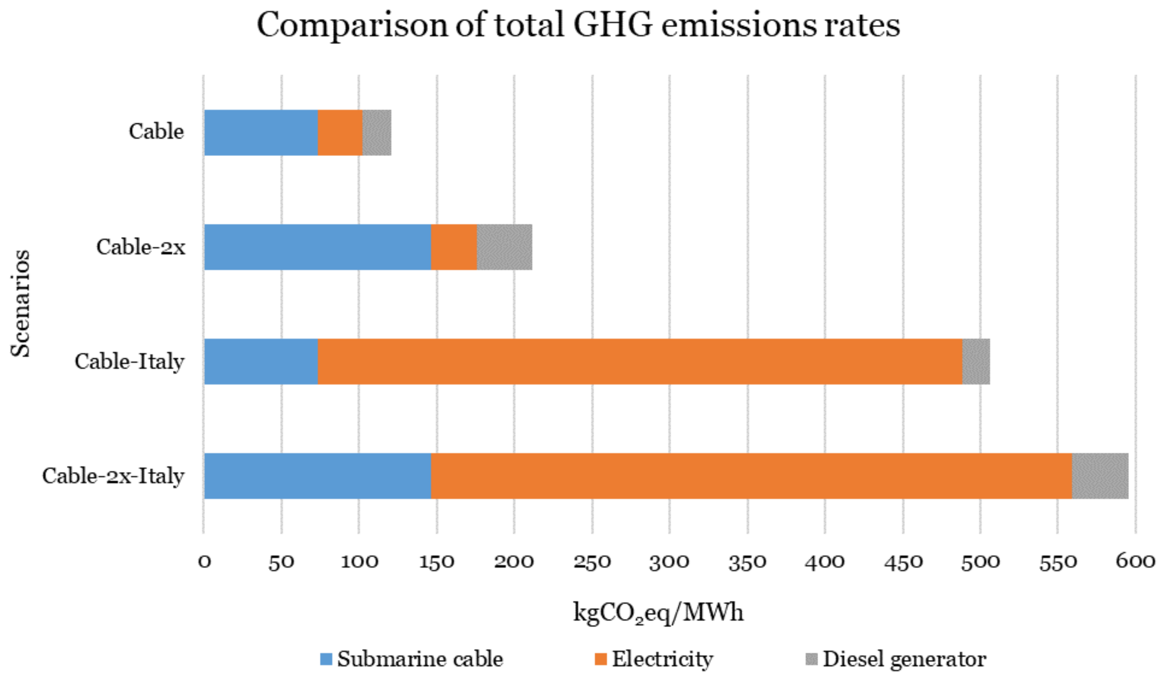

Figure 6-9: Comparison of the total GHG emissions rates of the Cable, Cable-2x, Cable-Italy and Cable-2x-Italy scenarios.

7 Conclusions

In the framework of a necessary energy transition, including the decarbonisation of energy sources, a larger and larger penetration of RES and the development of energy storage technologies, the integration of RES in hydrogen-based P2P storage systems is the most credible option with medium/long-term capacity and H_2 can be also used as a clean energy vector, flexibly transportable across different sectors and regions. In particular, islands and remote areas are optimal candidates to rely on local RES and P2P systems, becoming isolated micro-grids and avoiding more expensive and impacting solutions, such as submarine electric connections or on-site diesel generators.

In this thesis, a holistic LCA environmental analysis (in terms of CO_2 equivalent emissions with time horizon of 100 years) of the complete hydrogen-based P2P storage system relying on local RES, located in the Froan Islands in Norway and designed in the demo case 4 of the European Remote project, has been carried on, in comparison with the climate impacts of additional scenarios. The resulting GHG emissions of the different scenarios are presented in Figure 7-1 and in Table 7-1.

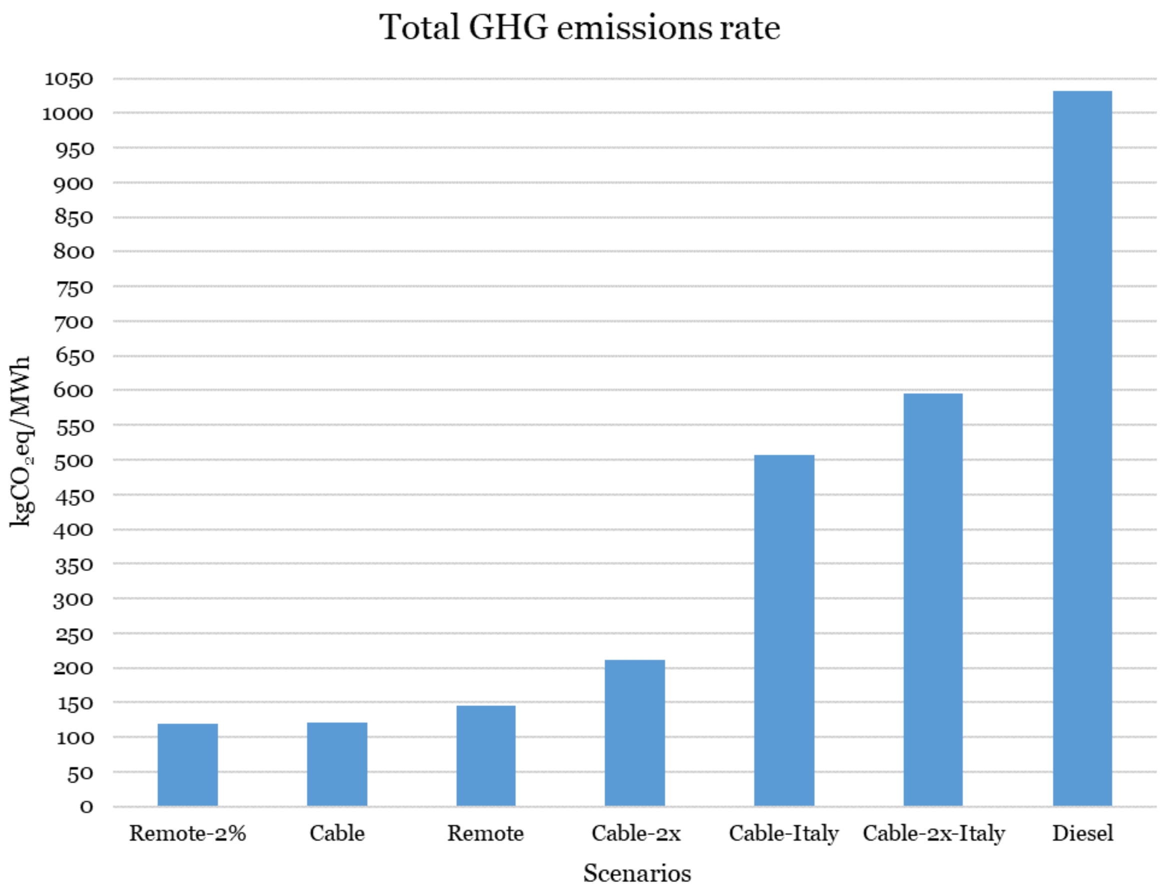

Figure 7-1: Comparison of the total GHG emissions rates of all the analysed scenarios.

Table 7-1: Comparison of the total GHG emissions rates of all the analysed scenarios with the relative contribution of each subsystem.

GHG emissions rate										
$kgCO_2eq/MWh$										
Scenario	PV panels	Wind turbines	Battery	Water electrolyser	Hydrogen tank	Fuel cell	Submarine cable	Electricity	Diesel generator	**Total**
Remote-2%	33.455	47.627	10.069	1.525	4.749	3.631	-	-	18.430	**119.485**
Cable	-	-	-	-	-	-	73.307	29.030	18.430	**120.768**
Remote	33.455	47.627	10.069	1.525	4.749	3.631	-	-	44.662	**145.716**
Cable-2x	-	-	-	-	-	-	146.615	28.879	35.918	**211.412**
Cable-Italy	-	-	-	-	-	-	73.307	414.842	18.430	**506.579**
Cable-2x-Italy	-	-	-	-	-	-	146.615	412.684	35.918	**595.216**
Diesel	-	-	-	-	-	-	-	-	1031.920	**1031.920**

The resulting LCA environmental impact of the Remote scenario is 145.7 $kgCO_2eq/MWh$, mainly due to the energy production systems (86.29%), including WTs (32.68%), PV panels (22.96%) and diesel generator (30.65%). The hybrid storage system has instead a lower impact (13.71%) equally distributed between the Li-ion batteries (6.91%) and the hydrogen P2P system (6.80%), which represents the less impacting subsystem of the power plant. As expected, the fossil fuel reference scenario has the highest GHG emissions (1,031.9 $kgCO_2eq/MWh$), more or less 7 times the emissions of the Remote scenario and producing around 12,657.2 tons of CO_2 equivalent more than the hydrogen-based P2P plant, during the 25 years lifetime. The environmental impact is mainly caused by the direct carbon dioxide produced in the diesel combustion on-site (84.74%), followed by the diesel production phase (14.18%) and the manufacture of the generators (1.08%). The Cable scenario, instead, seems an environmentally friendly solution and it presents a lower impact (120.8 $kgCO_2eq/MWh$) than the Remote scenario. The biggest contribution is related to the installed submarine cable (60.70%), followed by the electricity produced in the Norwegian mainland (24.04%) and the emissions related to the diesel generator (15.26%), including its manufacture and the diesel production and combustion. The relatively low GHG emissions produced in the Cable case are determined by several possible factors. The small contribution of the diesel generator to the total load (2%), a value lower than the one assumed in the Remote scenario (5%), limits the GHG emissions related to the fossil fuel subsystem. The length of the submarine cable, determined by the distance of the islands from the mainland, is also an important parameter influencing the environmental impact. In fact, a longer cable would have meant higher GHG emissions. Moreover, the Norwegian electricity transmitted and produced in the mainland is almost totally generated from RES (98% [V]), keeping low the total environmental impacts.

On the basis of these considerations, additional scenarios are studied. The lowest GHG emissions are produced by the Remote-2% case (119.5 $kgCO_2eq/MWh$), in which an higher availability of the renewable Remote plant and a consequent lower contribution of generators to the load are assumed (2% as in the Cable scenario), involving an expected decrease in the environmental impact of the diesel generator subsystem, more than halved with respect to the base Remote case. Higher emissions are instead found doubling the cables length in the Cable-2x scenario (211.4 $kgCO_2eq/MWh$), an increase of 75.1% compared to the base Cable case, caused by the doubled impact of the installed submarine cables and by the higher diesel generators contribution to cover the higher cables unavailability, which also causes a small decrease of the electricity transmitted. The environmental impacts are even larger in the Cable-Italy scenario (506.6 $kgCO_2eq/MWh$), where the higher carbon intensity of the electricity produced in Italy (417.0 against the 29.2 gCO_2eq/kWh_{el} of the Norwegian electricity) is assumed. This leads to a GHG emissions increase of more than four times compared to the base Cable case, entirely caused by the different mix of energy sources used to produce the electricity in the mainland, process which here dominates the final impacts (81.89%), followed by the submarine cables (14.47%) and by the diesel generators (3.64%) subsystems. Moreover, assuming also for this last case a double cables length, the Cable-2x-Italy scenario is analysed, showing a further increase in GHG emissions (595.2 $kgCO_2eq/MWh$), caused by the same factors already explained, but not so big in percentage (17.5% compared to 75.1% between the Cable and the Cable-2x scenarios), since the large environmental impact of the Cable-Italy scenario is mainly due to the electricity production and not to the submarine cable as in the Cable scenario.

In conclusion, apart from the very low GWI of the Cable scenario in the particular Froan Islands situation, the application of H_2-based P2P storage systems in remote isolated micro-grids offers high climate change benefits in comparison with other scenarios, especially with fossil fuel ones. Around the world, according to [23], there are more than 10,000 inhabited islands, with 750 million estimated islanders, and many of these islands (especially those in the range of 1,000-100,000 inhabitants) still rely on diesel generators instead of local RES. Considering also other isolated situations, such as mountains and remote areas, the number of potential remote sites compatible with the application of H_2-based P2P storage systems relying on local RES is even bigger. The incredibly large utilisation potentials, coupled with the environmentally favourable results obtained, show the very large extent of the potential climate change benefits (in terms of CO_2eq) obtainable with these systems.

Moreover, the analysis performed in the additional scenarios shows the high sensitivity of the final results to some relevant parameters, such as the contribution of diesel generation to the final load in case of unavailability of the main plant, the electrical connection cables length and the carbon intensity of the electricity produced and transmitted. Further relevant factors, not analysed in this thesis work, can be the focus of future works. For example, the number of inhabitants and then the required total load would impact both the size of each subsystem of the energy plant, both the section and the voltage of the transmission cables. The local RES potential and their timely distribution are also important factors influencing the choice of subsystems size, especially regarding the generation systems (WTs and PV panels) and the storage capacity, which can be smaller if RES production is more constant. In the particular case of our analysis, since the solar irradiation of the Norwegian scenario is quite low, assuming for example a different location with higher solar irradiation would mean a lower PV panels surface, causing an even lower final environmental impact. A greater consciousness and knowledge of these critical parameters would also enable and support future scale up analyses, in which the installation of H_2-based P2P storage systems, relying on local RES, would concern a large number of islands and remote locations and maybe further end uses of H_2 along with the electricity sector (mobility, heating,...), showing more widely the potential environmental benefits arising from the development of these systems.

Bibliography

[1] Allen, M.R., O.P. Dube, W. Solecki, F. Aragón-Durand, W. Cramer, S. Humphreys, M. Kainuma, J. Kala, N. Mahowald, Y. Mulugetta, R. Perez, M. Wairiu, and K. Zickfeld, 2018: Framing and Context. In: Global Warming of 1.5°C. An IPCC Special Report on the impacts of global warming of 1.5°C above pre-industrial levels and related global greenhouse gas emission pathways, in the context of strengthening the global response to the threat of climate change, sustainable development, and efforts to eradicate poverty [Masson-Delmotte, V., P. Zhai, H.-O. Pörtner, D. Roberts, J. Skea, P.R. Shukla, A. Pirani, W. Moufouma-Okia, C. Péan, R. Pidcock, S. Connors, J.B.R. Matthews, Y. Chen, X. Zhou, M.I. Gomis, E. Lonnoy, T. Maycock, M. Tignor, and T. Waterfield (eds.)]. In Press.

[2] IPCC, 2014: Climate Change 2014: Synthesis Report. Contribution of Working Groups I, II and III to the Fifth Assessment Report of the Intergovernmental Panel on Climate Change [Core Writing Team, R.K. Pachauri and L.A. Meyer (eds.)]. IPCC, Geneva, Switzerland, 151 pp.

[3] Rogelj, J., D. Shindell, K. Jiang, S. Fifita, P. Forster, V. Ginzburg, C. Handa, H. Kheshgi, S. Kobayashi, E. Kriegler, L. Mundaca, R. Séférian, and M.V. Vilariño, 2018: Mitigation Pathways Compatible with 1.5°C in the Context of Sustainable Development. In: Global Warming of 1.5°C. An IPCC Special Report on the impacts of global warming of 1.5°C above pre-industrial levels and related global greenhouse gas emission pathways, in the context of strengthening the global response to the threat of climate change, sustainable development, and efforts to eradicate poverty [Masson-Delmotte, V., P. Zhai, H.-O. Pörtner, D. Roberts, J. Skea, P.R. Shukla, A. Pirani, W. Moufouma-Okia, C. Péan, R. Pidcock, S. Connors, J.B.R. Matthews, Y. Chen, X. Zhou, M.I. Gomis, E. Lonnoy, T. Maycock, M. Tignor, and T. Waterfield (eds.)]. In Press.

[4] Transforming our world: the 2030 Agenda for Sustainable Development. Resolution adopted by the General Assembly, seventieth session, on 25 September 2015. United Nations.

[5] Edenhofer O., R. Pichs-Madruga, Y. Sokona, S. Kadner, J. C. Minx, S. Brunner, S. Agrawala, G. Baiocchi, I. A. Bashmakov, G. Blanco, J. Broome, T. Bruckner, M. Bustamante, L. Clarke, M. Conte Grand, F. Creutzig, X. Cruz-Núñez, S. Dhakal, N. K. Dubash, P. Eickemeier, E. Farahani, M. Fischedick, M. Fleurbaey, R. Gerlagh, L. Gómez-Echeverri, S. Gupta, J. Harnisch, K. Jiang, F. Jotzo, S. Kartha, S. Klasen, C. Kolstad, V. Krey, H. Kunreuther, O. Lucon, O. Masera, Y. Mulugetta, R. B. Norgaard, A. Patt, N. H. Ravindranath, K. Riahi, J. Roy, A. Sagar, R. Schaeffer, S. Schlömer, K. C. Seto, K. Seyboth, R. Sims, P. Smith, E. Somanathan, R. Stavins, C. von Stechow, T. Sterner, T. Sugiyama, S. Suh, D. Ürge-Vorsatz, K. Urama, A. Venables, D. G. Victor, E. Weber, D. Zhou, J. Zou, and T. Zwickel, 2014: Technical Summary. In: Climate Change 2014: Mitigation of Climate Change. Contribution of Working Group III to the Fifth Assessment Report of the Intergovernmental Panel on Climate Change [Edenhofer, O., R. Pichs-Madruga, Y. Sokona, E. Farahani, S. Kadner, K. Seyboth, A. Adler, I. Baum, S. Brunner, P. Eickemeier, B. Kriemann, J. Savolainen, S. Schlömer, C. von Stechow, T. Zwickel and J. C. Minx (eds.)]. Cambridge University Press, Cambridge, United Kingdom and New York, NY, USA.

[6] Adoption of the Paris agreement. Conference of the Parties, twenty-first session. Paris, 12 December 2015. Framework Convention on Climate Change. United Nations.

[7] Communication from the Commission to the European Parliament, the Council, the European Economic and Social Committee, the Committee of the Regions and the European Investment Bank, Second Report on the State of the Energy Union, Brussels, 1.2.2017, COM(2017) 53 final.

[8] Renewable energy in Europe-2018, Recent growth and knock-on effects, EEA Report No 20/2018, European Environment Agency, 2018.

[9] Report from the Commission to the European Parliament, the Council, the European Economic and Social Committee and the Committee of the Regions, Renewable Energy Progress Report, Brussels, 1.2.2017, COM(2017) 57 final.

[10] Communication from the Commission to the European Parliament, the Council, the European Economic and Social Committee, the Committee of the Regions and the European Investment Bank, Third Report on the State of the Energy Union, Brussels, 23.11.2017, COM(2017) 688 final.

[11] Energy production and imports. Statistics Explained. Eurostat. Data extracted in July 2019. 06/08/2019. https://ec.europa.eu/eurostat/statisticsexplained/Energy_production_and_imports.

[12] Renewable energy statistics. Statistics Explained. Eurostat. Data extracted in January 2019. 21/08/2019. https://ec.europa.eu/eurostat/statistics-explained/Renewable_energy_statistics.

[13] Europe 2020 indicators – climate change and energy. Statistics Explained. Eurostat. Data extracted in August 2019. 07/10/2019. https://ec.europa.eu/eurostat/statistics-explained/Europe_2020_indicators_climate_change_and_energy.

[14] Commercialisation of energy storage in Europe, Final report, March 2015.

[15] De Coninck, H., A. Revi, M. Babiker, P. Bertoldi, M. Buckeridge, A. Cartwright, W. Dong, J. Ford, S. Fuss, J.-C. Hourcade, D. Ley, R. Mechler, P. Newman, A. Revokatova, S. Schultz, L. Steg, and T. Sugiyama, 2018: Strengthening and Implementing the Global Response. In: Global Warming of 1.5°C. An IPCC Special Report on the impacts of global warming of 1.5°C above pre-industrial levels and related global greenhouse gas emission pathways, in the context of strengthening the global response to the threat of climate change, sustainable development, and efforts to eradicate poverty [Masson-Delmotte, V., P. Zhai, H.-O. Pörtner, D. Roberts, J. Skea, P.R. Shukla, A. Pirani, W. Moufouma-Okia, C. Péan, R. Pidcock, S. Connors, J.B.R. Matthews, Y. Chen, X. Zhou, M.I. Gomis, E. Lonnoy, T. Maycock, M. Tignor, and T. Waterfield (eds.)]. In Press.

[16] Luo X, Wang J, Dooner M, Clarke J. Overview of current development in electrical energy storage technologies and the application potential in power system operation. Appl Energy 2015; 137:511e36. http://dx.doi.org/10.1016/j.apenergy.2014.09.081.

[17] IRENA (2018), Hydrogen from renewable power: Technology outlook for the energy transition, International Renewable Energy Agency, Abu Dhabi.

[18] Hydrogen roadmap Europe, A sustainable pathway for the European energy transition, Fuel Cells and Hydrogen 2 Joint Undertaking, 2019.

[19] IRENA (2018), Power System Flexibility for the Energy Transition, Part 1: Overview for policy makers, International Renewable Energy Agency, Abu Dhabi.

[20] Off-grid renewable energy solutions to expand electricity access: An opportunity not to be missed, International Renewable Energy Agency, Abu Dhabi.

[21] REMOTE, Project n° 779541, "Remote area Energy supply with Multiple Options for integrated hydrogen-based TEchnologies". Deliverable D2.1. Analysis of the economic and regulatory framework of the technological demonstrators. WP2–Use cases: definition of the technical and business cases of the 4 DEMOs. T2.1–Analyses of the economic and regulatory framework for the four demonstrators. 16/05/2018 (Re-submitted 31/10/2018). Principal Authors: Kyrre Sundseth, Kjetil Midthun, Mats Aarlott, Adrian Werner (SINTEF). Contributors: Daniele Consoli, Martina Ciani Bassetti (EGP), Stella Chatzigavriil (HOR), Roberta Giuliano, Ilaria Schiavi, Manuel Lai (IRIS), Bernhard Kvaal (TREN), Alberto Carpita (POW).

[22] IRENA (2018), 'Off-grid renewable energy solutions: Global and regional status and trends'. IRENA, Abu Dhabi.

[23] REMOTE - PART B Sections 1-3 Excluding Section 2.2 [RESERVED].

[24] REMOTE, Project n° 779541, "Remote area Energy supply with Multiple Options for integrated hydrogen-based TEchnologies", Deliverable number 2.2, Technical specification of the technological demonstrators, 30/07/2018. Principal authors: Paolo Marocco, Domenico Ferrero, Marta Gandiglio, Massimo Santarelli (POLITO). Contributors: Villy Biltoft (BPSE), Daniele Consoli, Martina Ciani Bassetti (EGP), Ilaria Rosso, Lorenzo Cantone, Olivia Rigovacca (EPS), Stella Chatzigavriil (HOR), Denis Thomas, Stefan Knauf (HYG), Ilaria Schiavi, Roberta Giuliano, Manuel Lai (IRIS), Alberto Carpita, Maylis Duru (POW), Bernhard Kvaal (TE).

[25] C. Koroneos, A. Dompros, G. Roumbas, N. Moussiopoulos. Life cycle assessment of hydrogen fuel production processes. International Journal of Hydrogen Energy 29 (2004) 1443–1450. 2004 International Association for Hydrogen Energy. Published by Elsevier Ltd. http://dx.doi.org/10.1016/j.ijhydene.2004.01.016.

[26] Ahmet Ozbilen, Ibrahim Dincer, Marc A. Rosen. A comparative life cycle analysis of hydrogen production via thermochemical water splitting using a Cu-Cl cycle. International journal of hydrogen energy 36 (2011) 11321-11327. Hydrogen Energy Publications, LLC. Published by Elsevier Ltd.
http://doi.org/10.1016/j.ijhydene.2010.12.035.

[27] E. Cetinkaya, I. Dincer, G.F. Naterer. Life cycle assessment of various hydrogen production methods. International journal of hydrogen energy 37 (2012) 2071-2080. 2011, Hydrogen Energy Publications, LLC. Published by Elsevier Ltd. http://dx.doi.org/10.1016/j.ijhydene.2011.10.064.

[28] Javier Dufour, David P. Serrano, José L. Gálvez, Antonio González, Enrique Soria, José L.G. Fierro. Life cycle assessment of alternatives for hydrogen production from renewable and fossil sources. International journal of hydrogen energy 37 (2012) 1173-1183. 2011, Hydrogen Energy Publications, LLC. Published by Elsevier Ltd. http://dx.doi.org/10.1016/j.ijhydene.2011.09.135.

[29] Canan Acar, Ibrahim Dincer. Comparative assessment of hydrogen production methods from renewable and non-renewable sources. International journal of hydrogen energy 39 (2014) 1-12. Hydrogen Energy Publications, LLC. Published by Elsevier Ltd. http://dx.doi.org/10.1016/j.ijhydene.2013.10.060.

[30] Ahmet Ozbilen, Ibrahim Dincer, Marc A. Rosen. Comparative environmental impact and efficiency assessment of selected hydrogen production methods. Environmental Impact Assessment Review 42 (2013) 1–9. 2013 Elsevier Inc. http://dx.doi.org/10.1016/j.eiar.2013.03.003

[31] Ibrahim Dincer, Canan Acar. Review and evaluation of hydrogen production methods for better sustainability. International journal of hydrogen energy 40 (2015) 11094-11111. 2014, Hydrogen Energy Publications, LLC. Published by Elsevier Ltd. http://dx.doi.org/10.1016/j.ijhydene.2014.12.035.

[32] Andi Mehmeti, Athanasios Angelis-Dimakis, George Arampatzis, Stephen J. McPhail and Sergio Ulgiati. Life Cycle Assessment and Water Footprint of Hydrogen Production Methods: From Conventional to Emerging Technologies. Environments 2018, 5, 24. http://dx.doi.org/10.3390/environments5020024.

[33] Pamela L. Spath, Margaret K. Mann. Life Cycle Assessment of Renewable Hydrogen Production via Wind/Electrolysis. Milestone Report for the U.S. Department of Energy's Hydrogen Program Process Analysis Task. February 2001. National Renewable Energy Laboratory.

[34] Ramchandra Bhandari, Clemens A. Trudewind, Petra Zapp. Life cycle assessment of hydrogen production via electrolysis – a review. Journal of Cleaner Production 85 (2014) 151-163. Elsevier Ltd. http://dx.doi.org/10.1016/j.jclepro.2013.07.048.

[35] Mikhail Granovskii, Ibrahim Dincer, Marc A. Rosen. Life cycle assessment of hydrogen fuel cell and gasoline vehicles. International Journal of Hydrogen Energy 31 (2006) 337–352. 2005 International Association for Hydrogen Energy. Published by Elsevier Ltd. http://dx.doi.org/10.1016/j.ijhydene.2005.10.004.

[36] Christopher J. Greiner, Magnus Korpås, Arne T. Holen. A Norwegian case study on the production of hydrogen from wind power. International Journal of Hydrogen Energy 32 (2007) 1500–1507. 2006 International Association for Hydrogen Energy. Published by Elsevier Ltd. http://dx.doi.org/10.1016/j.ijhydene.2006.10.030.

[37] Ibrahim Dincer. Environmental and sustainability aspects of hydrogen and fuel cell systems. International Journal Of Energy Research 2007; 31:29–55. Published online 1 August 2006 in Wiley InterScience (www.interscience.wiley.com). http://dx.doi.org/10.1002/er.1226.

[38] Ximena C. Schmidt Rivera, Evangelia Topriska, Maria Kolokotroni, Adisa Azapagic. Environmental sustainability of renewable hydrogen in comparison with conventional cooking fuels. Journal of Cleaner Production 196 (2018) 863-879. 2018 Elsevier Ltd. https://doi.org/10.1016/j.jclepro.2018.06.033.

[39] E. Akyuz, Z. Oktay, I. Dincer. Performance investigation of hydrogen production from a hybrid wind-PV system. International journal of hydrogen energy 37 (2012) 16623-16630. 2012, Hydrogen Energy Publications, LLC. Published by Elsevier Ltd. http://dx.doi.org/10.1016/j.ijhydene.2012.02.149.

[40] Gerda Reiter, Johannes Lindorfer. Global warming potential of hydrogen and methane production from renewable electricity via power-to-gas technology. Int J Life Cycle Assess (2015) 20:477–489. Springer-Verlag Berlin Heidelberg 2015. https://doi.org/10.1007/s11367-015-0848-0.

[41] Jörg Burkhardt, Andreas Patyk, Philippe Tanguy, Carsten Retzke. Hydrogen mobility from wind energy – A life cycle assessment focusing on the fuel supply. Applied Energy 181 (2016) 54–64. 2016 Elsevier Ltd. http://dx.doi.org/10.1016/j.apenergy.2016.07.104.

[42] Kay Bareiß, Cristina de la Rua, Maximilian Möckl, Thomas Hamacher. Life cycle assessment of hydrogen from proton exchange membrane water electrolysis in future energy systems. Applied Energy 237 (2019) 862–872. Published by Elsevier Ltd. https://doi.org/10.1016/j.apenergy.2019.01.001.

[43] Mitja Mori, Miha Jensterle, Tilen Mržljak, Boštjan Drobnič. Life-cycle assessment of a hydrogen-based uninterruptible power supply system using renewable energy. Int J Life Cycle Assess (2014) 19:1810–1822 http://dx.doi.org/10.1007/s11367-014-0790-6.

[44] David Parra, Xiaojin Zhang, Christian Bauer, Martin K. Patel. An integrated techno-economic and life cycle environmental assessment of power-to-gas systems. Applied Energy 193 (2017) 440–454. 2017 Elsevier Ltd. http://dx.doi.org/10.1016/j.apenergy.2017.02.063.

[45] Karin Tschiggerl, Christian Sledz, Milan Topic. Considering environmental impacts of energy storage technologies: A life cycle assessment of power-to-gas business models. 2018 Elsevier Ltd. https://doi.org/10.1016/j.energy.2018.07.105.

[46] Akinyele DO, Rayudu RK, Nair NKC. Development of photovoltaic power plant for remote residential applications: the socio-technical and economic perspectives. Appl Energy 2015;155:131-49. http://dx.doi.org/10.1016/j.apenergy.2015.05.091.

[47] Kabakian V, McManus MC, Harajli H. Attributional life cycle assessment of mounted 1.8 kWp monocrystalline photovoltaic system with batteries and comparison with fossil energy production system. Appl Energy 2015;154:428-37. http://dx.doi.org/10.1016/j.apenergy.2015.04.125.

[48] Bhandari B, Lee KT, Lee CS, Song CK, Maskey RK, Ahn SH. A novel off-grid hybrid power system comprised of solar photovoltaic, wind, and hydro energy sources. Appl Energy 2014;133:236-42. http://dx.doi.org/10.1016/j.apenergy.2014.07.033.

[49] Tao Ma, Hongxing Yang, Lin Lu. A feasibility study of a stand-alone hybrid solar–wind–battery system for a remote island. 2014 Elsevier Ltd. http://dx.doi.org/10.1016/j.apenergy.2014.01.090.

[50] T. Adefarati, R.C. Bansal. Reliability, economic and environmental analysis of a microgrid system in the presence of renewable energy resources. Applied Energy 236 (2019) 1089–1114. 2018 Elsevier Ltd. https://doi.org/10.1016/j.apenergy.2018.12.050.

[51] Kristin Elise Skøyen Arnesen, Snorre Thorsønn Borgen. A Multi-Horizon Stochastic Programming Approach to Optimal Component Sizing for The Strategic Microgrid Design Problem. Master thesis in Industrial Economics and Technology Management. NTNU, Department of Industrial Economics and Technology Management. June 2017. http://hdl.handle.net/11250/2470453.

[52] A. Khosravi, R.N.N. Koury, L. Machado, J.J.G. Pabon. Energy, exergy and economic analysis of a hybrid renewable energy with hydrogen storage system. Energy 148 (2018) 1087-1102. 2018 Elsevier Ltd. https://doi.org/10.1016/j.energy.2018.02.008.

[53] Daniel Chade, Tomasz Miklis, David Dvorak. Feasibility study of wind-to-hydrogen system for Arctic remote locations e Grimsey island case study. Renewable Energy 76 (2015) 204-211. Elsevier Ltd. http://dx.doi.org/10.1016/j.renene.2014.11.023.

[54] Guangling Zhao, Eva Ravn Nielsen, Enrique Troncoso, Kris Hyde, Jesús Simón Romeo, Michael Diderich. Life cycle cost analysis: A case study of hydrogen energy application on the Orkney Islands. International journal of hydrogen energy 44 (2019) 9517-9528. 2018 Hydrogen Energy Publications LLC. Published by Elsevier Ltd. https://doi.org/10.1016/j.ijhydene.2018.08.015.

[55] Guangling Zhao, Allan Schrøder Pedersen. Life cycle assessment of hydrogen production and consumption in an isolated territory. 25th CIRP Life Cycle Engineering (LCE) Conference, 30 April – 2 May 2018, Copenhagen, Denmark. Published by Elsevier B.V. https://doi.org/10.1016/j.procir.2017.11.100.

[56] Øystein Ulleberg, Torgeir Nakken, Arnaud Eté. The wind/hydrogen demonstration system at Utsira in Norway: Evaluation of system performance using operational data and updated hydrogen energy system modeling tools. 2009 Professor T. Nejat Veziroglu. Published by Elsevier Ltd. http://dx.doi.org/10.1016/j.ijhydene.2009.10.077.

[57] Farrukh Khalid, Ibrahim Dincer, Marc A. Rosen. Analysis and assessment of an integrated hydrogen energy system. International journal of hydrogen energy 41 (2016) 7960-7967. 2016 Hydrogen Energy Publications LLC. Published by Elsevier Ltd. http://dx.doi.org/10.1016/j.ijhydene.2015.12.221.

[58] Giorgio Cau, Daniele Cocco, Mario Petrollese, Søren Knudsen Kær, Christian Milan. Energy management strategy based on short-term generation scheduling for a renewable microgrid using a hydrogen storage system. Energy Conversion and Management 87 (2014) 820–831. 2014 Elsevier Ltd. http://dx.doi.org/10.1016/j.enconman.2014.07.078.

[59] Roberto Carapellucci, Lorena Giordano. Modeling and optimization of an energy generation island based on renewable technologies and hydrogen storage systems. International journal of hydrogen energy 37 (2012) 2081-2093. 2011, Hydrogen Energy Publications, LLC. Published by Elsevier Ltd. http://dx.doi.org/10.1016/j.ijhydene.2011.10.073.

[60] Dimitris Ipsakis, Spyros Voutetakis, Panos Seferlis, Fotis Stergiopoulos, Costas Elmasides. Power management strategies for a stand-alone power system using renewable energy sources and hydrogen storage. International journal of hydrogen energy 34 (2009) 7081–7095. 2008 International Association for Hydrogen Energy. Published by Elsevier Ltd. http://dx.doi.org/10.1016/j.ijhydene.2008.06.051.

[61] Hakan Caliskan, Ibrahim Dincer, Arif Hepbasli. Exergoeconomic and environmental impact analyses of a renewable energy based hydrogen production system. International journal of hydrogen energy 38 (2013) 6104-6111. 2013, Hydrogen Energy Publications, LLC. Published by Elsevier Ltd. http://dx.doi.org/10.1016/j.ijhydene.2013.01.069.

[62] Manuel Castañeda, Antonio Cano, Francisco Jurado, Higinio Sánchez, Luis M. Fernández. Sizing optimization, dynamic modeling and energy management strategies of a stand-alone PV/hydrogen/battery-based hybrid system. International journal of hydrogen energy 38 (2013) 3830-3845. 2013, Hydrogen Energy Publications, LLC. Published by Elsevier Ltd. http://dx.doi.org/10.1016/j.ijhydene.2013.01.080.

[63] Kevork Hacatoglu, Ibrahim Dincer, Marc A. Rosen. Sustainability assessment of a hybrid energy system with hydrogen-based storage. International journal of hydrogen energy 40 (2015) 1559-1568. 2014, Hydrogen Energy Publications, LLC. Published by Elsevier Ltd. http://dx.doi.org/10.1016/j.ijhydene.2014.11.079.

[64] Yildiz Kalinci, Arif Hepbasli, Ibrahim Dincer. Techno-economic analysis of a stand-alone hybrid renewable energy system with hydrogen production and storage options. International journal of hydrogen energy 40 (2015) 7652-7664. 2014, Hydrogen Energy Publications, LLC. Published by Elsevier Ltd. http://dx.doi.org/10.1016/j.ijhydene.2014.10.147.

[65] Massimo Santarelli, Michele Calì, Sara Macagno. Design and analysis of stand-alone hydrogen energy systems with different renewable sources. International Journal of Hydrogen Energy 29 (2004) 1571-1586. 2004 International Association for Hydrogen Energy. Published by Elsevier Ltd. http://dx.doi.org/10.1016/j.ijhydene.2004.01.014.

[66] Faisal I. Khan, Kelly Hawboldt, M.T. Iqbal. Life Cycle Analysis of wind–fuel cell integrated system. Renewable Energy 30 (2005) 157–177. 2004 Elsevier Ltd. https://doi.org/10.1016/j.renene.2004.05.009.

[67] E.MacA. Gray, C.J. Webb, J. Andrews, B. Shabani, P.J. Tsai, S.L.I. Chan. Hydrogen storage for off-grid power supply. International journal of hydrogen energy 36 (2011) 654-663. 2010 Professor T. Nejat Veziroglu. Published by Elsevier Ltd. http://dx.doi.org/10.1016/j.ijhydene.2010.09.051.

[68] Ruiming Fang. Life cycle cost assessment of wind power-hydrogen coupled integrated energy system. International journal of hydrogen energy 44 (2019) 29399-29408. 2019 Hydrogen Energy Publications LLC. Published by Elsevier Ltd. https://doi.org/10.1016/j.ijhydene.2019.03.192.

[69] Geovanni Hernández Galvez, Oliver Probst, O. Lastres, Airel Núñez Rodríguez, Alina Juantorena Ugás, Edgar Andrade Durán, P. J. Sebastian. Optimization of autonomous hybrid systems with hydrogen storage: Life cycle assessment. International Journal of Energy Research, May 2012, Vol.36(6), pp. 749-763. 2011 John Wiley & Sons, Ltd. https://dx.doi.org/10.1002/er.1830.

[70] Pablo García, Juan P. Torreglosa, Luis M. Fernández, Francisco Jurado. Improving long-term operation of power sources in off-grid hybrid systems based on renewable energy, hydrogen and battery. Journal of Power Sources 265 (2014) 149-159. 2014 Elsevier B.V. http://dx.doi.org/10.1016/j.jpowsour.2014.04.118.

[71] David C. Young, Greig A. Mill, Rob Wall. Feasibility of renewable energy storage using hydrogen in remote communities in Bhutan. International Journal of Hydrogen Energy 32 (2007) 997–1009. 2006 International Association for Hydrogen Energy. Published by Elsevier Ltd. http://dx.doi.org/10.1016/j.ijhydene.2006.07.002.

[72] G. Tzamalis, E.I. Zoulias, E. Stamatakis, O.-S. Parissis, A. Stubos, E. Lois. Techno-economic analysis of RES & hydrogen technologies integration in remote island power system. International journal of hydrogen energy 38 (2013) 11646-11654. 2013, Hydrogen Energy Publications, LLC. Published by Elsevier Ltd. http://dx.doi.org/10.1016/j.ijhydene.2013.03.084.

[73] Qingsong Wang, Wei Liu, b, Xueliang Yuan, Hongrui Tang, Yuzhou Tang, Mansen Wang, Jian Zuo, Zhanlong Song, Jing Sun. Environmental impact analysis and process optimization of batteries based on life cycle assessment. Journal of Cleaner Production 174 (2018) 1262-1273. 2017 Elsevier Ltd. https://doi.org/10.1016/j.jclepro.2017.11.059.

[74] Laurent Vandepaer, Julie Cloutier, Ben Amor. Environmental impacts of Lithium Metal Polymer and Lithium-ion stationary batteries. Renewable and Sustainable Energy Reviews 78 (2017) 46–60. 2017 Elsevier Ltd. http://dx.doi.org/10.1016/j.rser.2017.04.057.

[75] Yuhan Liang, Jing Su, Beidou Xi, Yajuan Yuc, Danfeng Ji, Yuanyuan Sun, Chifei Cui, Jianchao Zhu. Life cycle assessment of lithium-ion batteries for greenhouse gas emissions. Resources, Conservation and Recycling 117 (2017) 285–293. 2016 Published by Elsevier B.V. http://dx.doi.org/10.1016/j.resconrec.2016.08.028.

[76] R. Stropnik, M. Sekavčnik, A.M. Ferriz, M. Mori. Reducing environmental impacts of the ups system based on PEM fuel cell with circular economy. Energy 165 (2018) 824-835. 2018 Elsevier Ltd. https://doi.org/10.1016/j.energy.2018.09.201.

[77] S. Avril, G. Arnaud, A. Florentin, M. Vinard. Multi-objective optimization of batteries and hydrogen storage technologies for remote photovoltaic systems. Energy 35 (2010) 5300-5308. 2010 Elsevier Ltd. http://dx.doi.org/10.1016/j.energy.2010.07.033.

[78] Mitavachan Hiremath, Karen Derendorf, Thomas Vogt. Comparative Life Cycle Assessment of Battery Storage Systems for Stationary Applications. Environ. Sci. Technol. 2015, 49, 4825−4833. American Chemical Society. http://doi.org/10.1021/es504572q.

[79] K. Agbossou, R. Chahine, J. Hamelin, F. Laurencelle, A. Anouar, J.-M. St-Arnaud, T. K. Bose. Renewable energy systems based on hydrogen for remote applications. Journal of Power Sources 96 (2001) 168-172. 2001 Elsevier Science B. V. https://dx.doi.org/10.1016/S0378-7753(01)00495-5.

[80] Nesrin Demir, Akif Taşkın. Life cycle assessment of wind turbines in Pınarbaşı-Kayseri. Journal of Cleaner Production 54 (2013) 253-263. 2013 Elsevier Ltd. http://dx.doi.org/10.1016/j.jclepro.2013.04.016.

[81] G. Tzamalis, E.I. Zoulias, E. Stamatakis, E. Varkaraki, E. Lois, F. Zannikos. Techno-economic analysis of an autonomous power system integrating hydrogen technology as energy storage medium. Renewable Energy 36 (2011) 118-124. 2010 Elsevier Ltd. https://dx.doi.org/10.1016/j.renene.2010.06.006.

[82] Fabio Magrassi, Elena Rocco, Stefano Barberis, Michela Gallo, Adriana Del Borghi. Hybrid solar power system versus photovoltaic plant: A comparative analysis through a life cycle approach. Renewable Energy 130 (2019) 290-304. 2018 Elsevier Ltd. https://doi.org/10.1016/j.renene.2018.06.072.

[83] Ameen Gargoom, Enamul Haque, Sajeeb Saha, Aman Oo. Hybrid Wind-Diesel Remote Area Power Systems with Hydrogen-based Energy Storage System. 2018 IEEE International Conference on Power Electronics, Drives and Energy Systems (PEDES), December 2018, pp. 1-6. https://dx.doi.org/10.1109/PEDES.2018.8707747.

[84] Benjamin Guinot, Bénédicte Champel, Florent Montignac, Elisabeth Lemaire, Didier Vannucci, Sebastien Sailler, Yann Bultel. Techno-economic study of a PV-hydrogen-battery hybrid system for off-grid power supply: Impact of performances' ageing on optimal system sizing and competitiveness. International journal of hydrogen energy 40 (2015) 623-632. 2014, Hydrogen Energy Publications, LLC. Published by Elsevier Ltd. http://dx.doi.org/10.1016/j.ijhydene.2014.11.007.

[85] Farivar Fazelpour, Nima Soltani, Marc A. Rosen. Economic analysis of standalone hybrid energy systems for application in Tehran, Iran. International journal of hydrogen energy 41 (2016) 7732-7743. 2016 Hydrogen Energy Publications LLC. Published by Elsevier Ltd. http://dx.doi.org/10.1016/j.ijhydene.2016.01.113.

[86] Stainless Steel and CO2: Facts and Scientific Observations. International Stainless Steel Forum (ISSF). 15 June 2015. http://www.worldstainless.org/Files/issf/non-image-files/PDF/ISSF_Stainless_steel_and_CO2.pdf.

[87] Xiaojin Zhang, Christian Bauer, Christopher L. Mutel, Kathrin Volkart. Life Cycle Assessment of Power-to-Gas: Approaches, system variations and their environmental implications. Applied Energy 190 (2017) 326–338. 2016 Elsevier Ltd. http://dx.doi.org/10.1016/j.apenergy.2016.12.098.

[88] Alberto Moro, Laura Lonza. Electricity carbon intensity in European Member States: Impacts on GHG emissions of electric vehicles. Transportation Research Part D 64 (2018) 5–14. 2017 Elsevier Ltd. http://dx.doi.org/10.1016/j.trd.2017.07.012.

[89] Rodolfo Dufo-López, José L. Bernal-Agustín, José M. Yusta-Loyo, José A. Domínguez-Navarro, Ignacio J. Ramírez-Rosado, Juan Lujano, Ismael Aso. Multi-objective optimization minimizing cost and life cycle emissions of stand-alone PV–wind–diesel systems with batteries storage. Applied Energy 88 (2011) 4033–4041. 2011 Elsevier Ltd. http://dx.doi.org/10.1016/j.apenergy.2011.04.019.

[90] Study on actual GHG data for diesel, petrol, kerosene and natural gas. Final report. Work order: ENER/C2/2013-643. July 2015. European Commission, DG ENER.

[91] N. Belmonte, V. Girgenti, P. Florian, C. Peano, C. Luetto, P. Rizzi, M. Baricco, "A comparison of energy storage from renewable sources through batteries and fuel cells: A case study in Turin, Italy", 2016, Hydrogen Energy Publications LLC. Published by Elsevier Ltd. http://dx.doi.org/10.1016/j.ijhydene.2016.07.260.

[92] Juhua Yang, Yuan Chang, Lixiao Zhang, Yan Hao, Qin Yan, Changbo Wang. The life-cycle energy and environmental emissions of a typical offshore wind farm in China. Journal of Cleaner Production 180 (2018) 316-324. 2018 Elsevier Ltd. https://doi.org/10.1016/j.jclepro.2018.01.082.

[93] Nadia Belmonte, Carlo Luetto, Stefano Staulo, Paola Rizzi, Marcello Baricco. Case Studies of Energy Storage with Fuel Cells and Batteries for Stationary and Mobile Applications. Challenges 2017, 8, 9. www.mdpi.com/journal/challenges. http://dx.doi.org/10.3390/challe8010009.

[94] Victor Nian, Yang Liu, Sheng Zhong. Life cycle cost-benefit analysis of offshore wind energy under the climatic conditions in Southeast Asia – Setting the bottom-line for deployment. Applied Energy 233–234 (2019) 1003–1014. 2018 Elsevier Ltd. https://doi.org/10.1016/j.apenergy.2018.10.042.

[95] Brian Fleck, Marc Huot. Comparative life-cycle assessment of a small wind turbine for residential off-grid use. Renewable Energy 34 (2009) 2688–2696. 2009 Elsevier Ltd. https://doi.org/10.1016/j.renene.2009.06.016.

[96] Datasheet HGM138 Googol Diesel Power Generator, Guangdong Honny Power-tech Co., Ltd. www.honnypower.com.

[97] O.V. Marchenko, S.V. Solomin. Modeling of hydrogen and electrical energy storages in wind/PV energy system on the Lake Baikal coast. International journal of hydrogen energy 42 (2017) 9361-9370. 2017 Hydrogen Energy Publications LLC. Published by Elsevier Ltd. http://dx.doi.org/10.1016/j.ijhydene.2017.02.076.

[98] Fatemeh Homayouni, Ramin Roshandel & Ali Asghar Hamidi (2017) Sizing and performance analysis of standalone hybrid photovoltaic/battery/hydrogen storage technology power generation systems based on the energy hub concept, International Journal of Green Energy, 14:2, 121-134. https://doi.org/10.1080/15435075.2016.1233423.

[99] Daniele Groppi, Davide Astiaso Garcia, Gianluigi Lo Basso, Fabrizio Cumo, Livio De Santoli. Analysing economic and environmental sustainability related to the use of battery and hydrogen energy storages for increasing the energy independence of small islands 2018 Elsevier Ltd. https://doi.org/10.1016/j.enconman.2018.09.063.

[100] IPCC, 2014: Annex II: Glossary [Mach, K.J., S. Planton and C. von Stechow (eds.)]. In: Climate Change 2014: Synthesis Report. Contribution of Working Groups I, II and III to the Fifth Assessment Report of the Intergovernmental Panel on Climate Change [Core Writing Team, R.K. Pachauri and L.A. Meyer (eds.)]. IPCC, Geneva, Switzerland, pp. 117-130.

[101] Norasikin Ahmad Ludin, Nur Ifthitah Mustafa, Marlia M. Hanafiah, Mohd Adib Ibrahim, Mohd Asri Mat Teridi, Suhaila Sepeai, Azami Zaharim, Kamaruzzaman Sopian. Prospects of life cycle assessment of renewable energy from solar photovoltaic technologies: A review. Renewable and Sustainable Energy Reviews 96 (2018) 11–28. 2018 Elsevier Ltd. https://doi.org/10.1016/j.rser.2018.07.048.

[102] Yuxuan Wang, Tianye Sun. Life cycle assessment of CO2 emissions from wind power plants: Methodology and case studies. Renewable Energy 43 (2012) 30-36. 2012 Elsevier Ltd. https://doi.org/10.1016/j.renene.2011.12.017.

[103] Varun, I.K. Bhat, Ravi Prakash. LCA of renewable energy for electricity generation systems—A review. Renewable and Sustainable Energy Reviews 13 (2009) 1067–1073. 2008 Elsevier Ltd. https://doi.org/10.1016/j.rser.2008.08.004.

[104] UNI EN ISO 14040: 2006. Environmental management – life cycle assessment – principles and framework.

[105] UNI EN ISO 14044: 2006. Environmental management – life cycle assessment – requirements and guidelines.

[106] Grond L, Schulze P, Holstein J. Systems analyses power to gas deliverable 1: technology review. Part of TKI project TKIG01038 – systems analyses Power-to-Gas pathways. Groningen: DNV KEMA Energy & Sustainability; 2013.

[107] Gardiner M. Energy requirements for hydrogen gas compression and liquefaction as related to vehicle storage needs; 2009.

[108] LGNeON®R solar module LG365Q1C-A5 datasheet. LG Electronics USA. https://www.lg.com/us/business/solar-panels/lg-LG365Q1C-A5.

[109] Umberto Desideri, Stefania Proietti, Francesco Zepparelli, Paolo Sdringola, Silvia Bini. Life Cycle Assessment of a ground-mounted 1778 kWp photovoltaic plant and comparison with traditional energy production systems. Applied Energy 97 (2012) 930–943. 2012 Elsevier Ltd. http://dx.doi.org/10.1016/j.apenergy.2012.01.055.

[110] Guofu Hou, Honghang Sun, Ziying Jiang, Ziqiang Pan, Yibo Wang, Xiaodan Zhang, Ying Zhao, Qiang Yao. Life cycle assessment of grid-connected photovoltaic power generation from crystalline silicon solar modules in China. Applied Energy 164 (2016) 882–890. 2015 Elsevier Ltd. http://dx.doi.org/10.1016/j.apenergy.2015.11.023.

[111] U. Desideri, F. Zepparelli, V. Morettini, E. Garroni. Comparative analysis of concentrating solar power and photovoltaic technologies: Technical and environmental evaluations. Applied Energy 102 (2013) 765–784. 2012 Elsevier Ltd. http://dx.doi.org/10.1016/j.apenergy.2012.08.033.

[112] V.M. Fthenakis, H.C. Kim. Photovoltaics: Life-cycle analyses. Solar Energy 85 (2011) 1609-1628. 2009 Elsevier Ltd. https://dx.doi.org/10.1016/j.solener.2009.10.002.

[113] Jinqing Peng, Lin Lu, Hongxing Yang. Review on life cycle assessment of energy payback and greenhouse gas emission of solar photovoltaic systems. Renewable and Sustainable Energy Reviews 19 (2013) 255–274. 2012 Elsevier Ltd. http://dx.doi.org/10.1016/j.rser.2012.11.035.

[114] Saïcha Gerbinet, Sandra Belboom, Angélique Léonard. Life Cycle Analysis (LCA) of photovoltaic panels: A review. Renewable and Sustainable Energy Reviews 38 (2014) 747–753. 2014 Elsevier Ltd. http://dx.doi.org/10.1016/j.rser.2014.07.043.

[115] Vestas wind turbine V27/225 datasheet.

[116] Begoña Guezuraga, Rudolf Zauner, Werner Pölz. Life cycle assessment of two different 2 MW class wind turbines. Renewable Energy 37 (2012) 37-44. 2011 Elsevier Ltd. http://dx.doi.org/10.1016/j.renene.2011.05.008.

[117] Cameron Smith, John Burrows, Eric Scheier, Amberli Young, Jessica Smith, Tiffany Young, Shabbir H. Gheewala. Comparative Life Cycle Assessment of a Thai Island's diesel/PV/wind hybrid microgrid. Renewable Energy 80 (2015) 85-100. 2015 Elsevier Ltd. http://dx.doi.org/10.1016/j.renene.2015.01.003.

[118] M.C. McManus. Environmental consequences of the use of batteries in low carbon systems: The impact of battery production. Applied Energy 93 (2012) 288–295. 2011 Elsevier Ltd. http://dx.doi.org/10.1016/j.apenergy.2011.12.062.

[119] Abdul Qayoom Jakhrani, Andrew Ragai Henry Rigit, Al-Khalid Othman, Saleem Raza Samo, Shakeel Ahmed Kamboh. Estimation of Carbon Footprints from Diesel Generator Emissions. 2012 International Conference in Green and Ubiquitous Technology. 2011 IEEE. https://dx.doi.org/10.1109/GUT.2012.6344193.

[120] Han Hao, Zhexuan Mu, Shuhua Jiang, Zongwei Liu and Fuquan Zhao. GHG Emissions from the Production of Lithium-Ion Batteries for Electric Vehicles in China. 2017 www.mdpi.com/journal/sustainability, 9, 504; http://doi.org/10.3390/su9040504.

[121] Linda Ager-Wick Ellingsen, Guillaume Majeau-Bettez, Bhawna Singh, Akhilesh Kumar Srivastava, Lars Ole Valøen, and Anders Hammer Strømman. Life Cycle Assessment of a Lithium-Ion Battery Vehicle Pack. www.wileyonlinelibrary.com/journal/jie. Journal of Industrial Ecology, 2013, by Yale University http://doi.org/10.1111/jiec.12072.

[122] Chris San Marchi, Brian P. Somerday. Comparison of stainless steels for high-pressure hydrogen service. Proceedings of the ASME 2014 Pressure Vessels & Piping Conference. PVP2014-28811. July 20-24, 2014, Anaheim, California, USA.

[123] R. García-Valverde, C. Miguel, R. Martínez-Béjar, A. Urbina. Life cycle assessment study of a 4.2 kWp stand-alone photovoltaic system. Solar Energy 83 (2009) 1434–1445. 2009 Elsevier Ltd. https://doi.org/10.1016/j.solener.2009.03.012.

[124] E. A. Alsema. Environmental life cycle assessment of solar home systems. Tech. rep. NWS-E-2000-15. Department of Science, Technology and Society, Utrecht University, Utrecht, The Netherlands; 2000.

[125] Benjamin K. Sovacool. Valuing the greenhouse gas emissions from nuclear power: A critical survey. Energy Policy 36 (2008) 2950–2963. 2008 Elsevier Ltd. https://doi.org/10.1016/j.enpol.2008.04.017.

[126] Luc Gagnon, Camille Bélanger, Yohji Uchiyama. Life-cycle assessment of electricity generation options: The status of research in year 2001. Energy Policy 30 (2002) 1267–1278. 2002 Elsevier Science Ltd. https://doi.org/10.1016/S0301-4215(02)00088-5.

[127] Sara Evangelisti, Carla Tagliaferri, Dan J.L. Brett, Paola Lettieri. Life cycle assessment of a polymer electrolyte membrane fuel cell system for passenger vehicles. Journal of Cleaner Production 142 (2017) 4339-4355. 2016 Elsevier Ltd. http://dx.doi.org/10.1016/j.jclepro.2016.11.159.

[128] Andrew Simons, Christian Bauer. A life-cycle perspective on automotive fuel cells. Applied Energy 157 (2015) 884–896. 2015 Elsevier Ltd. http://dx.doi.org/10.1016/j.apenergy.2015.02.049.

[129] Christine Birkeland. Assessing the Life Cycle Environmental Impacts of Offshore Wind Power Generation and Power Transmission in the North Sea. Master thesis of Science in Energy and Environment. NTNU, Department of Energy and Process Engineering. June 2011. http://hdl.handle.net/11250/257062.

[130] Daniel Garraín, Yolanda Lechón. Exploratory environmental impact assessment of the manufacturing and disposal stages of a new PEM fuel cell. International journal of hydrogen energy 39 (2014) 1769-1774. 2013, Hydrogen Energy Publications, LLC. Published by Elsevier Ltd. http://dx.doi.org/10.1016/j.ijhydene.2013.11.095.

[131] Martin Pehnt. Life-cycle assessment of fuel cell stacks. International Journal of Hydrogen Energy 26 (2001) 91-101. 2000 International Association for Hydrogen Energy. Published by Elsevier Science Ltd. https://doi.org/10.1016/S0360-3199(00)00053-7.

[132] L. Oliveira, M. Messagie, J. Mertens, H. Laget, T. Coosemans, J. Van Mierlo. Environmental performance of electricity storage systems for grid applications, a life cycle approach. Energy Conversion and Management 101 (2015) 326–335. 2015 Elsevier Ltd. http://dx.doi.org/10.1016/j.enconman.2015.05.063.

[133] John Warnock, David McMillan, James Pilgrim, Sally Shenton. Failure Rates of Offshore Wind Transmission Systems. Energies 2019, 12, 2682. www.mdpi.com/journal/energies. https://doi.org/10.3390/en12142682.

[134] P. Masoni, A. Zamagni. Reviewers/Advisory Board: P. Fullana I Palmer, M. Bode, M. Finkbeiner, K. Chomkhamsri. GUIDANCE DOCUMENT FOR PERFORMING LCA ON FUEL CELLS. Deliverable D3.3–Final guidance document. Work Package 3–Preparation and Consultation of the Guidance Document. 2011-09-30. Fuel cell and Hydrogen – Joint Undertaking.

[135] Kelly Benton, Xufei Yang, Zhichao Wang. Life cycle energy assessment of a standby diesel generator set. Journal of Cleaner Production 149 (2017) 265-274. 2017 Elsevier Ltd. http://dx.doi.org/10.1016/j.jclepro.2017.02.082.

[136] Svandís Hlín Karlsdóttir. Experience in transporting energy through subsea power cables: The case of Iceland. M.S. thesis, Faculty of Industrial Engineering, Mechanical Engineering and Computer Science. School of Engineering and Natural Sciences, University of Iceland. Reykjavik, 2013.

[137] T.Adefarati, R.C.Bansal. Chapter 2 - Energizing Renewable Energy Systems and Distribution Generation. Pathways to a Smarter Power System 2019, Pages 29-65. 2019 Elsevier Ltd. https://doi.org/10.1016/B978-0-08-102592-5.00002-8.

[138] Edgar Furuholt. Life cycle assessment of gasoline and diesel. Resources, Conservation and Recycling 14 (1995) 251-263. 1995 Elsevier Science B.V. https://doi-org.ezproxy.biblio.polito.it/10.1016/0921-3449(95)00020-J.

[139] Tom Beer, Tim Grant, David Williams, Harry Watson. Fuel-cycle greenhouse gas emissions from alternative fuels in Australian heavy vehicles. Atmospheric Environment 36 (2002) 753–763. 2002 Elsevier Science Ltd. https://doi.org/10.1016/S1352-2310(01)00514-3.

[140] Yu-Fong Huang, Xing-Jia Gan, Pei-Te Chiueh. Life cycle assessment and net energy analysis of offshore wind power systems. Renewable Energy 102 (2017) 98-106. 2016 Elsevier Ltd. http://dx.doi.org/10.1016/j.renene.2016.10.050.

[141] Sally D. Wright, Anthony L. Rogers, James F. Manwell, Anthony Ellis. Transmission options for offshore wind farms in the United States. Centre for Energy Efficiency and Renewable Energy, University of Massachusetts at Amherst. AWEA 2002.

[142] Datasheet submarine cable 2XS(FL)2YRAA 3x1x70 RM/16 6/10 (12)kV, Nexans. https://www.nexans.com.

[143] CIGRE Working Group B1.10. Update of Service Experience of HV Underground and Submarine Cables; CIGRE: Paris, France, 2009.

[144] CIGRE Working Group B1.21. Third-Party Damage to Underground and Submarine Cables; CIGRE: Paris, France, 2009.

[145] M. O'Connor, T. Lewis, G. Dalton. Weather window analysis of Irish west coast wave data with relevance to operations & maintenance of marine renewables. Renewable Energy 52 (2013) 57-66. 2012 Elsevier Ltd. http://dx.doi.org/10.1016/j.renene.2012.10.021.

[146] Stromme. RAM for NorNed cable HVDC project. 1998.

[147] NEEDS, 2008. New Energy Externalities Developments for Sustainability. RS1a: Life cycle approaches to assess emerging energy technologies (Final report on offshore wind technology), NEEDS projects, DONG Energy.

[148] Datasheet KD66W Kohler Diesel Power Generator, KOHLER Power Systems. www.KohlerPower.com.

[149] Stacey L. Dolan, Garvin A. Heath. Life Cycle Greenhouse Gas Emissions of Utility-Scale Wind Power: Systematic Review and Harmonization. Journal of Industrial Ecology, April 2012, Vol.16 (Supplement 1), pp. S136-S154. www.wileyonlinelibrary.com http://dx.doi.org/10.1111/j.1530-9290.2012.00464.x.

[150] Hanne Lerche Raadal, Luc Gagnon, Ingunn Saur Modahl, Ole Jørgen Hanssen. Life cycle greenhouse gas (GHG) emissions from the generation of wind and hydro power. Renewable and Sustainable Energy Reviews 15 (2011) 3417–3422. 2011 Elsevier Ltd. http://dx.doi.org/10.1016/j.rser.2011.05.001.

[151] IRENA (February 2018), Renewable Energy Prospects for the European Union, International Renewable Energy Agency, Abu Dhabi.

[152] Monaaf D.A. Al-falahi, S.D.G. Jayasinghe, H. Enshaei. A review on recent size optimization methodologies for standalone solar and wind hybrid renewable energy system. 2017 Elsevier Ltd. http://dx.doi.org/10.1016/j.enconman.2017.04.019.

[153] Dimitrios-Sotirios Kourkoumpas, Georgios Benekos, Nikolaos Nikolopoulos, Sotirios Karellas, Panagiotis Grammelis, Emmanouel Kakaras. A review of key environmental and energy performance indicators for the case of renewable energy systems when integrated with storage solutions. Applied Energy 231 (2018) 380–398. Elsevier Ltd. https://doi.org/10.1016/j.apenergy.2018.09.043.

[154] A.R. Dehghani-Sanij, E. Tharumalingam, M.B. Dusseault, R. Fraser. Study of energy storage systems and environmental challenges of batteries. Renewable and Sustainable Energy Reviews 104 (2019) 192–208. 2019 Elsevier Ltd. https://doi.org/10.1016/j.rser.2019.01.023.

[155] REMOTE, Project n° 779541, "Remote area Energy supply with Multiple Options for integrated hydrogen-based Technologies". Deliverable number 2.5, Control strategies of the 4 DEMOs. WP2–Use cases: definition of the technical and business cases of the 4 DEMOs. T2.4–Control strategies of the DEMO plants. 30/01/2019. Author(s): Alexandros Kafetzis, Chrysovalantou Ziogou, Kyriakos Panopoulos, Simira Papadopoulou, Panos Seferlis, Spyros Voutetakis.

[156] A. Lozanovski, Dr. O. Schuller, Dr. M. Faltenbacher. Reviewers/Advisory Board: P. Fullana I Palmer, M. Bode, M. Finkbeiner, K. Chomkhamsri. Guidance Document for Performing LCA on Hydrogen Production Systems. Deliverable D3.3–Final guidance document. Work Package 3–Preparation and Consultation of the Guidance Document. 2011-09-30. Fuel cell and Hydrogen – Joint Undertaking.

Websites

[I] https://sustainabledevelopment.un.org.

[II] https://www.un.org/sustainabledevelopment/news/communications-material/.

[III] https://ec.europa.eu.

[IV] https://cordis.europa.eu/project/rcn/97935/reporting/en.

[V] https://www.nve.no.

[VI] https://atlas.nve.no/.